REPORT DOCUMENTATION PAGE

Form Approved OMB No. 0704-0188

1. AGENCY USE ONLY (Leave blank)	2. REPORT DATE	3. REPORT TYPE AND DATES COVERED
	January 2010	Technical Report

4. TITLE AND SUBTITLE

Robust Multiple – Input – Output Communications

5. FUNDING NUMBERS

6. AUTHOR(S)

Songsri Sirianunpiboon

7. PERFORMING ORGANIZATION NAME(S) AND ADDRESS(ES)

DSTO

8. PERFORMING ORGANIZATION REPORT NUMBER

9. SPONSORING/MONITORING AGENCY NAME(S) AND ADDRESS(ES

Electronic Warfare and Radar Division
DSTO
PO Box 1500 Edinburg
South Australia 5111 Australia

10. SPONSORING/MONITORING AGENCY REPORT NUMBER

11. SUPPLEMENTARY NOTES

12a. DISTRIBUTION/AVAILABILITY STATEMENT

Approved for Public Release.

12b. DISTRIBUTION CODE

ABSTRACT (Maximum 200 words)

Multiple antennas at both the transmitter and receiver is known output (MIMO) as multiple-input multiple- system. This has emerged as the most promising technique for improving the performance of wireless digital transmission systems as well as allowing higher data rates to be obtained for a given bandwidth. A consequence of the MIMO wireless communications revolution is that multipath scattering of the transmitted signal has moved from being a problem to being a valuable resource. This has happened to such extent that MIMO systems have come to rely on this resource. However, away from dense urban and indoor environments such as Australian rural and remote areas with wide open spaces and flat or smooth undulating terrain such rich scattering can be hard to find.

This research seeks to develop MIMO schemes which will give robust and reliable performance in environments that can change rapidly from rich scattering environment to clear line of sight between transmitter and receiver. Wirelesss communications system which are robust to changing environment conditions are a particular important factor in military communication systems as well as for civilian emergency services. In this work, polarization is proposed as a source of diversity in wireless communications. Polarization diversity is particularly suited to the Australian rural and remote environment where wide open spaces and flat or smooth undulating terrain give rise to line of sight conditions between the transmitter and the receiver. The polarization diversity of transmitted signals is mostly preserved by the line-of-sight environment presenting an opportunity for transmitter and receiver diversity techniques ,

Another aspect of the research presented here is the development of fast, fixed complexity, decoding algorithms for space-time codes that are robust to the changing transmission conditions. Reliable high rate transmission over the MIMO system ca only be achieved through "space-time coding". The major drawback of a number of potentially useful space-time codes is the high computational complexity of the known decoding algorithms. This is particular true for a number of codes which. are best suited to the exploitation of polarization diversity. The existing "fast" decoding algorithm for this decoding problem, the so-called sphere decoder, h as performance which depends crucially on the channel conditions. When the channel is close to singular, that is, when the channel between the base station and terminal is close to pure line-of-sight' the sphere decoder defaults to an exhaustive search. If such conditions persist the communication system could be in outage purely due to computational overload. In this project we develop fast decoding algorithms which have fixed complexity across all channel conditions. In particular, we present the fastest known fixed complexity decoding algorithm for the Golden code, an important code used in the WiMax standard for fully mobile internet access.

14. SUBJECT TERMS

DSTO, Australia , Multiple antennas, Transmitter, Receiver, Multiple-input multiple-output (MIMO), Wireless digital transmission, Bandwidth

15. NUMBER OF PAGES

16. PRICE CODE

17. SECURITY CLASSIFICATION OF REPORT	18. SECURITY CLASSIFICATION OF THIS PAGE	19. SECURITY CLASSIFICATION OF ABSTRACT	20. LIMITATION OF ABSTRACT
CLASSIFIED	UNCLASSIFIED	UNCLASSIFIED	UL

Department of Defence
Defence Science and
Technology Organisation

DSTO FELLOWSHIP PROGRAM

Robust Multiple - Input Multiple - Output Communications

Songsri Sirianunpiboon

DSTO Science and Technology for a Secure World

Summary

Multiple antennas at both the transmitter and receiver is known as multiple-input multiple-output (MIMO) system. This has emerged as the most promising technique for improving the performance of wireless digital transmission systems as well as allowing higher data rates to be obtained for a given bandwidth. A consequence of the MIMO wireless communications revolution is that multipath scattering of the transmitted signal has moved from being a problem to being a valuable resource. This has happened to such extent that MIMO systems have come to rely on this resource. However, away from dense urban and indoor environments such as Australian rural and remote areas with wide open spaces and flat or smooth undulating terrain such rich scattering can be hard to find.

This research seeks to develop MIMO schemes which will give robust and reliable performance in environments that can change rapidly from rich scattering environment to clear line of sight between transmitter and receiver. Wireless communications system which are robust to changing environment conditions are a particular important factor in military communication systems as well as for civilian emergency services. In this work, polarization is proposed as a source of diversity in wireless communications. Polarization diversity is particularly suited to the Australian rural and remote environment where wide open spaces and flat or smooth undulating terrain give rise to line of sight conditions between the transmitter and the receiver. The polarization diversity of transmitted signals is mostly preserved by the line-of-sight environment, presenting an opportunity for transmitter and receiver diversity techniques.

Another aspect of the research presented here is the development of fast, fixed complexity, decoding algorithms for space-time codes that are robust to the changing transmission conditions. Reliable high rate transmission over the MIMO system can only be achieved through "space-time coding". The major drawback of a number of potentially useful space-time codes is the high computational complexity of the known decoding algorithms. This is particular true for a number of codes which are best suited to the exploitation of polarization diversity. The existing "fast" decoding algorithm for this decoding problem, the so-called sphere decoder, has performance which depends crucially on the channel conditions. When the channel is close to singular, that is, when the channel between the base station and terminal is close to pure line-of-sight, the sphere decoder defaults to an exhaustive search. If such conditions persist the communication system could be in outage purely due to computational overload. In this project we develop fast decoding algorithms which have fixed complexity across all channel conditions. In particular, we present the fastest known fixed complexity decoding algorithm for the Golden code, an important code used in the WiMax standard for fully mobile internet access.

Author

Dr Songsri Sirianunpiboon
Electronic Warfare and Radar Division

Songsri Sirianunpiboon received her PhD in Applied Mathematics from La Trobe University, Melbourne, Australia in 1989. She emigrated to Australia after a number of years teaching mathematics at Silpakorn University in Thailand. She joined DSTO with Defence System Analysis Division in 2001. In 2002 she joined Secure Communications Branch, C3ID where she has been involved in research in the area of statistical signal processing for electronic surveillance and communications. From 2007-2009, Songsri was awarded a DSTO Fellowship to work in the area of MIMO communications. Currently Songsri is with Electronic Warfare and Radar Division where she pursues research in statistical signal processing for intercepted radar signals.

Fellowship Publications and Presentations

1. S. Sirianunpiboon, Y. Wu, A. R. Calderbank and S. D. Howard, "Fast Optimal Decoding of Multiplexed Orthogonal Designs by Conditional Optimization", *IEEE Trans. Information Theory*, Vol, 56, No.3, March 2010.

2. L. M. Davis, S. Srinivasan and S. Sirianunpiboon, "Flexible Complexity Fast Decoding of Multiplexed Alamouti Codes in Spaee-Time-Polarization Systems", in *Proc. IEEE VTC 2010 -Spring*, Taipei, Taiwan 2010.

3. S. Sirianunpiboon, S. D. Howard and A. R. Calderbank, "A Scheme for Fully Polarimetric MIMO Multiuser Detection", in *Proc. Asilomar Conference on Signal, System and Computers*, Paeifie Grove, USA, Nov 2009.

4. S. Sirianunpiboon, S. D. Howard, A. R. Calderbank and L. M. Davis, "Fully-Polarimetric MIMO to Improve Throughput and Reliability aeross Propagation Conditions", in *Proc. IEEE VTC 2009-Fall*, Anchorage, Alaska, Sept, 2009.

5. S. D. Howard, S. Sirianunpiboon and A. R. Calderbank, "Low Complexity Essentially Maximum likelihood Decoding of Perfect Space-Time Codes", in *Proc. IEEE ICASSP*, Taipei, Taiwan, 19-24 Apr 2009.

6. S. Sirianunpiboon, L. M. Davis and A. R. Calderbank, "Performance of the Golden Code in the Presence of Polarization Diversity", in *Proc. IEEE AusCTW*, Sydney, 4-6 Feb. 2009.

7. A. R. Calderbank, S. Sirianunpiboon and S. D. Howard, "Spaee-Time Codes: The Value of Correlation at the Transmitter ", a book ehapter in *New Directions in Wireless Communication Research*, V. Tarokh, editor, Springer, 2008.

8. S. Sirianunpiboon, A. R. Calderbank and S. D. Howard, "Bayesian Analysis of Interferenee Cancellation for Alamouti Multiplexing", *IEEE Trans. Information Theory*, vol.54, no.10, pp. 4755-4761, Oet 2008.

9. S. Sirianunpiboon, A. R. Calderbank and S. D. Howard, "Cognitive Decoding and the Golden Code", in *Proc. 16th European Signal Processing Conference*, Lausanne, 25-29 Aug, 2008.

10. S. Sirianunpiboon, A. R. Calderbank and S. D. Howard, "Fast Essentially Maximum likelihood Decoding of the Golden Code", submitted to *IEEE Trans. Information Theory*, Jun 2008.

11. S. D. Howard, S. Sirianunpiboon and A. R. Calderbank, "Fast Decoding of the Golden Code by Diophantine Approximation", in *Proc. IEEE ITW*, Lake Tahoe, CA. USA, 2-6 Sept 2007.

12. S. Sirianunpiboon, A. R. Calderbank and S. D. Howard, "Diversity Gains Across Line of Sight and Rieh Seattering Environments from Spaee-Polarization-Time Codes", in *Proc. Information Theory for Wireless Network (ITW)* Bergen, Norway, 1-6 July 2007.

Contents

List of Figures

Acknowledgments

This work was carried out under the Defence Science and Technology Organisation (DSTO) Fellowship Program during 2007-2009. I would like to thank DSTO for awarding me this Fellowship.

I would also like to thank Dr. Bruce Ward and Dr. Warren Marwood for their full and continuing support in pursuing this Fellowship.

My thanks also go to Prof. Calderbank at Princeton University, for his support and lending his considerable expertise to this project.

A large portion of this research is based on collaborative work with Prof. Robert Calderbank, Assoc. Prof. Linda Davis and Dr. Stephen Howard.

Preface

The primary characteristic of wireless communications is variability. Any change in the position of the transmitter or receiver, or in fact, of any object in the vicinity of the wireless system can cause the quality of the transmission to change. This effect is referred to as fading. Fading is caused by the transmitted signal making its way to the receiver via multiple paths, and these *multipath* components can then destructively interfere to significantly reduce the received power. Another important characteristic of wireless communications is that users must share a common resource, *bandwidth*.

Consideration of these problems and limitations led to the development of *multiple-input multiple-output* (MIMO) wireless communication systems in the mid 1990s and this technique has emerged as the most promising technique for improving the performance of wireless digital transmission systems [1, 2]. This improvement is two-fold. First, the limited resources of a wireless communication system, such as spectrum and power, can be efficiently used with multiple antennas to provide good quality and large capacity to a wide range of applications requiring high data rates. In short, MIMO techniques allow higher data rates to be obtained for a given bandwidth. The second advantage obtained through the use of MIMO systems is robustness to fading caused by multipath propagation of the radio transmissions. As a consequence of these benefits, MIMO has gone through the adoption curve for commercial wireless systems to the point that today (2009), all high throughput commercial standards (i.e. WiMax, Wi-Fi etc.) have adopted MIMO as part of the optional, if not mandatory, portions of their standards [3].

A consequence of the MIMO wireless communications revolution is that multipath scattering of the transmitted signal has moved from being a problem to being a valuable resource. This has happened to such an extent that MIMO systems have come to rely on this resource. However, away from dense urban and indoor environments, for example, in Australian rural and remote areas with wide open spaces and flat or smooth undulating terrain such rich scattering can be hard to find.

The research reported in this work seeks to develop MIMO schemes which will give robust and reliable performance in environments that can change rapidly from a rich scattering environment to clear line of sight between transmitter and receiver. Wireless communications systems which are robust to changing environmental conditions are a particularly important factor in military communication systems as well as for civilian emergency services.

Central to this research program is the introduction of a new degree of freedom at the physical layer of the wireless network, called polarization. The polarization of the electromagnetic wave carrying the information from the transmitter to the receiver is defined by the orientation of the electric field vector in the plane perpendicular to the direction of propagation. Traditionally, wireless communication systems have used a single transmit antenna and a single receive antenna with linear vertical polarization. Linear horizontal and circular polarization are also possible and have found application in wireless point-to-point (e.g. IEEE 802.11 WiFi) and satellite communication systems respectively. By introducing either dual-polarized antennas and/or multiple antennas with different polarization, the dimension of polarization is added to those of time, frequency and space for wireless transmission at the physical layer [4].

Some existing wireless systems (e.g. many WiFi access points) exploit polarization in an implicit way. These implicit techniques are analogous to traditional selection diversity [4]. The signal is launched with a single polarization, the propagation medium then couples some

energy into the cross-polarization plane, and the signal is received with a cross-polarized antenna [5]. Exploitation of implicit polarization diversity is suited to rich scattering (e.g. dense urban and indoor) environments [6]. In this work, polarization is proposed as a source of explicit diversity in wireless communications. Explicit polarization diversity is particularly suited to the Australian rural and remote environment where wide open spaces and flat or smooth undulating terrain give rise to line of sight (LOS) conditions between the transmitter and the receiver. The polarization diversities of transmitted signals are mostly preserved by the LOS environment, presenting an opportunity for transmitter diversity as well as receiver diversity techniques.

Another aspect of the research reported here is to develop fast, fixed complexity, decoding algorithms for space-time codes that are robust to the changing environment. The major drawback of space-time codes is the high complexity of their decoding algorithms. This is particularly true for a number of codes which are best suited to the exploitation of polarization diversity. The existing "fast" decoding algorithm for this problem, the so-called *sphere decoder*, has performance which depends crucially on the channel conditions. When the channel is close to singular, that is, when the channel between the base station and terminal is close to pure line of sight, the sphere decoder defaults to an exhaustive search. If such conditions persist the communication system could be in outage purely due to computational overload. The fast decoding algorithms developed here have fixed complexity across all channel conditions.

The report is essentially divided into three parts. The first part, Chapters 1 and 2, give the necessary background on MIMO communications and space-time block codes and goes on to develop some new techniques which we later use to analyse polarimetric MIMO schemes.

The second part consists of Chapters 3 and 4. It reports on our development of fast decoding algorithms for space-time codes. We develop fast decoding algorithms for a number of important space-time codes, that have fixed complexity across channel conditions. Our fast decoding algorithms are based on a technique called *conditional optimization*, which is widely used in statistical estimation and signal processing to reduce the search space of an optimization problem by taking advantage of the possibility of analytically optimizing over some subset of the parameters, conditioned on the remaining parameters. This technique has hardly been exploited in discrete optimization problems associated with decoding in wireless communications. We show how to apply this method to a large class of full-rate, full-diversity space-time block codes, which includes multiplexed orthogonal designs, to give fast maximum likelihood (ML) detection with low computational complexity. The technique is also applied to the Golden Code and perfect space-time block codes, in an approximate form, to obtain essentially maximum likelihood performance with greatly reduced complexity. Chapter 4 analyses, in a general way, the structure of space-time codes that allow fast maximum likelihood decoding. We show that the perfect space-time codes of Oggier et al. [7] are in fact, multiplexed quasi-orthogonal designs and so have fast, fixed complexity, exact ML decoding algorithms.

The third part of this report explores the benefit of polarization diversity for MIMO systems. In Chapter 2 we analyse interference cancellation for multiple Alamouti schemes using a Bayesian approach which provides a unified framework with which to understand the relationship between various signal detection techniques. The approach leads to a new parameter which can be used to predict the performance of systems based on Alamouti coding, without needing to resort to simulations. This parameter is used to analyse various transmission schemes involving polarization diversity in Chapter 5. We show that a certain scheme which multiplexes space-time codes across polarization gives significant benefits in stability of per-

formance for the MIMO system in the presence of even a small LOS component. In particular, this scheme is shown to give inherent stability with respect to the relative orientation of a pair of spatially separated dual polarized transmit antenna. This provides an important indication of how polarization can be used to develop more robust and reliable wireless communication systems. We go on to investigate systems using dual polarized transmit and dual polarized receive antenna in various conditions from pure LOS, Ricean and pure scattering. It is shown that the performance of the Golden Code can be made stable across propagation conditions by the use of dual polarized transmit and dual polarized receive antennas. However, this is true only if the transmitter and/or receiver are fixed in position or are allowed to rotate in a plane of alignment.

In mobile communications, the transmitter and/or receiver rotate with respect to each other, throwing the dual polarimetric antennas out of alignment and degrading the performance significantly. To improve the stability in transmission and/or reception under the rotation of the transmitter and/or receiver, we investigate the use of a triad antenna at the transmitter and the receiver in Chapter 6. We analytically show that the capacity of a system using triad antennas is preserved under the relative rotation of the transmitter and receiver. This is not the case for the dual polarized system. We introduce a 3×3 space-time code suitable for the triad system which gives full rate, through which the gains achievable with triad antennas are demonstrated. This code also has the advantage of being fast to decode due to our fast decoding algorithm.

Notation

E	Expectation
$\mathbf{I}_n$	$n \times n$ Identity matrix
$\mathrm{Q}(\cdot)$	Quantiser (Slicer)
det	Determinant of matrix
$\mathbb{Z}$	Integer
$\mathbb{Z}[i]$	Gaussian integer
$\mathbb{C}$	Complex number
$\mathbb{R}$	Real number
$\mathbb{Q}$	Rational number
$\mathbb{C}^{N \times M}$	$N \times M$ matrices of complex number
$\mathbb{R}^n$	n dimensional vectors of real numbers
Tr	Trace of matrix
diag	Diagonal of a matrix
$*$	complex conjugate
$\dagger$	Hermitian conjugate
$\Re(\cdot)$	real part

Abbreviations

AWGN	Additive White Gaussian Noise
BLAST	Bell Lab Layered Space-Time Architecture
CDMA	Code Division Multiple Access
CSI	Channel State Information
EDGE	Enhanced Data for Global Evolution
GSM	Global System for Mobile
IC	Interference Cancellation
LDC	Linear Dispersion Code
LOS	Line-of-Sight
MAP	Maximum a Posteriori
MIMO	Multiple-Input Multiple-Output
ML	Maximum Likelihood
OD	Orthogonal Design
OSTBC	Orthogonal Space-Time Block Code
PCS	Personal Communication System
QOD	Quasi-Orthogonal Design
QOSTBC	Quasi-Orthogonal Space-Time Block Codes
SINR	Signal to Interference and Noise Ratio
SM	Spatial Multiplexing
SNR	Signal to Noise Ratio
STBC	Space-Time Block Code
UMTS	Universal Mobile Telecommunications System
WiFi	Wireless Fidelity
WiMAX	Worldwide Interoperability for Microwave Access
XPD	Cross Polarization Discrimination
ZF	Zero Forcing

Chapter 1: MIMO Communications

1.1 Introduction

Recent advances in wireless communication systems have provided high speed, high throughput over wireless channels, providing high quality information exchange between portable devices located anywhere in the world. Wired communication has more stability, better performance and higher reliability, but it greatly constrains the environments or locations in which the system can be used. Wireless communication provides the benefits of portability, mobility and accessibility. However, this represents both freedom to the end user and also a number of challenges for the system designer [8].

Wireless communication is the transfer of information over a distance without the use of electrical conductors or wires. Instead, the information rides on electromagnetic waves, with the consequence that the information undergoes attenuation (fading) due to the interaction of the electromagnetic waves with the physical environment. The signal attenuation by wireless propagation may be due to the distance between communicating nodes, referred to as *path loss*, or due to *shadowing* from obstacles such as buildings, or due to constructive and destructive interference of multiple reflections of the electromagnetic wave, referred to as *multipath propagation*. Figure 1.1 illustrates a typical outdoor wireless propagation environment where the mobile node is communicating with a wireless access point (base station). The signal transmitted from the mobile may reach the base station directly (line of sight) or through multiple reflections on local scatterers such as buildings, trees, hills etc. The received signal is a combination of multiple delayed copies of the transmitted signal. This multipath propagation makes wireless a challenging communication environment.

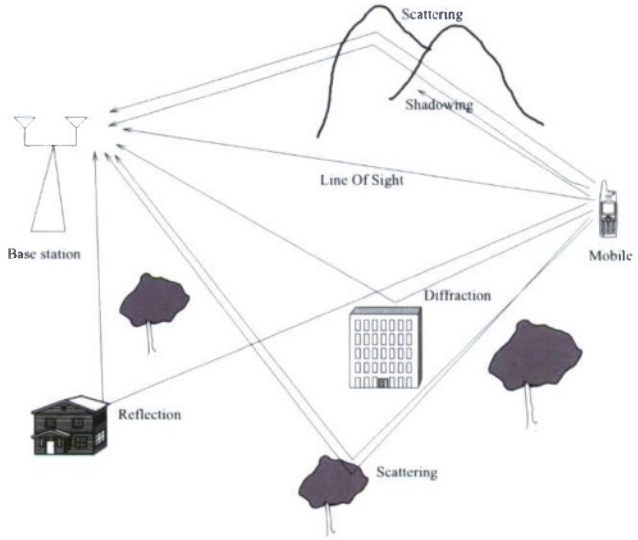

Figure 1.1: Radio propagation environment

Fortunately, this challenge can be turned into an opportunity through the use of multiple antennas. The multiple antennas may be in spatially separate locations and/or have different polarizations (*polarization diversity*). Due to different local scattering environments, sufficiently separated antenna elements provide almost independent fading channels. How much separation is appropriate depends on the environment. In rural macro cells, many wavelengths of separation may be required to de-correlate antennas, whereas in indoor environments a half wavelength separation may be sufficient [9]. With sufficient spacing, multiple antennas at both ends of a wireless link can be used to exploit the statistical independence of the multiple channels connecting transmitter to receiver to increase spectral efficiency thought the uses of *spatial multiplexing*. The existence of multiple independent channels can also be used to improve link reliability through the use of *transmit diversity* techniques. A transmit diversity technique which spreads the transmitted information across the multiple independent paths, and which is particularly attractive because it does not require channel state information (CSI) at the transmitter, is *space-time coding* [10].

1.2 Spatial Multiplexing

Spatial multiplexing (SM) is a technique which uses multiple antennas at both the transmitter and receiver to increase the transmission rate by exploiting multipath. That is, it uses the scattering characteristics of the propagation environment to enhance the transmission rate by treating the multiplicity of scattering paths as separate parallel sub-channels. Bell Labs was the first to demonstrate a laboratory prototype in 1998, known as BLAST (Bell Labs Layered Space-Time Architecture, see Figure 1.2), where SM is the principal technique used to improve the performance of a wireless communication system. Bell Labs accomplished this by splitting a single user's data stream into multiple sub-streams and using an array of transmitter antennas to simultaneously launch the parallel sub-streams. All the sub-streams are transmitted in the same frequency band, so spectrum is used very efficiently. Since the user's data is being sent in parallel over multiple antennas, the effective transmission rate increases roughly linearly with the number of antennas.

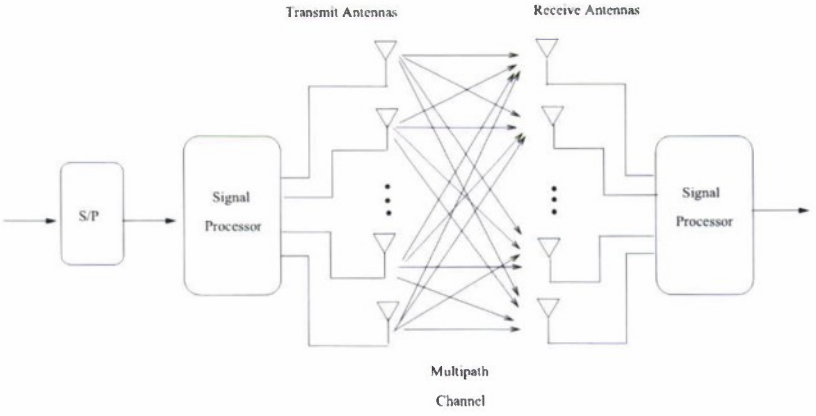

Figure 1.2: MIMO system

At the receiver, if the multipath scattering is sufficient, i.e. the channel matrix has full rank, then the received signal at each receive antenna is a non-zero linear combination of independent transmitted sub-streams. Using sophisticated signal processing, these slight differences in scattering allow the sub-streams to be separated and recovered. In its most basic form known as vertical (V)-BLAST, the detection process uses a combination of nulling and symbol cancellation to successively compute the decision statistics which are then used to form estimates of the underlying data symbols.

Spatial multiplexing relies on the scattering richness in the propagation environment. The lack of such conditions reduces the achievable rates of spatial multiplexing techniques from their theoretical projections under ideal assumptions [11, 12].

1.3 Space-Time Block Codes

Space-time block codes (STBC) introduced by Tarokh et al. [10], improve the reliability of communication over fading channels by correlating signals across different transmit antennas. The transmitted data stream is encoded in blocks which are distributed across space and time.

Consider a communication system with n_t transmit and n_r receive antennas. Assume that the transmitted symbols from the n_t transmit antennas at time slot t is

$$\boldsymbol{x}_t = (x_t^1, x_t^2, \ldots, x_t^{n_t}), \quad 1 \leq t \leq T \tag{1.1}$$

where x_t^i is the transmitted symbol from antenna i at time slot t, and all transmitted symbols have the same duration. A $n_t \times T$ space-time codeword matrix can be defined as

$$\mathbf{X} = (\boldsymbol{x}_1, \boldsymbol{x}_2, \ldots, \boldsymbol{x}_T) = \begin{pmatrix} x_1^1 & x_2^1 & \ldots & x_T^1 \\ x_1^2 & x_2^2 & \ldots & x_T^2 \\ \vdots & \vdots & \vdots & \vdots \\ x_1^{n_t} & x_2^{n_t} & \ldots & x_T^{n_t} \end{pmatrix} \tag{1.2}$$

The i^{th} row $\boldsymbol{x}^i = (x_1^i, x_2^i, \ldots, x_T^i)$ is the data sequence transmitted from the i^{th} transmit antenna and the j^{th} column $x_j = (x_j^1, x_j^2, \ldots, x_j^{n_t})$ is the space-time symbol transmitted at time $j, 1 \leq j \leq T$. In a general form, an STBC can be seen as a mapping of T complex symbols $(x_1, x_2, \ldots, x_T)$ onto a matrix $\mathbf{X}$ of dimension $n_t \times T$:

$$(x_1, x_2, \ldots, x_T) \rightarrow \mathbf{X} \tag{1.3}$$

1.3.1 Diversity

Error probability on an additive white Gaussian noise (AWGN) channel decays exponentially with SNR, and the challenge of communication over Rayleigh fading channels is that error probability decays only inversely with SNR. The received symbols $\boldsymbol{y}$ are given by

$$\boldsymbol{y} = \boldsymbol{h}\mathbf{X} + \boldsymbol{n} \tag{1.4}$$

where $\mathbf{X}$ is the transmitted codeword, $\boldsymbol{h}$ is the vector of fading (or channel) coefficients, and $\boldsymbol{w}$ is Gaussian noise. We assume a quasi-static model where the fading coefficients are constant over a frame and change independently from one frame to the next. If we normalize $\mathbf{X}$ so that

the average energy per complex symbol is 1 (SNR $= 1/N_0$), then the probability of error given perfeet channel state information is

$$\Pr(\mathbf{X}_i \rightarrow \mathbf{X}_j | \boldsymbol{h}) = Q\left(\frac{\|\boldsymbol{h}(\mathbf{X}_i - \mathbf{X}_j)\|}{2\sqrt{N_0/2}}\right) \tag{1.5}$$

and averaging over the channel statistics gives

$$\Pr(\mathbf{X}_i \rightarrow \mathbf{X}_j) = E\left\{Q\left(\frac{\sqrt{\mathrm{SNR}\,\boldsymbol{h}(\mathbf{X}_i - \mathbf{X}_j)(\mathbf{X}_i - \mathbf{X}_j)^\dagger \boldsymbol{h}^\dagger}}{2}\right)\right\} \tag{1.6}$$

where

$$Q(x) = \frac{1}{\sqrt{2\pi}} \int_x^\infty \exp\left(\frac{-y^2}{2}\right) dy. \tag{1.7}$$

The matrix $(\mathbf{X}_i - \mathbf{X}_j)(\mathbf{X}_i - \mathbf{X}_j)^\dagger$ is Hermitian, so there is a unitary matrix U for which

$$U(\mathbf{X}_i - \mathbf{X}_j)(\mathbf{X}_i - \mathbf{X}_j)^\dagger U^\dagger = \mathrm{diag}(\lambda_1^2, \cdots, \lambda_{n_t}^2) \tag{1.8}$$

where the entries λ_i are the singular values of $\mathbf{X}_i - \mathbf{X}_j$. The change of basis $\boldsymbol{h} \rightarrow U\boldsymbol{h}$ preserves the Rayleigh distribution of $\boldsymbol{h}$ and if $\lambda_1, \cdots, \lambda_{n_t}$ are nonzero, then

$$\Pr(\mathbf{X}_i \rightarrow \mathbf{X}_j) = \frac{(\mathrm{SNR}/2)^{-n_t}}{\lambda_1^2 \cdots \lambda_{n_t}^2}, \tag{1.9}$$

and the matrix $\mathbf{X}_i - \mathbf{X}_j$ is nonsingular and maximal diversity is achieved. We ean associate the following quantities with a space-time code:

- The *diversity gain* is the minimum of the rank of $\mathbf{X}_i - \mathbf{X}_j$ over all codewords in the code.
- The *coding gain* is the minimum value of the product of the non-zero singular values of $\mathbf{X}_i - \mathbf{X}_j$ over all codewords.

There is a fundamental trade-off between using the multipath to improve throughput by multiplexing and improving reliability through using a space-time code. This ean be quantified using the following definitions of *diversity order* and *multiplexing rate*.

A scheme which has an average error probability $\overline{P}_e(SNR)$ as a funetion of SNR that satisfies

$$\lim_{\mathrm{SNR}\rightarrow\infty} \log \frac{\overline{P}_e(\mathrm{SNR})}{\log \mathrm{SNR}} = -d \tag{1.10}$$

is said to have a *diversity order* of d. In other words, a scheme with diversity order d has an error probability at high SNR that behaves as $\overline{P}_e(SNR) \sim \mathrm{SNR}^{-d}$.

A scheme which has a transmission rate of R(SNR) as a funetion of SNR is said to have a *multiplexing rate* r if

$$\lim_{\mathrm{SNR}\rightarrow\infty} \frac{\log R(\mathrm{SNR})}{\log \mathrm{SNR}} = r. \tag{1.11}$$

In other words, the system has a rate of $r \log \mathrm{SNR}$ at high SNR. There is a trade-off between achievable diversity and multiplexing rate which is expressed in terms of the supremum $d^{\mathrm{opt}}(r)$ of the diversity gain achievable by any scheme with multiplexing rate r. The following theorem is due to Zheng and Tse [13],

Theorem 1 *Let $K = min(n_t, n_r)$ where n_t and n_r are the number of transmit and receive antennas and suppose that the code block length $N > n_t + n_r - 1$. Then the optimal trade-off curve $d^{opt}(r)$ is given by the piecewise linear function connecting points in $(k, d^{opt}(k))$, $k = 0, \cdots, K$ where*

$$d^{opt}(k) = (n_t - k)(n_r - k). \tag{1.12}$$

It implies that high multiplexing rate comes at the price of decreased diversity gain and high diversity gain comes at the price of low multiplexing rate.

We now give a description of some of the most important space-time codes.

1.3.2 Alamouti Code

The most famous space-time block code was discovered by Alamouti [14], and is described by a 2×2 matrix where the columns represent different time slots, the rows represent different antennas, and the entries are the symbols to be transmitted. The Alamouti codeword is represented as

$$\mathbf{X} = \begin{pmatrix} x_1 & x_2 \\ -x_2^* & x_1^* \end{pmatrix}. \tag{1.13}$$

The two rows (or columns) of $\mathbf{X}$ are orthogonal to each other,

$$\mathbf{X}\mathbf{X}^\dagger = (|x_1|^2 + |x_2|^2)\mathbf{I}_2. \tag{1.14}$$

Thus, given two codewords $\mathbf{X}$ and $\mathbf{Y}$ we see that

$$\det(\mathbf{X} - \mathbf{Y})(\mathbf{X} - \mathbf{Y})^\dagger = (|x_1 - y_1|^2 + |x_2 - y_2|^2)^2. \tag{1.15}$$

This means that a subcode of the Alamouti code corresponding to symbol pairs $\boldsymbol{x}_j = (x_{j_1}, x_{j_2}) \in \mathbb{C}^2$, $j = 1, \cdots, N$, has

Diversity gain: 2
Coding gain: $\min_{j,k \in \{1,\cdots,N\}} \|\boldsymbol{x}_j - \boldsymbol{x}_k\|^2$

At the receiver, the signals r_1, r_2 received over two consecutive time slots are given by

$$\begin{pmatrix} r_1 \\ -r_2^* \end{pmatrix} = \begin{pmatrix} h_1 & h_2 \\ -h_2^* & h_1^* \end{pmatrix} \begin{pmatrix} x_1 \\ x_2 \end{pmatrix} + \begin{pmatrix} n_1 \\ n_2 \end{pmatrix} \tag{1.16}$$

where h_1, h_2 are the path gains from the two transmit antennas to the receiver, and the noise samples n_1, n_2 are independent samples of a zero-mean complex Gaussian random variable with variance $2\sigma^2$ per complex dimension. Equation (1.16) can be represented as

$$\boldsymbol{r} = \mathcal{H}\boldsymbol{x} + \boldsymbol{n} \tag{1.17}$$

where the equivalent matrix channel (induced channel) $\mathcal{H}$ is orthogonal i.e. $\mathcal{H}^\dagger\mathcal{H} = \mathbf{I}_2$. Throughout this work we consider the case of coherent detection i.e. the receiver is assumed to have perfect knowledge of the Channel State Information (CSI). In practice CSI can be obtained by introducing some pilot transmissions that enable accurate channel estimation. With $\mathcal{H}$ known, the following processing can be done at the receiver

$$\mathcal{H}^\dagger\boldsymbol{r} = (|h_1|^2 + |h_2|^2)\boldsymbol{x} + \boldsymbol{n}'. \tag{1.18}$$

The new noise term $\boldsymbol{n}'$ is still white, so the ML detection of x_1, x_2 is decoupled.

The Alamouti code provides full diversity at full transmission rate for any real or complex signal constellation, it does not require CSI at the transmitter, and the ML decoding requires only linear complexity processing. For these reasons, the Alamouti code has been adopted in several wireless standards such as WCDMA [15] and CDMA2000 [16]. The Alamouti code also facilitates higher data rates through multiplexing of parallel data streams and the addition of a second antenna at the receiver that performs interference cancellation. Data rates of 4 bits/s/Hz have been demonstrated for several wireless channels including UTMS, GSM, EDGE, IEEE 802.11n and IEEE 802.16 [17]. This scheme is investigated in the next chapter with a view to extending its use to a polarization diverse MIMO systems.

1.3.3 Orthogonal Space-Time Block Codes

The Alamouti code is an example of an *Orthogonal Space-Time Block Code* (OSTBC) for two transmit antennas and its success provided an impetus for investigating the existence of OSTBCs for more than two transmit antennas. OSTBCs are also referred to as *orthogonal designs* (OD) and have the property that ML decoding is linear. At the same time these codes achieve full diversity. In order to describe OSTBCs, first consider an STBC, written in the form of a linear dispersion code (LDC)[18] (note that LDC are discussed in some detail in Section 4.1)

$$\mathbf{X} = \sum_{i=1}^{2T} x_i A_i \tag{1.19}$$

where A_i is a $n_t \times T$ complex matrix and $\{x_i\}_{i=1}^{2T}$ is a set of real scalar symbols.

Definition 1 *A STBC* (1.19) *is an OSTBC if it satisfies the following*

$$\mathbf{X}\mathbf{X}^\dagger = \sum_{i=1}^{2T} x_i^2 \mathcal{D}_i, \tag{1.20}$$

where each $\mathcal{D}_i$ is a diagonal matrix. It follows that

$$\begin{aligned} A_i A_i^\dagger &= \mathcal{D}_i, i = 1, \ldots, 2T \\ A_i A_j^\dagger + A_j A_i^\dagger &= 2\delta_{ij}\mathcal{D}_i, 1 \le i < j \le 2T. \end{aligned} \tag{1.21}$$

Tarokh et al. [19] showed that, in general, full-rate or orthogonal designs exist for all real constellations but only for two, four, or eight transmit antennas, while they exist for all complex constellations only for two transmit antennas (the Alamouti scheme). However, for particular constellations, it might be possible to construct orthogonal designs for other cases. Moreover, if a rate loss is acceptable, orthogonal designs exist for an arbitrary number of transmit antennas [19]. It is also shown by Wang and Xia [20] that the rate of a generalized complex orthogonal design cannot exceed $3/4$ for more than two antennas. An example of the $R = 3/4$ rate code for four transmit antennas is the following:

$$\mathbf{X} = \begin{pmatrix} x_1 & x_2 & x_3 & 0 \\ -x_2^* & x_1^* & 0 & x_3 \\ -x_3^* & 0 & x_1^* & -x_2 \\ 0 & -x_3^* & x_2^* & x_1 \end{pmatrix} \tag{1.22}$$

1.3.4 Quasi-Orthogonal Space-Time Block Codes

As mentioned above, Tarokh et al. [19] showed that full-rate orthogonal designs with complex elements in its transmission matrix are impossible for more than two transmit antennas. This has motivated Jafarkhani [21] to develop a full-rate complex design for four transmit antennas for which pairs of symbols could be decoded independently. This is only possible if one accepts a loss of diversity compared to a true orthogonal design. Jafarkhani called this class of codes quasi-orthogonal space-time block codes (QOSTBC) and introduced the 4×4 code

$$\mathbf{X} = \begin{pmatrix} x_1 & x_2 & x_3 & x_4 \\ -x_2^* & x_1^* & -x_4^* & x_3^* \\ -x_3^* & -x_4^* & x_1^* & x_2^* \\ x_4 & -x_3 & -x_2 & x_1 \end{pmatrix} \tag{1.23}$$

where the structure of the 2×2 blocks mirrors that of the Alamouti code. The columns $\mathbf{X}_i, i = 1, 2, 3, 4$ of the matrix $\mathbf{X}$ divide into two groups $\{\mathbf{X}_1, \mathbf{X}_4\}$ and $\{\mathbf{X}_2, \mathbf{X}_3\}$ with the columns from different groups being orthogonal. Jafarkhani showed that the maximum likelihood decision metric is a sum $f(x_1, x_4) + g(x_2, x_3)$ where f is independent of x_2, x_3 and g is independent of x_1, x_4. The decoder finds the pair (x_1, x_4) that minimizes $f(x_1, x_4)$ and (independently) the pair (x_2, x_3) that minimizes $g(x_2, x_3)$. Thus decoding complexity is quadratic in the size of the signal constellation.

The main issue with QOSTBCs is that they do not have full diversity. However, as we will discuss in Chapter 4 a number of full-rate, full-diversity codes can be constructed by multiplexing quasi-orthogonal STBCs. We show that codes with this type of structure admit fast ML decoding algorithms based on *conditional optimization*. Next we will consider other methods for design of STBCs.

1.4 Design Criteria for Space-Time Block Codes

Under the assumption that perfect channel state information is known at the receiver, Tarokh et al. [10] developed the following two design criteria for the high SNR regime.

- **Rank Criterion:** Maximize the *diversity gain*, i.e. the minimum rank r of the codewords difference $\mathbf{X}_i - \mathbf{X}_j$ over all distinct pairs of space-time codewords $\mathbf{X}_i, \mathbf{X}_j$.
- **Determinant Criterion:** For a given diversity r, maximize the *coding gain*, i.e. the minimum product of the nonzero singular values of the difference $\mathbf{X}_i - \mathbf{X}_j$ over all distinct pairs of space-time codewords $\mathbf{X}_i, \mathbf{X}_j$.

If $r = n_t$ for all pairs $(\mathbf{X}_i, \mathbf{X}_j)$, we say that the code is *full rank*. If $\mathbf{X}$ is full rank, we have

$$\det(\mathbf{A}_{ij}) \neq 0 \quad \text{for all} \quad \mathbf{A}_{ij} \tag{1.24}$$

where $\mathbf{A}_{ij} = (\mathbf{X}_i - \mathbf{X}_j)(\mathbf{X}_i - \mathbf{X}_j)^\dagger$, and we say that the code has *full diversity*. This means that we can exploit all the $n_r n_t$ independent channels available in the MIMO system.

1.5 Algebraic Space-Time Block Codes

In order to increase reliability, STB codes are designed to have full diversity with a large minimum determinant. Such codes can be constructed by looking at matrix representations of

algebraic objects such as Galois fields and cyclic division algebras. In this section, we give descriptions of this class of codes which have become known as *perfect* space-time codes.

An interesting result of our research is that these perfect codes can be seen as multiplexed quasi-orthogonal designs, (see Chapter 3 and Chapter 4), which admit fast ML decoding algorithms. The most important of these codes is the 2×2 MIMO system known as the Golden Code.

1.5.1 The Golden Code

The Golden Code [22] is a 2×2 block space-time code that encodes four complex symbols over two time slots and achieves full diversity. It is known to be the best 2×2 STBC in having the largest coding gain. It achieves a trade off between rate and reliability for both one and two receive antennas that is the best possible in terms of the diversity-multiplexing bound derived by Zheng and Tse [13]. In fact, the Golden Code is incorporated into the IEEE 802.16e (WiMAX) standard [23].

Codewords in the Golden Code take the form

$$\mathbf{X} = \frac{1}{\sqrt{5}} \begin{pmatrix} \alpha & 0 \\ 0 & \bar{\alpha} \end{pmatrix} \begin{pmatrix} x_1 + \tau x_2 & x_3 + \tau x_4 \\ i(x_3 + \mu x_4) & x_1 + \mu x_2 \end{pmatrix}, \tag{1.25}$$

where $\{x\}_{i=1}^{4} \in \mathcal{C} \subset \mathbb{Z}[i]$ are the transmitted symbols, and $\mathcal{C}$ is a signal constellation taken to be 2^m–QAM. The parameters $\tau = (1+\sqrt{5})/2$ and $\mu = (1-\sqrt{5})/2$ are the Golden Ratio. The diagonal matrix $\mathrm{diag}[\alpha, \bar{\alpha}]$, where $\alpha = (1 + i\mu), \bar{\alpha} = (1 + i\tau)$, serves to equalize transmitted signal power across the two transmit antennas. The entries of Golden Code codewords are drawn from $\mathbb{Z}[i][\sqrt{5}] \subset \mathbb{Q}(i, \sqrt{5})$. Note that $\mathbb{Z}[i][\sqrt{5}]$ is the ring of elements of the form $(n_1 + in_2) + (n_3 + in_4)\sqrt{5}, n_i \in \mathbb{Z}$ and $\mathbb{Q}(i, \sqrt{5})$ is the field of elements of the form $(a_1 + ia_2) + (a_3 + ia_4), a_i \in \mathbb{Q}$. Following [24] we rewrite (1.25) as

$$\mathbf{X} = \frac{1}{\sqrt{5}} \begin{pmatrix} \alpha & 0 \\ 0 & \alpha \end{pmatrix} \left[\begin{pmatrix} x_1 & x_3 \\ ix_3 & x_1 \end{pmatrix} + \begin{pmatrix} \tau & 0 \\ 0 & \mu \end{pmatrix} \begin{pmatrix} x_2 & x_4 \\ ix_4 & x_2 \end{pmatrix} \right], \tag{1.26}$$

The set of integer matrices of the form

$$\begin{pmatrix} x & y \\ iy & x \end{pmatrix}, \quad x, y \in \mathbb{Z}[i]. \tag{1.27}$$

forms a matrix representation of the cyclotomic ring $\mathbb{Z}[\zeta_8]$, where ζ_8 is a primitive 8^{th} root of unity. This can be seen explicitly by making the identification

$$\zeta_8 \rightarrow \begin{pmatrix} 0 & 1 \\ i & 0 \end{pmatrix}, \tag{1.28}$$

and for simplicity, we will drop the subscript and write $\zeta = \zeta_8$.

The cyclotomic ring $\mathbb{Z}[\zeta]$ is the ring of algebraic integers in the cyclotomic field $\mathbb{Q}(\zeta)$ and any element of this field can be written in the form

$$\alpha = a_0 + a_1\zeta + a_2\zeta^2 + a_3\zeta^3, \tag{1.29}$$

with $a_0, a_1, a_2, a_3 \in \mathbb{Q}$. The identification (1.28) extends to the matrix representation

$$\alpha \rightarrow A_\alpha = \begin{pmatrix} a_0 + ia_2 & a_1 + ia_3 \\ i(a_1 + ia_3) & a_0 + ia_2 \end{pmatrix}. \tag{1.30}$$

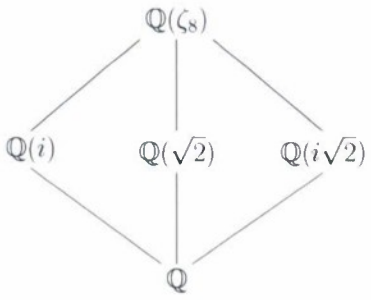

Figure 1.3: The subfield structure of $\mathbb{Q}(\zeta)$

The field $\mathbb{Q}(\zeta)$ is a Galois extension of degree 4 over $\mathbb{Q}$ with $\mathrm{Gal}(\mathbb{Q}(\zeta)/\mathbb{Q}) \cong D_2$, the dihedral group of order 4. There are four field automorphisms, σ_j, j=1, 3, 5, 7, given by

$$\sigma_j(\zeta) = \zeta^j. \tag{1.31}$$

In fact, $\mathrm{Gal}(\mathbb{Q}(\zeta)/\mathbb{Q}) = \langle \sigma_3, \sigma_5 \rangle$. The subfield structure of $\mathbb{Q}(\zeta)$ is shown in Figure 1.3, where we note that $\zeta^2 = i$, $\zeta - \zeta^3 = \sqrt{2}$ and $\zeta + \zeta^3 = i\sqrt{2}$. Given any element $\alpha \in \mathbb{Q}(\zeta)$, the field norm is defined by

$$\begin{aligned} N_{\mathbb{Q}(\zeta)/\mathbb{Q}}(\alpha) &= \prod_{\sigma \in \mathrm{Gal}(\mathbb{Q}(\zeta)/\mathbb{Q})} \sigma(\alpha) \\ &= (a_0^2 + a_2^2)^2 + (a_1^2 + a_3^2)^2 + 4a_1a_3(a_0^2 - a_2^2) + 4a_0a_2(a_3^2 - a_1^2). \end{aligned} \tag{1.32}$$

In terms of the matrix representation (1.30) we see that

$$N_{\mathbb{Q}(\zeta)/\mathbb{Q}}(\alpha) = |\det(A_\alpha)|^2. \tag{1.33}$$

In fact, in terms of the relative norm $N_{\mathbb{Q}(\zeta)/\mathbb{Q}(i)}$, which is defined by,

$$N_{\mathbb{Q}(\zeta)/\mathbb{Q}(i)}(\alpha) = \sigma_1(\alpha)\sigma_5(\alpha), \tag{1.34}$$

we have

$$N_{\mathbb{Q}(\zeta)/\mathbb{Q}(i)}(\alpha) = \det(A_\alpha). \tag{1.35}$$

Another norm on $\mathbb{Q}(\zeta)$ we will find useful is defined by

$$\|\alpha\|^2 = \frac{1}{2}\left(\sigma_1(\alpha)\sigma_7(\alpha) + \sigma_3(\alpha)\sigma_5(\alpha)\right) \tag{1.36}$$

$$= a_0^2 + a_2^2 + a_1^2 + a_3^2 \tag{1.37}$$

$$= \frac{1}{2}\|A_\alpha\|_F^2, \tag{1.38}$$

where $\|\cdot\|_F$ denotes the matrix Frobenius norm.

The Golden Code can be written in the form

$$\mathbf{X} = \frac{1}{\sqrt{5}} B_1 \begin{pmatrix} x_1 & x_3 \\ ix_3 & x_1 \end{pmatrix} + \frac{1}{\sqrt{5}} B_2 \begin{pmatrix} x_2 & x_4 \\ ix_4 & x_2 \end{pmatrix} \tag{1.39}$$

where

$$B_1 = \begin{pmatrix} \alpha & 0 \\ 0 & \overline{\alpha} \end{pmatrix} \quad \text{and} \quad B_2 = -i \begin{pmatrix} \overline{\alpha} & 0 \\ 0 & \alpha \end{pmatrix} \tag{1.40}$$

The matrices B_1 and B_2 satisfy

$$\mathrm{Tr}\left(B_i B_j^{\dagger}\right) = 5\delta_{ij}, \tag{1.41}$$

for $i, j = 1, 2$. A consequence of the structure of the Golden Code is that for any two code words $\mathbf{X}_i$ and $\mathbf{X}_j$ their difference $\mathbf{X}_i - \mathbf{X}_j$ is rank 2 and

$$\det(\mathbf{X}_i - \mathbf{X}_j)(\mathbf{X}_i - \mathbf{X}_j)^{\dagger} \geq 16/25. \tag{1.42}$$

An observation that may potentially lead to fast decoding algorithms for the Golden Code is that the cyclotomic ring $\mathbb{Z}[\zeta] \subset \mathbb{Q}(\zeta)$ is a Euclidean domain with respect to the field norm $N_{\mathbb{Q}(\zeta)/\mathbb{Q}}$. We refer the reader to the survey of cyclotomic Euclidean number fields by Akhtar [25] for more details. The observation that $\mathbb{Q}(\zeta)$ is Euclidean goes back to Eisenstein in 1850. Thus, for any two elements of $a, b \in \mathbb{Z}[\zeta]$ with $b \neq 0$, there exist $q, r \in \mathbb{Z}[\zeta]$ such that

$$a = qb + r, \tag{1.43}$$

with $r = 0$ or $N_{\mathbb{Q}(\zeta)/\mathbb{Q}}(r) < N_{\mathbb{Q}(\zeta)/\mathbb{Q}}(b)$. In fact, we have

$$q = \lfloor a/b \rceil \quad \text{and} \quad r = a - \lfloor a/b \rceil b, \tag{1.44}$$

where for any $\alpha \in \mathbb{Q}(\zeta)$, we define $\lfloor \alpha \rceil \in \mathbb{Z}[\zeta]$ by

$$\lfloor \alpha \rceil = \lfloor a_0 \rceil + \lfloor a_1 \rceil \zeta + \lfloor a_2 \rceil \zeta^2 + \lfloor a_3 \rceil \zeta^3, \tag{1.45}$$

where for $x \in \mathbb{R}$, $\lfloor x \rceil$ denotes the nearest integer to x. The Euclidean algorithm in $\mathbb{Z}[\zeta]$ enables the efficient computation of a greatest common divisor for any pair of cyclotomic integers a, $b \in \mathbb{Z}[\zeta]$. This provides the basis for possible fast decoding schemes based on the extension of an inhomogeneous Diophantine approximation schemes such as Cassel's algorithm [26]. Research in this area is ongoing.

Finally it is interesting to note that the IEEE 802.16e specifications include three MIMO profiles having 2 transmit antennas, from which two are defined as MIMO schemes on both the down-link and up-link transmission of mobile WiMAX systems. The first one is the Alamouti code, which is described in Section 1.3.2, namely, Matrix A, which achieves full transmit diversity at the expense of rate loss. The second one is spatial multiplexing, namely Matrix B, which achieves full rate at the expense of diversity loss. On the other hand, the third MIMO profile with two transmit antennas in IEEE 802.16e specifications, known as Matrix C, is both a full-rate and full-diversity code. More specifically, Matrix C is a variant of the Golden Code.

1.5.2 The Pefect Space-Time Block Codes

One of our aims is the development of polarization-time codes for fully polarimetric MIMO systems. For this application we need codes which have similar properties to the Golden Code but which are appropriate for more than 2 transmit antennas. The *Perfect* space time block codes will turn out to be very good candidates.

Perfect STBCs were first introduced by Oggiere et al. [7] to have full-rate, full-diversity, non-vanishing determinant and to be information lossless. These codes are constructed for

$2 \times 2, 3 \times 3, 4 \times 4$ and 6×6 MIMO systems. An example of a 2×2 perfect STBC is the Golden Code. The following are descriptions of 3×3 and 4×4 perfect STBCs. These are written in a novel form that we have introduced in order to assist in the development of our fast decoding algorithms which are discussed in Chapter 3.

3×3 **Perfect STBC:** The perfect 3×3 STBC transmits nine complex (usually from an $N-$HEX constellation) information symbols $\{x_i\}_{i=1}^{9}$ over three time slots from three transmit antennas. The transmit codewords of the 3×3 perfect STBC can be expressed as

$$\mathbf{X} = \sum_{i=0}^{2} B_{i+1} \begin{pmatrix} x_{3i+1} & x_{3i+2} & x_{3i+3} \\ jx_{3i+3} & x_{3i+1} & x_{3i+2} \\ jx_{3i+2} & jx_{3i+3} & x_{3i+1} \end{pmatrix} \tag{1.46}$$

where the diagonal matrices B_i are

$$\begin{aligned} B_1 &= (1+j)\mathbf{I}_3 + \Theta \\ B_2 &= (-1-2j)\mathbf{I}_3 + j\Theta^2 \\ B_3 &= (-1-2j)\mathbf{I}_3 + (1+j)\Theta + (1+j)\Theta^2 \end{aligned} \tag{1.47}$$

with $\Theta = \mathrm{diag}(\theta_1, \theta_2, \theta_3), \theta_i = 2\cos(2^i\pi/7), j = e^{2\pi i/3}$. The B_i satisfy

$$\mathrm{Tr}(B_j B_m^\dagger) = 7\delta_{jm} \tag{1.48}$$

4×4 **Perfect STBC:** The 4×4 perfect STBC transmits 16 complex ($N-$QAM constellation) information symbols $\{x_i\}_{i=1}^{16}$ over four time slots from four transmit antennas. The codewords can be expressed as

$$\mathbf{X} = \sum_{i=0}^{3} B_{i+1} \begin{pmatrix} x_{4i+1} & x_{4i+2} & x_{4i+3} & x_{4i+4} \\ ix_{4i+4} & x_{4i+1} & x_{4i+2} & x_{4i+3} \\ ix_{4i+3} & ix_{4i+4} & x_{4i+1} & x_{4i+2} \\ ix_{4i+2} & ix_{4i+3} & ix_{4i+4} & x_{4i+1} \end{pmatrix} \tag{1.49}$$

where

$$\begin{aligned} B_1 &= (1-3i)\mathbf{I}_4 + i\Theta^2 \\ B_2 &= (1-3i)\Theta + i\Theta^3 \\ B_3 &= -i\mathbf{I}_4 + (-3+4i)\Theta + (1-i)\Theta^3 \\ B_4 &= (-1+i)\mathbf{I}_4 - 3\Theta + \Theta^2 + \Theta^3 \end{aligned} \tag{1.50}$$

with $\Theta = \mathrm{diag}(\theta_1, \theta_2, \theta_3, \theta_4), \theta_i = 2\cos(2^i\pi/15)$. The B_i satisfy

$$\mathrm{Tr}(B_j B_m^\dagger) = 15\delta_{jm} \tag{1.51}$$

1.5.3 Multiplexed Alamouti Blocks

One approach to high data rates is to multiplex Alamouti blocks where a high rate space-time code might be constructed as a "linear" combination of Alamouti blocks. These codes are 2×2 STBC with full-rate, full-diversity and have the structure that allows fast maximum likelihood decoding which will be discussed in detail in Chapter 3.

Hottinen–Tirkkonen–Kashaev [27, 28]: These authors considered the 2×2 full-rate, full-diversity STBC which has the form

$$\mathbf{X} = \begin{pmatrix} x_1 & -x_2^* \\ x_2 & x_1^* \end{pmatrix} + T \begin{pmatrix} z_1 & -z_2^* \\ z_2 & z_1^* \end{pmatrix} \tag{1.52}$$

where $\{x_i\}_{i=1}^4 \in \mathbb{Z}[i]$,

$$T = \begin{pmatrix} 1 & 0 \\ 0 & -1 \end{pmatrix}, \quad \begin{pmatrix} z_1 \\ z_2 \end{pmatrix} = U \begin{pmatrix} x_3 \\ x_4 \end{pmatrix} \tag{1.53}$$

and

$$U = \frac{1}{\sqrt{7}} \begin{pmatrix} 1+i & -1+2i \\ 1+2i & 1-i \end{pmatrix}, \tag{1.54}$$

which is a unitary matrix. This code is also known as the Silver Code [29].

Sezginer–Sari [30]: Sezginer and Sari proposed a full-rate, full-diversity 2×2 STBC which can be expressed as

$$\mathbf{X} = \begin{pmatrix} ax_1 + bx_3 & -cx_2^* - dx_4^* \\ ax_2 + bx_4 & cx_1^* + dx_3^* \end{pmatrix} \tag{1.55}$$

where a, b, c and d are complex-valued design parameters that are chosen to optimize coding gain. In terms of the transmitted power, Sezginer and Sari have expressed the desired conditions as

$$\begin{aligned} |a|^2 + |b|^2 &= 1 = |c|^2 + |d|^2 \\ |a|^2 + |c|^2 &= 1 = |b|^2 + |d|^2 \end{aligned} \tag{1.56}$$

The first condition ensures an equal transmit power at each symbol time, while the second condition ensures that equal total power is transmitted for each symbol. These conditions imply that all the design parameters should have the same magnitude, i.e.

$$|a| = |b| = |c| = |d| = 1/\sqrt{2} \tag{1.57}$$

Rabiei–Al-Dhahir [31]: These authors have considered a full-rate, full-diversity STBC for 2 transmit antennas which takes the form

$$\mathbf{X} = \begin{pmatrix} \alpha_1 x_1 - \beta_1 x_2^* & \beta_1 x_3^* + \alpha_1 x_4 \\ \alpha_2 x_3 - \beta_2 x_4^* & \beta_2 x_1^* + \alpha_2 x_2 \end{pmatrix} \tag{1.58}$$

where $\alpha_1, \alpha_2, \beta_1$ and β_2 are real design parameters chosen to guarantee that the code is an information lossless STBC and to maximize its coding gain. For this purpose, the following conditions must be satisfied

$$\exists(\alpha_1, \beta_1, \alpha_2, \beta_2) \in \mathbb{R} \quad \text{such that} \begin{cases} \alpha_1^2 + \beta_1^2 & = 1 \\ \alpha_2^2 + \beta_2^2 & = 1 \\ \alpha_1\alpha_2 - \beta_1\beta_2 & = 0 \end{cases} \tag{1.59}$$

1.6 Multiple-Antenna Channel Capacity

One important aspect of the use of STBCs is their effect on the capacity of the communication channel [32, 19, 33, 34]. That is, if we insist on using a particular STBC do we degrade the channel's capacity to carry information. In this section we briefly discussed the mutual information and capacity of a MIMO system which will be useful for later discussion on system performance, particularly for polarimetric channels.

Consider a MIMO Gaussian channel characterized by a fixed $n_r \times n_t$ complex matrix $\mathbf{H} = [h_{ij}]$, where h_{ij} is the complex number representing path gain between transmit antenna i and receive antenna j. At each symbol time, the n_r-dimensional receive signal vector is represented by

$$\boldsymbol{y} = \mathbf{H}\boldsymbol{x} + \boldsymbol{n} \tag{1.60}$$

where $\boldsymbol{x}$ is the n_t-dimensional transmitted vector and the noise $\boldsymbol{n}$ is a Gaussian vector with n_r i.i.d. components. Assuming that the vector $\boldsymbol{x}$ has circularly complex Gaussian distributed components and $\mathbf{H}$ is deterministic, Teletar [2] showed that the mutual information can be expressed as

$$I(\boldsymbol{x}; \boldsymbol{y}|\mathbf{H}) = \log_2 \det\left(\mathbf{I}_{n_r} + \frac{1}{2\sigma^2}\mathbf{H}\mathbf{Q}\mathbf{H}^\dagger\right) \tag{1.61}$$

where $\mathbf{I}_{n_r}$ is the $n_r \times n_r$ identity matrix, σ^2 is the variance per real dimension of the noise $\boldsymbol{n}$ and $\mathbf{Q}$ is the covariance matrix of $\boldsymbol{x}$,

$$\mathbf{Q} = E[\boldsymbol{x}\boldsymbol{x}^\dagger]. \tag{1.62}$$

When $\mathbf{H}$ is known perfectly at the transmitter, then the mutual information can be optimized with water-filling [2, 35] to give the capacity

$$C = \max_{\mathbf{Q}, \mathrm{Tr}(\mathbf{Q}) \leq P_{\boldsymbol{x}}} I(\boldsymbol{x}, \boldsymbol{y}) \tag{1.63}$$

where $P_{\boldsymbol{x}}$ is the maximum power available at the transmitter.

Consider the case where the channel state information, $\mathbf{H}$ is perfectly known only at the receiver. Teletar [2] conjectures that when the channel matrix is random, non-ergodic, then in the high SNR region, the optimal covariance matrix for the source is given by

$$\mathbf{Q}_{\text{opt}} = (P_{\boldsymbol{x}}/n_t)\mathbf{I}_{n_t}. \tag{1.64}$$

The corresponding mutual information is

$$I(\boldsymbol{x}; \boldsymbol{y}) = \log_2 \det\left(\mathbf{I}_{n_r} + \frac{\rho}{n_t}\mathbf{H}\mathbf{H}^\dagger\right) \tag{1.65}$$

where $\rho = P_{\boldsymbol{x}}/2\sigma^2$. The channel capacity is then given by

$$C = E_{\mathbf{H}}\left[\log_2 \det\left(\mathbf{I}_{n_r} + \frac{\rho}{n_t}\mathbf{H}\mathbf{H}^\dagger\right)\right] \tag{1.66}$$

where the expectation E is taken over the possible channel matrices $\mathbf{H}$.

1.6.1 Space-Time Coding and Channel Capacity

Consider a MIMO system with n_t transmit and n_r receive antennas. A space-time code $\mathbf{X}$ represents a STBC codeword to be transmitted from n_t transmit antennas, extending over T time slots. The case $T = 1$ is just spatial multiplexing. The $n_r \times T$ received signal matrix is given by

$$\mathbf{Y} = \sqrt{\frac{\rho}{n_t}}\mathbf{H}\mathbf{X} + \mathbf{W} \tag{1.67}$$

where $\mathbf{W} \in \mathbb{C}^{n_r \times T}$ is the additive white Gaussian noise matrix with entries distributed as $\mathcal{CN}(0, 2\sigma^2)$.

In order to understand the impact of the STBC on channel capacity, a new capacity $\overline{C}$ can be derived with the induced (equivalent) channel matrix. To this end we first rewrite (1.67) as

$$\boldsymbol{y} = \sqrt{\frac{\rho}{n_t}}\mathcal{H}\boldsymbol{x} + \boldsymbol{n} \tag{1.68}$$

where $\boldsymbol{y}$ is the $Tn_r \times 1$ received signal vector and $\boldsymbol{x}$ is a vector of information symbols and $\mathcal{H}$ is an equivalent channel matrix. Then the capacity of the new equivalent channel $\mathcal{H}$ is given by

$$\overline{C} = E_{\mathcal{H}}\left[\frac{1}{T}\log_2 \det\left(\mathbf{I}_{Tn_r} + \frac{\rho}{n_t}\mathcal{H}\mathcal{H}^{\dagger}\right)\right]. \tag{1.69}$$

If $\overline{C} = C$ in equation (1.66) then the STBC $\mathbf{X}$ is described as *information lossless*. An example of an information lossless code is the Alamouti code for a 2×1 MIMO system.

Chapter 2: Bayesian Approach to Interference Cancellation

The famous space-time block code discovered by Alamouti [14] is a remarkable signaling scheme as it allows simple maximum likelihood (ML) decoding. The Alamouti code also facilitates higher data rates through multiplexing of parallel data streams and the addition of a second antenna at the receiver that performs interference cancellation. In this chapter, we consider interference cancellation for multiple Alamouti schemes using a Bayesian approach.

Interference cancellation for two Alamouti users has been studied and analysed previously in [36, 32, 37]. Here we want to be able to extend this two Alamouti scheme to more complex and varied situations and in particular to use it with polarization diverse transmit and receive antennas. Our Bayesian approach provides a unified framework with which to understand the relationship between various signal detection techniques and leads to a new parameter which can be used to predict the performance of the Alamouti scheme system without needing to resort to simulations.

2.1 System Model

The encoding rule for the Alamouti STBC is described by a 2×2 matrix

$$(x_1, x_2) \rightarrow \begin{pmatrix} x_1 & x_2 \\ -x_2^* & x_1^* \end{pmatrix} \tag{2.1}$$

where the rows represent different antennas, the columns represent different time slots, and the entries are the symbols to be transmitted.

Consider two co-channel users, each using the Alamouti code. Let $\boldsymbol{c} = (x_1, x_2)$ and $\boldsymbol{s} = (x_3, x_4)$ be the codewords transmitted by the first and second users respectively; r_{ij} is the signal received at the antenna i at time slot j, and h_{ij} denotes the channel gain from transmit antenna i to the receive antenna j. The received signals at the two receive antennas can be represented as,

$$\begin{aligned}(r_{11}, r_{12}) &= (h_{11}, h_{21}) \begin{pmatrix} x_1 & -x_2^* \\ x_2 & x_1^* \end{pmatrix} + (h_{31}, h_{41}) \begin{pmatrix} x_3 & -x_4^* \\ x_4 & x_3^* \end{pmatrix} + (n_{11}, n_{12}) \\ (r_{21}, r_{22}) &= (h_{12}, h_{22}) \begin{pmatrix} x_1 & -x_2^* \\ x_2 & x_1^* \end{pmatrix} + (h_{32}, h_{42}) \begin{pmatrix} x_3 & -x_4^* \\ x_4 & x_3^* \end{pmatrix} + (n_{21}, n_{22})\end{aligned} \tag{2.2}$$

where the noise samples n_{ij} are independent samples of a complex Gaussian random variable with zero mean and variance $2\sigma^2$. Equation (2.2) can be rewritten as

$$\begin{aligned}\boldsymbol{r}_1 &= \boldsymbol{c}\mathcal{H}_1 + \boldsymbol{s}\mathcal{G}_1 + \boldsymbol{n}_1 \\ \boldsymbol{r}_2 &= \boldsymbol{c}\mathcal{H}_2 + \boldsymbol{s}\mathcal{G}_2 + \boldsymbol{n}_2\end{aligned} \tag{2.3}$$

where $\boldsymbol{r}_1 = (r_{11}, -r_{12}^*), \boldsymbol{r}_2 = (r_{21}, -r_{22}^*)$ and

$$\begin{aligned}\mathcal{H}_1 &= \begin{pmatrix} h_{11} & -h_{21}^* \\ h_{21} & h_{11}^* \end{pmatrix} \quad \mathcal{H}_2 = \begin{pmatrix} h_{31} & -h_{41}^* \\ h_{31} & h_{41}^* \end{pmatrix} \\ \mathcal{G}_1 &= \begin{pmatrix} h_{12} & -h_{22}^* \\ h_{22} & h_{12}^* \end{pmatrix} \quad \mathcal{G}_2 = \begin{pmatrix} h_{32} & -h_{42}^* \\ h_{32} & h_{42}^* \end{pmatrix}.\end{aligned} \tag{2.4}$$

Rewrite (2.3) as

$$\boldsymbol{r} = c\mathcal{H} + s\mathcal{G} + \boldsymbol{n}, \tag{2.5}$$

where

$$\boldsymbol{r} = (\boldsymbol{r}_1\ \boldsymbol{r}_2), \mathcal{H} = (\mathcal{H}_1\ \mathcal{H}_2) \text{ and } \quad \mathcal{G} = (\mathcal{G}_1\ \mathcal{G}_2). \tag{2.6}$$

The problem here is to detect c and s. The challenge is that the solution involves a great deal more computation than the simple Alamouti scheme, particularly for large symbol constellations, due to cross correlation terms in the likelihood function.

The Alamouti code is in fact a matrix representation of the Quaternions. Thus the analysis of multiple Alamouti codes is facilitated by an understanding of the properties of quaternions and quaternion linear algebra. We turn to this now.

2.2 Properties of the Quaternions

The quaternions $\mathbb{H}$ are a non-commutative extension of the complex numbers. A general quaternion can be written as

$$q = q_0 + q_1\boldsymbol{i} + q_2\boldsymbol{j} + q_3\boldsymbol{k} \tag{2.7}$$

where $q_0, q_1, q_2, q_3 \in \mathbb{R}$ and $\boldsymbol{i}$, $\boldsymbol{j}$ and $\boldsymbol{k}$ satisfy the defining relations

$$\boldsymbol{i}^2 = \boldsymbol{j}^2 = \boldsymbol{k}^2 = -1, \tag{2.8}$$

$$\boldsymbol{ijk} = -1. \tag{2.9}$$

The conjugate of a quaternion q is defined as

$$q^* = q_0 - q_1\boldsymbol{i} - q_2\boldsymbol{j} - q_3\boldsymbol{k}. \tag{2.10}$$

The set $\mathbb{H}$ is closed under addition, multiplication, inversion and conjugation. One can compute with the quaternions using these relations just as one does with complex numbers using $i^2 = -1$. The quaternions have a norm defined by

$$\|q\| = \sqrt{q^*q} = \sqrt{q_0^2 + q_1^2 + q_2^2 + q_3^2}. \tag{2.11}$$

We can also define the real part of a quaternion to be $\Re(q) = q_0$ and note that for any quaternion

$$q^* + q = 2\Re(q), \tag{2.12}$$

and

$$q^* = q \iff q = \Re(q). \tag{2.13}$$

There is a faithful representation of $\mathbb{H}$ in terms of 2×2 complex matrices defined by

$$q_0 + q_1\boldsymbol{i} + q_2\boldsymbol{j} + q_3\boldsymbol{k} \to \begin{pmatrix} q_0 + iq_1 & q_2 + iq_3 \\ -q_2^* + iq_3^* & q_0^* - iq_1^* \end{pmatrix}. \tag{2.14}$$

The 2×2 matrix here has the Alamouti space-time block code structure

$$\begin{pmatrix} h_1 & h_2 \\ -h_2^* & h_1^* \end{pmatrix} \tag{2.15}$$

with $h_1 = q_0 + iq_1, h_2 = q_2 + iq_3 \in \mathbb{C}$. Note that in (2.14) we identified the real quaternions q_0 with real multiples of the identity $q_0\mathbf{I}_2$. Furthermore, it can be seen the quaternion conjugation corresponds to Hermitian conjugation for the matrix representation. If H is a matrix of the form (2.15), the quaternion properties (2.11)–(2.13) correspond to:

[Q1] $\|H\|^2 = \frac{1}{2}\mathrm{Tr}(H^\dagger H)$.

[Q2] $H^\dagger H = HH^\dagger = \|H\|^2 \mathbf{I}_2$.

[Q3] $H + H^\dagger = 2\Re(h_1)\mathbf{I}_2$.

[Q4] $H = H^\dagger \iff H = \Re(h_1)\mathbf{I}_2$.

2.3 Properties of Block Quaternion Matrices

Here we consider some properties of vectors and matrices with entries that are quaternions. For example a 2×2 quaternion matrix takes the form

$$S = \begin{pmatrix} s_1 & s_2 \\ s_3 & s_4 \end{pmatrix} \tag{2.16}$$

where $s_1, s_2, s_3, s_4 \in \mathbb{H}$. If such a quaternion matrix is Hermitian symmetric, i.e. $S = S^\dagger$, we refer to S as a quaternion symmetric matrix. Such a matrix has real quaternions on the diagonal.

Theorem 2 *A quaternion symmetric matrix S has the following properties:*

[B1] If $q_1, q_2, \cdots, q_N \in \mathbb{H}$ are quaternions then

$$(q_1^* \;\; q_2^* \;\; \cdots \;\; q_N^*)\, S\, (q_1 \;\; q_2 \cdots \;\; q_N)^T = \alpha, \tag{2.17}$$

for some real quaternion α.

[B2] S has real eigenvalues and complete set of orthonormal quaternion eigenvectors.

[B3] If S is nonsingular then S^{-1} is also a quaternion symmetric matrix.

We note that in the 2×2 matrix representation defined in (2.14) quaternion matrices are complex matrices built from 2×2 quaternion blocks of the form (2.15) and that the real quaternions are real multiples of $\mathbf{I}_2$. Since the represention (2.14) is faithful we can use it to prove algebraic relations (as we do below) which are true for the abstract quaternions.

Proof: Property B1 follows from the fact that the left hand side of (2.17) evaluates to a quaternion α which satisfies $\alpha^* = \alpha$ and so must be real.

Property B2 follows from the fact that S is a complex Hermitian symmetric matrix. Define column vectors $\boldsymbol{h}_1$ and $\boldsymbol{h}_2$ by

$$(\boldsymbol{h}_1, \boldsymbol{h}_2) = (H_1 \;\; H_2 \;\; \ldots \;\; H_N)^T. \tag{2.18}$$

The vectors $\boldsymbol{h}_1$ and $\boldsymbol{h}_2$ are orthogonal and satisfy $\|\boldsymbol{h}_1\| = \|\boldsymbol{h}_2\|$. We then have by Property B1, that the Rayleigh quotient is

$$\frac{\boldsymbol{h}_1^\dagger S \boldsymbol{h}_1}{\boldsymbol{h}_1^\dagger \boldsymbol{h}_1} = \frac{\boldsymbol{h}_2^\dagger S \boldsymbol{h}_2}{\boldsymbol{h}_2^\dagger \boldsymbol{h}_2}. \tag{2.19}$$

Thus, if $\boldsymbol{h}_1$ is an eigenvector of S, then $\boldsymbol{h}_2$ is also an eigenvector corresponding to the same eigenvalue. Overall we can write S as

$$S = \sum_{j=1}^{N} \kappa_j K_j K_j^{\dagger}, \tag{2.20}$$

where the κ_j are the real eigenvalues of S and where the K_j are the corresponding normalized quaternion eigenvectors. The quaternion eigenvectors satisfy $K_j^{\dagger} K_\ell = \delta_{j,\ell} \mathbf{I}_2$. Finally, if S is non-singular, then hy (2.20), S^{-1} is block quaternion symmetric. ■

We note that the relation (2.19) explains the computational "miracle" reported in [36] where the filter that estimates $\boldsymbol{c}$ is independent of the interfering signal $\boldsymbol{s}$.

2.4 Bayesian Detection

The model (2.5) described above implies that the likelihood function of codewords $\boldsymbol{c}$ and $\boldsymbol{s}$ given the received signal $\boldsymbol{r}$ is given hy

$$p(\boldsymbol{r}|\boldsymbol{c}, \boldsymbol{s}) = \frac{1}{\pi^2 \sigma^4} \exp\left(-\frac{1}{2\sigma^2} \left\| \boldsymbol{r} - \boldsymbol{c}\mathcal{H} - \boldsymbol{s}\mathcal{G} \right\|^2 \right). \tag{2.21}$$

Our prior knowledge of symbols x_i is that they are selected from the same constellation $\mathcal{C}$ independently, and that each symbol in $\mathcal{C}$ is transmitted with equal probability. We will also assume that the constellation is centered and normalized so that

$$\begin{aligned} E\{\boldsymbol{c}\} &= 0 \quad \text{and} \quad E\{\boldsymbol{c}^{\dagger}\boldsymbol{c}\} = \mathbf{I}_2, \\ E\{\boldsymbol{s}\} &= 0 \quad \text{and} \quad E\{\boldsymbol{s}^{\dagger}\boldsymbol{s}\} = \mathbf{I}_2. \end{aligned} \tag{2.22}$$

From Bayes' rule the posterior probability of $\boldsymbol{c}$ and $\boldsymbol{s}$ given the received data $\boldsymbol{r}$ is given by

$$\begin{aligned} p(\boldsymbol{c}, \boldsymbol{s}|\boldsymbol{r}) &= \frac{p(\boldsymbol{c})p(\boldsymbol{s})p(\boldsymbol{r}|\boldsymbol{c}, \boldsymbol{s})}{\sum_{\boldsymbol{c},\boldsymbol{s}\in\mathcal{C}^2} p(\boldsymbol{c})p(\boldsymbol{s})p(\boldsymbol{r}|\boldsymbol{c}, \boldsymbol{s})} \\ &= \frac{p(\boldsymbol{r}|\boldsymbol{c}, \boldsymbol{s})}{\sum_{\boldsymbol{c},\boldsymbol{s}\in\mathcal{C}^2} p(\boldsymbol{r}|\boldsymbol{c}, \boldsymbol{s})}. \end{aligned} \tag{2.23}$$

In the Bayesian approach to decision theory we introduce a loss function $L(\boldsymbol{c}, \boldsymbol{s}|\hat{\boldsymbol{c}}, \hat{\boldsymbol{s}})$ which quantifies the loss incurred in deciding the transmitted symbols are $\hat{\boldsymbol{c}}$ and $\hat{\boldsymbol{s}}$ when $\boldsymbol{c}$ and $\boldsymbol{s}$ were transmitted [38]. Bayesian decision theory then seeks to minimize the expected loss

$$\rho(\hat{\boldsymbol{c}}, \hat{\boldsymbol{s}}) = \sum_{\boldsymbol{c},\boldsymbol{s}\in\mathcal{C}^2} L(\boldsymbol{c}, \boldsymbol{s}|\hat{\boldsymbol{c}}, \hat{\boldsymbol{s}}) p(\boldsymbol{c}, \boldsymbol{s}|\boldsymbol{r}). \tag{2.24}$$

If we take L to be the 0-1 loss function

$$L(\boldsymbol{c}, \boldsymbol{s}|\hat{\boldsymbol{c}}, \hat{\boldsymbol{s}}) = \begin{cases} 0, & \text{if } \boldsymbol{c} = \hat{\boldsymbol{c}} \text{ and } \boldsymbol{s} = \hat{\boldsymbol{s}}, \\ 1, & \text{otherwise}, \end{cases} \tag{2.25}$$

then $\rho(\hat{\boldsymbol{c}}, \hat{\boldsymbol{s}})$ is minimized by the maximum *a posteriori* (MAP) estimate

$$(\hat{\boldsymbol{c}}, \hat{\boldsymbol{s}}) = \arg\max_{\boldsymbol{c},\boldsymbol{s}\in\mathcal{C}^2} p(\boldsymbol{c}, \boldsymbol{s}|\boldsymbol{r}), \tag{2.26}$$

and the expected loss is

$$\rho(\hat{\boldsymbol{c}}, \hat{\boldsymbol{s}}) = \sum_{(\boldsymbol{c},\boldsymbol{s}) \neq (\hat{\boldsymbol{c}},\hat{\boldsymbol{s}})} p(\boldsymbol{c}, \boldsymbol{s}|\boldsymbol{r}), \tag{2.27}$$

which is the posterior probability of error. If as we have assumed $p(\boldsymbol{c}) = 1/|\mathcal{C}|^2$ and $p(\boldsymbol{s}) = 1/|\mathcal{C}|^2$, then (2.26) is equivalent to the maximum likelihood estimate

$$(\hat{\boldsymbol{c}}, \hat{\boldsymbol{s}}) = \arg\max_{\boldsymbol{c},\boldsymbol{s} \in \mathcal{C}^2} p(\boldsymbol{r}|\boldsymbol{c}, \boldsymbol{s}). \tag{2.28}$$

Let $\boldsymbol{x} = (\boldsymbol{c}\ \boldsymbol{s})$, $A = (\mathcal{H}\ \mathcal{G})^{\mathrm{T}}$, then from the likelihood function $p(\boldsymbol{r}|\boldsymbol{c}, \boldsymbol{s})$ given in (2.21), we have

$$p(\boldsymbol{r}|\boldsymbol{c}, \boldsymbol{s}) \propto \exp\left(-\frac{1}{2}(\boldsymbol{x} - \tilde{\boldsymbol{x}})R^{-1}(\boldsymbol{x} - \tilde{\boldsymbol{x}})^{\dagger}\right), \tag{2.29}$$

where

$$\tilde{\boldsymbol{x}} = \boldsymbol{r}A^{\dagger}(AA^{\dagger})^{-1}, \tag{2.30}$$

and

$$R^{-1} = \frac{1}{\sigma^2}A^{\dagger}A = \frac{1}{\sigma^2}\begin{pmatrix} \|\mathcal{H}\|^2 \mathbf{I}_2 & \mathcal{H}\mathcal{G}^{\dagger} \\ \mathcal{G}\mathcal{H}^{\dagger} & \|\mathcal{G}\|^2 \mathbf{I}_2 \end{pmatrix}, \tag{2.31}$$

where $\|\cdot\|^2 = \frac{1}{2}\|\cdot\|_F^2$. For a given constellation $\mathcal{C}$, the performance of (2.28) in decoding $\boldsymbol{c}$ and $\boldsymbol{s}$ is determined by the determinant of R^{-1}. We have from [39],

$$\det(R^{-1}) = \frac{\|\mathcal{H}\|^4 \|\mathcal{G}\|^4}{\sigma^8}(1 - |\lambda|^2)^2, \tag{2.32}$$

where

$$\lambda = \frac{\mathcal{H}\mathcal{G}^{\dagger}}{\|\mathcal{H}\| \|\mathcal{G}\|}. \tag{2.33}$$

The parameter λ is an inner product of two unit quaternion vectors, and measures the angle between the desired signal channel vector $\mathcal{H}$ and the interference signal channel vector $\mathcal{G}$. We show in Section 5.3 [40] that this parameter is fundamental in the analysis of detection performance for multiple Alamouti schemes involving polarization.

Clearly, the MAP detector in (2.28) involves a complex search for a large constellation, as $(\boldsymbol{c}, \boldsymbol{s}) \in \mathcal{C}^4$. For example, a 2^4 symbol constellation involves 2^{16} evaluations of the likelihood function. This motivates the development of a number of alternative sub-optimal solutions which we will discuss from a Bayesian perspective.

2.5 Bayesian Interference Cancellation

The motivation behind interference cancellation is that the computation of full MAP/ML detection can be reduced if one of the signals, $\boldsymbol{s}$ say, can be canceled out. We would then only need to search over $\boldsymbol{c} \in \mathcal{C}^2$. This implies that we should attempt to marginalize the joint posterior distribution for $\boldsymbol{c}$ and $\boldsymbol{s}$ with respect to $\boldsymbol{s}$. This leads to

$$p(\boldsymbol{c}|\boldsymbol{r}) \propto \sum_{\boldsymbol{s}_1,\boldsymbol{s}_2 \in \mathcal{C}} p(\boldsymbol{r}|\boldsymbol{c}, \boldsymbol{s}) \tag{2.34}$$

and the MAP decision rule is

$$\hat{\boldsymbol{c}} = \arg\max_{\boldsymbol{c}\in\mathcal{C}^2} p(\boldsymbol{c}|\boldsymbol{r}). \tag{2.35}$$

It is evident that this does not help as the sum over $\boldsymbol{s}$ cannot be evaluated analytically, and so the evaluation of (2.34) requires just as many likelihood function evaluations as (2.26) or (2.28). However, we notice that if the sum in (2.34) were to be replaced by a Gaussian integral the marginalization could be computed analytically. In Bayesian terms, the trick is to forget something that we know in order to reduce computation. Instead of using the fact that $\boldsymbol{s}$ lies in some constellation, we simply recall from (2.22) that

$$E\{\boldsymbol{s}\} = 0 \quad \text{and} \quad E\{\boldsymbol{s}^\dagger \boldsymbol{s}\} = \mathbf{I}_2. \tag{2.36}$$

The prior for $\boldsymbol{s}$ is then taken to be the maximum entropy distribution satisfying the constraints (2.22). This is the Gaussian distribution with zero mean and unit variance, i.e. $p(\boldsymbol{s}) \propto \exp\left(-\frac{\boldsymbol{s}\boldsymbol{s}^\dagger}{2}\right)$. The new prior for $\boldsymbol{s}$ is perfectly consistent with our partial prior knowledge of $\boldsymbol{s}$, it just doesn't represent all that we know. Overall this means we allow some increase in the probability of error in detecting codewords $\boldsymbol{c}$ (and $\boldsymbol{s}$), for reduced computational load. We substitute (2.21) and the prior $p(\boldsymbol{s})$ into (2.26) and marginalize the posterior distribution with respect to $\boldsymbol{s}$ to obtain

$$\begin{aligned} p(\boldsymbol{c}|\boldsymbol{r}) &\propto \int_{\mathbb{C}^2} \exp\left(-\frac{1}{2\sigma^2}\left\|\boldsymbol{r} - \boldsymbol{c}\mathcal{H} - \boldsymbol{s}\mathcal{G}\right\|^2\right) \exp\left(-\frac{\boldsymbol{s}\boldsymbol{s}^\dagger}{2}\right) d\boldsymbol{s} \\ &\propto \exp\left(-\frac{1}{2}(\boldsymbol{c} - \tilde{\boldsymbol{c}})\mathcal{H}R^{-1}\mathcal{H}^\dagger(\boldsymbol{c} - \tilde{\boldsymbol{c}})^\dagger\right) \end{aligned} \tag{2.37}$$

where

$$R^{-1} = \frac{\mathbf{I}_4}{\sigma^2} - \frac{\mathcal{G}^\dagger\mathcal{G}}{\sigma^2(\|\mathcal{G}\|^2 + \sigma^2)}, \tag{2.38}$$

and

$$\tilde{\boldsymbol{c}} = \boldsymbol{r}R^{-1}\mathcal{H}^\dagger(\mathcal{H}R^{-1}\mathcal{H}^\dagger)^{-1}, \tag{2.39}$$

and we have dropped terms independent of $\boldsymbol{c}$.

Since R^{-1} is a quaternion symmetric matrix, we have from Theorem 2,

$$\mathcal{H}R^{-1}\mathcal{H}^\dagger = \beta^2\mathbf{I}_2, \tag{2.40}$$

where β^2 is real and positive. This is the projection of interference plus noise onto the signal subspace. Substituting (2.40) into (2.37) we obtain two independent maximization problems for decoding symbols x_1 and x_2 as

$$p(\boldsymbol{c}|\boldsymbol{r}) \propto \exp\left(-\frac{\beta_c^2}{2}|x_1 - \tilde{x}_1|^2 - \frac{\beta_c^2}{2}|x_2 - \tilde{x}_2|^2\right), \tag{2.41}$$

where

$$\tilde{\boldsymbol{c}} = \frac{1}{\beta_c^2}\boldsymbol{r}R^{-1}\mathcal{H}^\dagger, \tag{2.42}$$

and

$$\beta_c^2 = \frac{\|\mathcal{H}\|^2}{\sigma^2}\left(1 - \frac{|\lambda|^2}{1+\sigma^2/\|\mathcal{G}\|^2}\right). \tag{2.43}$$

This captures the solution obtained in [36], [32], and will be called the IC solution for convenience. Note that if $\mathcal{G} = 0$, then the performance described by (2.43) will be reduced to the performance of a single STBC user with 2 receive antennas, that is

$$\beta_{\text{ISTBC}}^2 = \frac{\|\mathcal{H}\|^2}{\sigma^2} = \frac{\|\mathcal{H}_1\|^2}{\sigma^2} + \frac{\|\mathcal{H}_2\|^2}{\sigma^2}. \tag{2.44}$$

If either $\mathcal{H}_1 = 0$ or $\mathcal{H}_2 = 0$ then we obtain the performance of a single STBC user with one receive antenna.

Assuming that symbols $\boldsymbol{c}$ from the first terminal have been decoded correctly, the receiver then cancels the contribution of the first terminal in the received signal vector $\boldsymbol{r}$. The receiver decodes symbol $\boldsymbol{s}$ by applying MAP decoding (2.28) to the received signal vector after canceling signals from the first terminal. This gives

$$p(\boldsymbol{s}|\boldsymbol{r}') \propto \exp\left(-\frac{\beta_s^2}{2}|x_3 - \tilde{x}_3|^2 - \frac{\beta_s^2}{2}|x_4 - \tilde{x}_4|^2\right), \tag{2.45}$$

where

$$\boldsymbol{r}' = \boldsymbol{r} - \boldsymbol{c}\mathcal{H}, \quad (\tilde{x}_3, \tilde{x}_4) = \frac{1}{\|\mathcal{G}\|^2}\boldsymbol{r}'\mathcal{G}^\dagger \quad \text{and} \quad \beta_s^2 = \frac{\|\mathcal{G}\|^2}{\sigma^2}. \tag{2.46}$$

Assuming that the symbols x_1 and x_2 have been decoded correctly, we can see from (2.46) that the performance for the decoded symbols $\boldsymbol{s}$ is equivalent to that of 1 user with 2 transmit and 2 receive antennas as previously noted in [32]. The performance for decoding symbols $\boldsymbol{c}$ and $\boldsymbol{s}$ is given by

$$\beta_{\text{IC1}}^2 = \frac{\|\mathcal{H}\|^4\|\mathcal{G}\|^4}{\sigma^8}\left(1 - \frac{|\lambda|^2}{1+\sigma^2/\|\mathcal{G}\|^2}\right)^2. \tag{2.47}$$

At this point we note that it is clearly advantageous to have chosen to cancel the Alamouti channel with the lower SNR. Thus, if $\|\mathcal{G}\| > \|\mathcal{H}\|$, we would exchange the roles of $\mathcal{H}$ and $\mathcal{G}$ in the above algorithm and analysis. We further note that x_1 and x_2 are assumed to have been decoded correctly, therefore (2.47) provides an upper bound for the performance of the IC solutions.

Alternatively, symbols $\boldsymbol{s}$ could be decoded in a similar fashion to the decoding of symbols $\boldsymbol{c}$. In this case the posterior probability for $\boldsymbol{s}$ given $\boldsymbol{r}$ becomes

$$p(\boldsymbol{s}|\boldsymbol{r}) \propto \exp\left(-\frac{\beta_s^2}{2}|x_3 - \tilde{x}_3|^2 - \frac{\beta_s^2}{2}|x_4 - \tilde{x}_4|^2\right), \tag{2.48}$$

where

$$\tilde{\boldsymbol{s}} = \frac{1}{\beta_s^2}\boldsymbol{r}R^{-1}\mathcal{G}^\dagger, \tag{2.49}$$

$$\beta_s^2 = \frac{\|\mathcal{G}\|^2}{\sigma^2}\left(1 - \frac{|\lambda|^2}{1+\sigma^2/\|\mathcal{H}\|^2}\right), \tag{2.50}$$

and

$$R^{-1} = \frac{\mathbf{I}_4}{\sigma^2} - \frac{\mathcal{H}^\dagger\mathcal{H}}{\sigma^2(\|\mathcal{H}\|^2 + \sigma^2)}. \tag{2.51}$$

The performanee is then given by

$$\beta_{\mathrm{IC2}}^2 = \frac{\|\mathcal{H}\|^4 \|\mathcal{G}\|^4}{\sigma^8} \left(1 - \frac{|\lambda|^2}{1+\sigma^2/\|\mathcal{G}\|^2}\right)^2 \left(1 - \frac{|\lambda|^2}{1+\sigma^2/\|\mathcal{H}\|^2}\right)^2. \tag{2.52}$$

2.6 The Zero-Forcing Decoder

Naguib and Seshadri [37] show that if

$$W = \begin{pmatrix} \mathbf{I}_2 & -\mathcal{G}_1\mathcal{G}_2^{-1} \\ -\mathcal{H}_2\mathcal{H}_1^{-1} & \mathbf{I}_2 \end{pmatrix}, \tag{2.53}$$

then

$$W \begin{pmatrix} \boldsymbol{r}_1 \\ \boldsymbol{r}_2 \end{pmatrix} = \begin{pmatrix} \boldsymbol{r}_1' \\ \boldsymbol{r}_2' \end{pmatrix} = \begin{pmatrix} \mathcal{H}' & 0 \\ 0 & \mathcal{G}' \end{pmatrix} \begin{pmatrix} \boldsymbol{c} \\ \boldsymbol{s} \end{pmatrix} + \begin{pmatrix} \boldsymbol{n}_1' \\ \boldsymbol{n}_2' \end{pmatrix}, \tag{2.54}$$

where

$$\mathcal{H}' = \mathcal{H}_1 - \mathcal{G}_1\mathcal{G}_2^{-1}\mathcal{H}_2 \quad \text{and} \quad \mathcal{G}' = \mathcal{G}_2 - \mathcal{H}_2\mathcal{H}_1^{-1}\mathcal{G}_1. \tag{2.55}$$

The matrix W transforms the problem of joint deteetion of two co-channel users into separate deteetion of two individual spaee-time users. Furthermore, the algebraie strueture of the bloek spaee-time code (elosure under addition, multiplieation and taking inverses) implies that the matriees $\mathcal{H}'$ and $\mathcal{G}'$ have the same strueture as the matriees $\mathcal{H}_1, \mathcal{H}_2, \mathcal{G}_1$ and $\mathcal{G}_2$. Now the new noise veetors $\boldsymbol{n}_1'$ and $\boldsymbol{n}_2'$ are eorrelated, and if we take these eorrelations into account and design the optimal deteetor we would just be back to (2.26). The key to reducing eomputation is to again forget something that we know. In this ease we forget that the noise veetors $\boldsymbol{n}_1'$ and $\boldsymbol{n}_2'$ are eorrelated and replaee the joint distribution of $\boldsymbol{n}_1'$ and $\boldsymbol{n}_2'$ by the higher entropy produet of marginals.

This reduces the problem of joint deteetion of codewords $\boldsymbol{c}$ and $\boldsymbol{s}$ to four independent maximization problems. That is we have the likelihood of the codewords given the reeeived signal

$$p(\boldsymbol{r}_1'|\boldsymbol{c}) \propto \exp\left(-\frac{\beta_c^2}{2}|x_1 - \tilde{x}_1|^2 - \frac{\beta_c^2}{2}|x_2 - \tilde{x}_2|^2\right), \tag{2.56}$$

$$p(\boldsymbol{r}_2'|\boldsymbol{s}) \propto \exp\left(-\frac{\beta_s^2}{2}|x_3 - \tilde{x}_3|^2 - \frac{\beta_s^2}{2}|x_4 - \tilde{x}_4|^2\right), \tag{2.57}$$

where

$$(\tilde{\boldsymbol{c}}, \tilde{\boldsymbol{s}}) = \left(\frac{\boldsymbol{r}_1'\mathcal{H}'^{\dagger}}{\|\mathcal{H}\|^2(1-|\lambda|^2)}, \frac{\boldsymbol{r}_2'\mathcal{G}'^{\dagger}}{\|\mathcal{G}\|^2(1-|\lambda|^2)}\right), \tag{2.58}$$

with

$$\beta_c^2 = \frac{\|\mathcal{H}\|^2(1-|\lambda|^2)}{\sigma^2} \quad \text{and} \quad \beta_s^2 = \frac{\|\mathcal{G}\|^2(1-|\lambda|^2)}{\sigma^2}. \tag{2.59}$$

The performanee of the zero-forcing deeoder for symbols $\boldsymbol{c}$ and $\boldsymbol{s}$ is given by

$$\beta_{\mathrm{ZF}}^2 = \frac{\|\mathcal{H}\|^4 \|\mathcal{G}\|^4}{\sigma^8}(1-|\lambda|^2)^4. \tag{2.60}$$

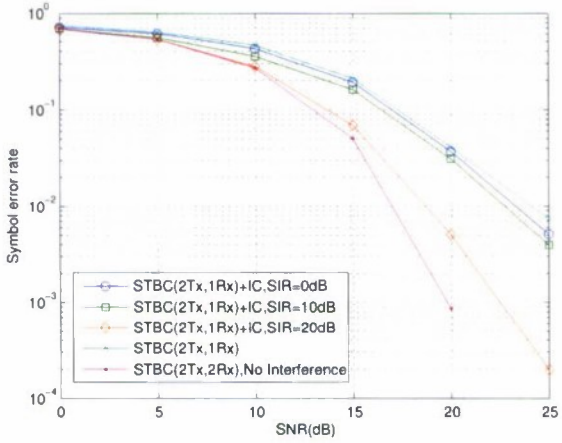

Figure 2.1: Behaviour of IC for two users of Alamouti code, at different SINR

2.7 Performance Analysis

First note that the expressions in (2.32), (2.47), (2.52) and (2.60) give the effective SNR when estimating $\boldsymbol{c}$ and $\boldsymbol{s}$. This effective SNR includes both noise and interference. Now consider the performance expression described in (2.43) or (2.50), if the power of the interfering path is small i.e. if $\|\mathcal{G}\|^2 \to 0$ then $\beta^2 \to \|\mathcal{H}\|^2/\sigma^2$. That is, the performance improves as the interference power decreases and converges to that of a single space-time user and a receiver with two antennas [36]. Figure 2.1 shows the simulation results which demonstrate this behavior.

To compare the performance of the three different solutions, we first determine the effective SNR of a symbol for each method by taking a fourth order root in (2.32),(2.60) and (2.52), to obtain

$$\mathrm{SNR}_{\mathrm{MAP}} = \frac{\|\mathcal{H}\|\,\|\mathcal{G}\|}{\sigma^2}\sqrt{1-|\lambda|^2}, \tag{2.61}$$

$$\mathrm{SNR}_{\mathrm{ZF}} = \frac{\|\mathcal{H}\|\,\|\mathcal{G}\|}{\sigma^2}(1-|\lambda|^2), \tag{2.62}$$

$$\mathrm{SNR}_{\mathrm{IC}} = \frac{\|\mathcal{H}\|\,\|\mathcal{G}\|}{\sigma^2}\sqrt{\left(1-\frac{|\lambda|^2}{1+\sigma^2/\|\mathcal{G}\|^2}\right)\left(1-\frac{|\lambda|^2}{1+\sigma^2/\|\mathcal{H}\|^2}\right)}. \tag{2.63}$$

If the channels $\mathcal{H}$ and $\mathcal{G}$ are orthogonal i.e. $|\lambda|^2 = 0$ then there is no difference in the performance of the three solutions. From (2.61)-(2.63), it is clear that when $|\lambda|^2 \neq 0$, the maximum likelihood solution outperforms the zero-forcing and IC solutions. Furthermore, the performance gap (the ratio or difference in dB for a given error rate) between zero-forcing , IC

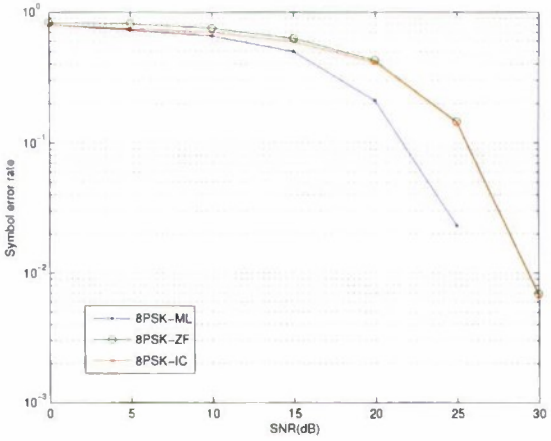

Figure 2.2: Performance comparison of the three different detection algorithms for two users of Alamouti code

solution and maximum likelihood solution can be explicitly described as follows:

$$\frac{\mathrm{SNR}_{\mathrm{ZF}}}{\mathrm{SNR}_{\mathrm{MAP}}} = \sqrt{1-|\lambda|^2}, \tag{2.64}$$

$$\frac{\mathrm{SNR}_{\mathrm{IC}}}{\mathrm{SNR}_{\mathrm{MAP}}} = \sqrt{\frac{\left(1-\frac{|\lambda|^2}{1+\sigma^2/\|\mathcal{G}\|^2}\right)\left(1-\frac{|\lambda|^2}{1+\sigma^2/\|\mathcal{H}\|^2}\right)}{(1-|\lambda|^2)}}. \tag{2.65}$$

Figure 2.2 shows the simulation results of interference cancellation for two co-channel users, each using the Alamouti scheme with 8PSK modulation comparing the three different solutions. The channels $\mathcal{H}$ and $\mathcal{G}$ are taken to have the channel separation $|\lambda|^2 = 0.8$ with a tolerance of 0.05, or in other words, the angle between the two channels is $\approx 37°$. In order to show that the performance expressions obtained above are valid, Figure 2.3 shows the result of shifting the zero-forcing and IC solutions shown in Figure 2.2 by the performance gap given in (2.64) and (2.65) respectively. As shown all curves are now aligned.

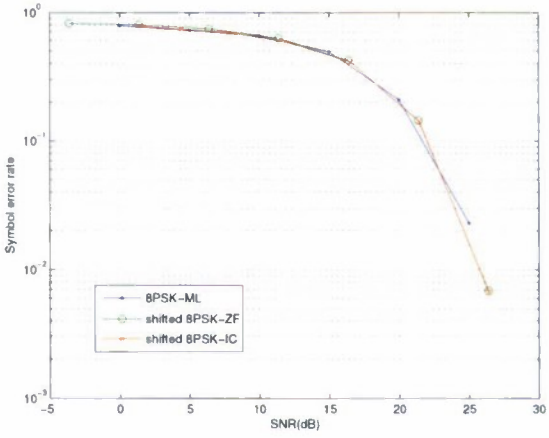

Figure 2.3: Performance of the three different detection algorithms agree after the SNR is shifted by the differences given in (2.64) *and* (2.65)

2.8 Generalization to N Alamouti Users

We now extend the analysis of Section 2 to detection of N co-channel users using N receive antennas, where eaeh user employs the Alamouti STBC. The generalization of (2.5) is straightforward, and the reeeived signal ean be written as

$$\boldsymbol{r} = \sum_{n=1}^{N} \boldsymbol{x}_n \mathsf{G}_n + \boldsymbol{n} \tag{2.66}$$

where $\mathsf{G}_n = (\mathcal{G}_{n,1}, \mathcal{G}_{n,2}, \cdots, \mathcal{G}_{n,N})$ are the channel matrices from user n to reeeiver antennas $1, 2, \cdots, N$ and $\boldsymbol{x}_n = (x_{n,1}\ x_{n,2})$ is the codeword transmitted by user n.

2.8.1 MAP/ML Detection

Let $\boldsymbol{x} = (\boldsymbol{x}_1, \boldsymbol{x}_2, \cdots, \boldsymbol{x}_N)$ and $A = (\mathsf{G}_1, \mathsf{G}_2, \cdots, \mathsf{G}_N)^{\mathrm{T}}$ then the posterior distribution $p(\boldsymbol{x}_1, \cdots, \boldsymbol{x}_N | \boldsymbol{r})$ is given by

$$p(\boldsymbol{x}_1, \cdots, \boldsymbol{x}_N | \boldsymbol{r}) \propto \exp\left(-(\boldsymbol{x} - \tilde{\boldsymbol{x}}) R^{-1} (\boldsymbol{x} - \tilde{\boldsymbol{x}})^{\dagger}\right), \tag{2.67}$$

where $R^{-1} = AA^{\dagger}$ and is obtained by

$$R^{-1} = \frac{1}{2\sigma^2} \begin{pmatrix} \|\mathsf{G}_1\|^2 \mathbf{I}_2 & \mathsf{G}_1 \mathsf{G}_2^{\dagger} & \cdots & \mathsf{G}_1 \mathsf{G}_N^{\dagger} \\ \mathsf{G}_2 \mathsf{G}_1^{\dagger} & \|\mathsf{G}_2\|^2 \mathbf{I}_2 & \cdots & \mathsf{G}_2 \mathsf{G}_N^{\dagger} \\ \vdots & \vdots & & \vdots \\ \mathsf{G}_N \mathsf{G}_1^{\dagger} & \mathsf{G}_N \mathsf{G}_2^{\dagger} & \cdots & \|\mathsf{G}_N\|^2 \mathbf{I}_2 \end{pmatrix}. \tag{2.68}$$

The performance of the MAP/ML detector is determined by

$$\beta_{ML}^2 = \det R^{-1} = \frac{\|\mathsf{G}_1\|^4 \|\mathsf{G}_2\|^4 \cdots \|\mathsf{G}_N\|^4}{\sigma^{4N}} V^2, \tag{2.69}$$

where

$$V^2 = \det \begin{pmatrix} \mathbf{I}_2 & \lambda_{1,2} & \cdots & \lambda_{1,N} \\ \lambda_{1,2}^\dagger & \mathbf{I}_2 & \cdots & \lambda_{2,N} \\ \vdots & \vdots & & \vdots \\ \lambda_{1,N}^\dagger & \lambda_{2,N}^\dagger & \cdots & \mathbf{I}_2 \end{pmatrix}, \tag{2.70}$$

with

$$\lambda_{m,n} = \frac{\mathsf{G}_m \mathsf{G}_n^\dagger}{\|\mathsf{G}_m\| \|\mathsf{G}_n\|}. \tag{2.71}$$

Writing $(\boldsymbol{g}_{n,1}, \boldsymbol{g}_{n,2}) = \mathsf{G}_n / \|\mathsf{G}_n\|$ we see that the quantity V is the volume of the parallelotope generated by the complex vectors $\{\boldsymbol{g}_{n,1}, \boldsymbol{g}_{n,2} | n = 1, \cdots, N\}$. It is a function of the pairwise quaternion angles between the users. Since the vectors $\boldsymbol{g}_{n,1}$ are normalized, $0 \leq V \leq 1$. We refer to V as the normalized channel volume. In terms of V, we can define the signal to noise ratio per user symbol as the $(2N)^{\text{th}}$-root of (2.69), that is,

$$\mathrm{SNR}_{ML} = \mathcal{G}\left(\mathrm{SNR}_1, \mathrm{SNR}_2, \cdots, \mathrm{SNR}_N\right) V^{1/N}, \tag{2.72}$$

where $\mathrm{SNR}_n = \|\mathsf{G}_n\|^2 / \sigma^2$, is the SNR of the n^{th} user and $\mathcal{G}$ denotes the geometric mean. For the two user case described in Section 2.5, the normalized channel volume $V = 1 - |\lambda|^2$.

2.8.2 Bayesian Interference Cancellation

Bayesian interference cancellation in the N user case is analogous to the two user case, although it becomes tedious to marginalize the posterior probability $p(\boldsymbol{x}_1, \boldsymbol{x}_2, \cdots, \boldsymbol{x}_N | \boldsymbol{r})$ with respect to $\boldsymbol{x}$ because of the multiple integrations. However, since we assume the prior distribution for $\boldsymbol{x}_2, \boldsymbol{x}_3, \cdots, \boldsymbol{x}_N$ to be Gaussian with zero mean and unit variance, we have

$$\left(\sum_{n=2}^{N} s_n \mathsf{G}_n + \boldsymbol{n} \right) \sim \mathcal{N}(0, R), \tag{2.73}$$

where

$$R = \sigma^2 \mathbf{I}_{2N} + \sum_{n=2}^{N} \mathsf{G}_n^\dagger \mathsf{G}_n. \tag{2.74}$$

Thus, we can write down the posterior distribution $p(\boldsymbol{x}_1 | \boldsymbol{r})$ directly as

$$p(\boldsymbol{x}_1 | \boldsymbol{r}) \propto \exp\left(-\frac{\beta^2}{2} |x_{1,1} - \tilde{x}_{1,1}|^2 - \frac{\beta^2}{2} |x_{1,2} - \tilde{x}_{1,2}|^2 \right) \tag{2.75}$$

where

$$\tilde{\boldsymbol{s}}_1 = \frac{1}{\beta^2} \boldsymbol{r} R^{-1} \mathsf{G}_1^\dagger, \tag{2.76}$$

and β will be computed below. Note that the reduced MAP decoding now consists of two independent maximization problems for decoding symbols $s_{1,1}$ and $s_{1,2}$.

In order to judge the performance of this reduced MAP decoding scheme we expand the positive semi-definite block quaternion symmetric covariance matrix R' given by

$$R' = \sum_{n=2}^{N} \mathsf{G}_n^{\dagger} \mathsf{G}_n \tag{2.77}$$

in terms of its block quaternion eigenveetors, (See Appendix), so that

$$R = \sigma^2 \mathbf{I}_{2N} + \sum_{n=2}^{N} \mathsf{K}_n^{\dagger} \mathsf{K}_n, \tag{2.78}$$

where $\mathsf{K}_n^{\dagger} \mathsf{K}_j = 0$, if $n \neq j$, and we have normalized the eigenvectors K_n so that $\|K_n\|^2 = \kappa_n$, their corresponding eigenvalues. In general some of the κ_j could be zero and so they would not contribute. Thus, we have replaced the Alamouti signaling interferers G_n hy an equivalent set of mutually orthogonal Alamouti signaling interferers K_n. Interference caneellation ean now be analyzed in terms of these equivalent interferers.

Applying the Matrix Inversion Lemma [41], the inverse of R is seen to be

$$R^{-1} = \frac{1}{\sigma^2} \mathbf{I}_{2N} - \frac{1}{\sigma^2} \sum_{n=2}^{N} \frac{\mathsf{K}_n \mathsf{K}_n^{\dagger}}{\|\mathsf{K}_n\|^2 + \sigma^2}, \tag{2.79}$$

and so we have

$$\beta^2 = \frac{\|\mathsf{G}_1\|^2}{\sigma^2} \left(1 - \sum_{n=2}^{N} \frac{|\lambda_n|^2}{1 + \sigma^2 / \|\mathsf{K}_n\|^2} \right), \tag{2.80}$$

where

$$\lambda_n = \frac{\mathsf{G}_1 \mathsf{K}_n^{\dagger}}{\|\mathsf{G}_1\| \, \|\mathsf{K}_n\|}. \tag{2.81}$$

$|\lambda_n|^2$ measures the angle hetween the desired signal channel G_1 and the n^{th} equivalent interferer channel K_n.

As with the IC algorithm described in Section 2.5, interference caneellation is first carried out to separate the user G_j with the highest signal to noise ratio. The transmitted symhols for this user are estimated (detected) and then substituted in (2.66) to ohtain

$$\boldsymbol{r}' = \boldsymbol{r} - \hat{\boldsymbol{s}}_j \mathsf{G}_j = \sum_{\substack{n=1 \\ n \neq j}}^{N} \boldsymbol{s}_n \mathsf{G}_n + \boldsymbol{n}. \tag{2.82}$$

The above procedure is then repeated with the Alamouti channel having the next highest SNR and so on. This algorithm is the counterpart of Foschini's scheme [42] for space-time multiplexing one dimensional signals. Here we are multiplexing 2×2 matrix signals.

2.9 Summary

Our Bayesian analysis of interference cancellation provides a unified framework with which to understand the relationship between various techniques for signal detection. We ohtained simple new results for performance analysis in terms of SNR. The analysis also leads to a

new parameter which measures the angle between a pair of block quaternion channel vectors. This parameter provides new theoretical insight to understanding and being able to predict the performance of different decoding algorithms as a function of signal to noise ratio. In Chapter 5 we apply this parameter to analyse the performance of various coding schemes for dual polarimetric antennas.

Chapter 3: Conditional Optimization and Fast Decoding Algorithms for Space-Time Block Codes

The drawback of the full-rate full-diversity STBCs listed in Section 1.5 is the decoding complexity. The sphere decoder was developed [43, 44, 45] to reduce the computational complexity by limiting the search to only within a sphere of given radius. However, the initial radius of the sphere depends on the signal-to-noise ratio and the channel condition number. When the channel matrix is close to singular, the preprocessing stage of the sphere decoding algorithm yields a plane of possibilities rather than a single initial estimate. When this occurs, the lattice point search degenerates to an exhaustive search, and consequently the overall complexity of the sphere decoder is no better than the exhaustive search. In wireless communication, when the channel between base station and terminal is line-of-sight, the induced channel is rank 1. This has motivated us to develop fast decoding algorithms for a number of important codes which have fixed low complexity across channel conditions, i.e. across propagation conditions from pure line-of-sight to rich scattering environments.

Our fast decoding algorithms are based on a technique called conditional optimization. This technique is used widely in statistical estimation and signal processing to reduce the search space of an optimization problem by taking advantage of the possibility of analytically optimising over some subset of the parameters conditioned on the remaining parameters. The approach is applied to a large class of full-rate, full-diversity space-time block codes. This approach can also be applied in an approximate form to the Golden Code and perfect space-time block codes to obtain essentially ML performance with reduced complexity [46, 47] compared to exact ML decoding.

3.1 Two Users of Alamouti Signaling

In Chapter 2 we considered an interference cancellation approach to the detection of two users of Alamouti codes, which provides linear complexity processing with a corresponding trade-off in performance. We show here that such systems have the structure that allows fast ML decoding with complexity $\mathcal{O}(N^2)$, where N is the size of the underlying constellation.

From (2.3), the received signal for a two Alamouti user system is given by

$$\begin{aligned} \boldsymbol{r}_1 &= \boldsymbol{c}\mathcal{H}_1 + \boldsymbol{s}\mathcal{G}_1 + \boldsymbol{n}_1 \\ \boldsymbol{r}_2 &= \boldsymbol{c}\mathcal{H}_2 + \boldsymbol{s}\mathcal{G}_2 + \boldsymbol{n}_2 \end{aligned} \tag{3.1}$$

where $\boldsymbol{c} = (x_1, x_2)$, $\boldsymbol{s} = (x_3, x_4)$,

$$\begin{aligned} \mathcal{H}_1 &= \begin{pmatrix} h_{11} & -h_{21}^* \\ h_{21} & h_{11}^* \end{pmatrix}, \quad \mathcal{G}_1 = \begin{pmatrix} h_{31} & -h_{41}^* \\ h_{41} & h_{31}^* \end{pmatrix}, \\ \mathcal{H}_2 &= \begin{pmatrix} h_{12} & -h_{22}^* \\ h_{22} & h_{12}^* \end{pmatrix}, \quad \mathcal{G}_2 = \begin{pmatrix} h_{32} & -h_{42}^* \\ h_{42} & h_{32}^* \end{pmatrix}. \end{aligned} \tag{3.2}$$

Interference cancellation as described in Chapter 2 is a suboptimal approach with linear complexity, [48, 37]. Here we show that two-user ML detection of Alamouti signals is possible with complexity $\mathcal{O}(N^2)$.

3.2 Code Multiplexed Alamouti Blocks

An approach to constructing high data rate codes is to multiplex existing codes. For example, a high rate space-time code might be constructed as a "linear" combination of Alamouti blocks [27, 30, 31, 49] of the general form

$$\mathbf{X} = \begin{pmatrix} x_1 & -x_2^* \\ x_2 & x_1^* \end{pmatrix} + \Lambda \begin{pmatrix} x_3 & -x_4^* \\ x_4 & x_3^* \end{pmatrix}, \tag{3.3}$$

where the matrix

$$\Lambda = \begin{pmatrix} \varphi_1 & \varphi_3 \\ \varphi_2 & \varphi_4 \end{pmatrix}$$

is usually taken to be a unitary matrix [50]. This restriction on Λ leads to code properties such as cubic shaping and information losslessness (see [7] for details on cubic shaping). However, we note our fast decoding algorithms do not depend on this property and will work for arbitrary non-singular Λ.

Remark 1 *If Λ is a unitary matrix of the form*

$$\Lambda = \begin{pmatrix} \varphi_1 & -\varphi_2^* \\ \varphi_2 & \varphi_1^* \end{pmatrix} \tag{3.4}$$

then (3.3) *reduces to Alamouti signaling with a non-standard constellation and decoding is essentially linear in complexity. One example is Alamouti signaling with 16-QAM viewed as a multiplexing of Alamouti blocks employing 4-QAM. However a disadvantage of this construction is that the value of adding a second receive antenna does not extend beyond noise averaging, in contrast to codes such as the Golden Code where it provides additional diversity gain.*

A number of codes proposed in the literature are of this multiplexed form. We discuss these examples in turn.

Hottinen–Tirkkonen–Kashaev [49, 27] These authors considered the family of 2×2 full-rate, full-diversity STBCs as described in (1.52). This code can be expressed in the form of (3.3) with

$$\Lambda = \frac{1}{\sqrt{7}} \begin{pmatrix} 1+i & -1+2i \\ -1-2i & -1+i \end{pmatrix}. \tag{3.5}$$

At the receiver, the received signal is represented as in (3.1) where $\mathcal{H}_1, \mathcal{H}_2$ are matrices as defined in (3.2), and

$$\mathcal{G}_1 = \begin{pmatrix} g_{11} & -g_{21}^* \\ g_{21} & g_{11}^* \end{pmatrix}, \quad \mathcal{G}_2 = \begin{pmatrix} g_{12} & -g_{22}^* \\ g_{22} & g_{12}^* \end{pmatrix} \tag{3.6}$$

where

$$(g_{11}, g_{21}) = (h_{11}, h_{21})\Lambda, \quad (g_{12}, g_{22}) = (h_{12}, h_{22})\Lambda. \tag{3.7}$$

Sezginer–Sari [30] Sezginer and Sari proposed a 2×2 full-rate, full-diversity STBC given in (1.55) which can be written in the form of (3.3),

$$\mathbf{X} = \begin{pmatrix} ax_1 & -cx_2^* \\ ax_2 & cx_1^* \end{pmatrix} + \begin{pmatrix} 0 & 1 \\ 1 & 0 \end{pmatrix} \begin{pmatrix} bx_4 & dx_3^* \\ bx_3 & -dx_4^* \end{pmatrix}, \tag{3.8}$$

and also leads to the received signal expressions as in (3.1) with

$$\begin{aligned}\mathcal{H}_1 &= \begin{pmatrix} ah_{11} & -c^* h_{21}^* \\ ah_{21} & c^* h_{11}^* \end{pmatrix}, \quad \mathcal{G}_1 = \begin{pmatrix} bh_{11} & -d^* h_{21}^* \\ bh_{21} & d^* h_{11}^* \end{pmatrix} \\ \mathcal{H}_2 &= \begin{pmatrix} ah_{12} & -c^* h_{22}^* \\ ah_{22} & c^* h_{12}^* \end{pmatrix}, \quad \mathcal{G}_2 = \begin{pmatrix} bh_{12} & -d^* h_{22}^* \\ bh_{22} & d^* h_{12}^* \end{pmatrix}\end{aligned} \tag{3.9}$$

Rabiei–Al-Dhahir [31] Rabiei and Al-Dhahir propose the code given in (1.58) which can be rewritten as

$$\mathbf{X} = \begin{pmatrix} x_1\alpha_1 & x_4\alpha_1 \\ -x_4^*\beta_2 & x_1^*\beta_2 \end{pmatrix} + \begin{pmatrix} 0 & 1 \\ 1 & 0 \end{pmatrix} \begin{pmatrix} x_3\alpha_2 & x_2\alpha_2 \\ -x_2^*\beta_1 & x_3^*\beta_1 \end{pmatrix}, \tag{3.10}$$

and the received signal can also be expressed as in (3.1) with

$$\begin{aligned} \boldsymbol{c} &= (x_1, x_4^*), \quad \boldsymbol{s} = (x_3, x_2^*), \\ \boldsymbol{r}_1 &= (r_{11}, r_{12}^*), \quad \boldsymbol{r}_2 = (r_{21}, r_{22}^*), \\ \mathcal{H}_1 &= \begin{pmatrix} h_{11}\alpha_1 & h_{21}^*\beta_2 \\ -h_{21}\beta_2 & h_{11}^*\alpha_1 \end{pmatrix}, \mathcal{G}_1 = \begin{pmatrix} h_{21}\alpha_2 & h_{11}^*\beta_1 \\ -h_{11}\beta_1 & h_{21}^*\alpha_2 \end{pmatrix}, \\ \mathcal{H}_2 &= \begin{pmatrix} h_{12}\alpha_1 & h_{22}^*\beta_2 \\ -h_{22}\beta_2 & h_{12}^*\alpha_1 \end{pmatrix}, \mathcal{G}_2 = \begin{pmatrix} h_{22}\alpha_2 & h_{12}^*\beta_1 \\ -h_{12}\beta_1 & h_{22}^*\alpha_2 \end{pmatrix}. \end{aligned} \tag{3.11}$$

3.3 Fast Optimal Decoding

As shown in the last section, the decoding problem for all cases takes the form

$$\begin{aligned} \boldsymbol{r}_1 &= \boldsymbol{c}\mathcal{H}_1 + \boldsymbol{s}\mathcal{G}_1 + \boldsymbol{n}_1 \\ \boldsymbol{r}_2 &= \boldsymbol{c}\mathcal{H}_2 + \boldsymbol{s}\mathcal{G}_2 + \boldsymbol{n}_2 \end{aligned} \tag{3.12}$$

where $\boldsymbol{c}$ and $\boldsymbol{s}$ are vectors of a pair of symbols x_i and $\mathcal{H}_1$, $\mathcal{H}_2$, $\mathcal{G}_1$ and $\mathcal{G}_2$ are Alamouti blocks. Assume that symbols $x_i, i = 1, \ldots, 4$ are selected from some QAM constellation $\mathcal{C}$ of size N. We now show that *exact* ML can be implemented with complexity $O(N^2)$, through a very simple algorithm. First write (3.12) as

$$\boldsymbol{r} = \boldsymbol{c}\mathcal{H} + \boldsymbol{s}\mathcal{G} + \boldsymbol{n} \tag{3.13}$$

where $\boldsymbol{r} = (\boldsymbol{r}_1, \boldsymbol{r}_2)$, $\mathcal{H} = (\mathcal{H}_1, \mathcal{H}_2)$, $\mathcal{G} = (\mathcal{G}_1, \mathcal{G}_2)$ and $\boldsymbol{n} = (\boldsymbol{n}_1, \boldsymbol{n}_2)$. The likelihood function for (3.13) is

$$p(\boldsymbol{r}|\boldsymbol{s}, \boldsymbol{c}) \propto \exp\left(-\frac{1}{2\sigma^2} \|\boldsymbol{r} - \boldsymbol{c}\mathcal{H} - \boldsymbol{s}\mathcal{G}\|^2\right) \tag{3.14}$$

and the ML estimate is given by

$$(\hat{\boldsymbol{c}}, \hat{\boldsymbol{s}}) = \arg\max_{\boldsymbol{c}, \boldsymbol{s} \in \mathcal{C}^2} p(\boldsymbol{r}|\boldsymbol{s}, \boldsymbol{c}). \tag{3.15}$$

At first glance this optimization seems to involve a search over $\mathcal{C}^4$. However, conditional optimization can be applied to optimize (3.14) exactly as follows. First maximize (3.14) with

respect to $\boldsymbol{c}$ given $\boldsymbol{s}$, by expanding (3.14) and completing the square, we obtain

$$\begin{aligned} p(\boldsymbol{r}|\boldsymbol{s},\boldsymbol{c}) \propto & \exp\left(-\frac{1}{2\sigma^2}(\boldsymbol{r}-\boldsymbol{s}\mathcal{G})\left(\mathbf{I}_4-\frac{\mathcal{H}^\dagger\mathcal{H}}{\|\mathcal{H}\|^2}\right)(\boldsymbol{r}-\boldsymbol{s}\mathcal{G})^\dagger\right) \\ & \times \exp\left(-\frac{\|\mathcal{H}\|^2}{2\sigma^2}\|\boldsymbol{c}-\tilde{\boldsymbol{c}}(s)\|^2\right), \end{aligned} \tag{3.16}$$

where

$$\tilde{\boldsymbol{c}}(\boldsymbol{s}) = \frac{\boldsymbol{r}\mathcal{H}^\dagger - \boldsymbol{s}\mathcal{G}\mathcal{H}^\dagger}{\|\mathcal{H}\|^2}, \tag{3.17}$$

and $\|\mathcal{H}\|^2 = \frac{1}{2}\|\mathcal{H}\|_F^2$. Thus the ML estimate of $\boldsymbol{c}$ given $\boldsymbol{s}$ is

$$\hat{\boldsymbol{c}}(\boldsymbol{s}) = \mathrm{Q}\left(\tilde{\boldsymbol{c}}(\boldsymbol{s})\right). \tag{3.18}$$

Substituting (3.18) into (3.14), we obtain the optimization problem for $\boldsymbol{s}$ alone:

$$\hat{\boldsymbol{s}} = \arg\max_{\boldsymbol{s}\in\mathcal{C}^2} \|\boldsymbol{r} - \hat{\boldsymbol{c}}(\boldsymbol{s})\mathcal{H} - \boldsymbol{s}\mathcal{G}\|^2. \tag{3.19}$$

Thus, (3.19) and (3.18) provide an algorithm for obtaining the ML solution of $\boldsymbol{c}$ and $\boldsymbol{s}$, which involves at most $|\mathcal{C}|^2 = N^2$ evaluations of the likelihood function. That is, we have an $\mathcal{O}(N^2)$ algorithm for estimating $\boldsymbol{s}$ and $\boldsymbol{c}$.

Remark 2 *Above we have assumed that a QAM constellation is used. This is not necessary for conditional optimization to provide a computational benefit, but does, along with certain other lattice based constellations, provide maximum computational benefit. For an arbitrary constellation the quantization step* (3.18) *is replaced by a search which is at most* $\mathcal{O}(|\mathcal{C}|)$*, while if the constellation is a Cartesian product of two real constellations, i.e.* $\mathcal{C} = \mathcal{R}\times\mathcal{R}$ *then this search is at most* $\mathcal{O}(\sqrt{|\mathcal{C}|})$*. Finally, if the constellation is a subset of one of a number of lattices, such as the QAM or HEX constellations, then the quantization step is* $\mathcal{O}(1)$*.*

3.4 Conditional Optimization

In the previous section we used a conditional optimization approach to develop fast ML decoding algorithms for multiplexed Alamouti codes. Here we consider conditional optimization from a more general perspective and discuss its application to fast decoding of space-time codes.

Conditional optimization is a technique widely used in statistical estimation and signal processing. The goal of this technique is to reduce the search space of the optimization by taking advantages of the possibility of analytically optimizing over some subset of the parameters conditioned on the remaining parameters, or at least more efficiently than an exhaustive search. An archetypal example of this approach is Rife and Boorstyn's [51]. This reduces the parameter estimation problem for a single tone in noise, which involves the estimation of three parameters, to an optimization problem involving only the frequency of the tone.

In general, suppose that we wish to maximize a likelihood function of the form

$$p(\boldsymbol{r}|\Theta) \tag{3.20}$$

where $\boldsymbol{r}$ is some data and Θ is a set of parameters we need to optimize over. If the parameter set can be split $\Theta = (\theta_1, \theta_2)$ such that optimization over θ_1 given θ_2 can be carried out analytically or at least very efficiently, then the optimization problem can be efficiently carried out as:

$$\hat{\theta}_2 = \arg\max_{\theta_2} p(\boldsymbol{r}|\theta_2, \hat{\theta}_1(\theta_2)), \tag{3.21}$$

where

$$\hat{\theta}_1(\theta_2) = \arg\max_{\theta_1} p(\boldsymbol{r}|\theta_2, \theta_1), \tag{3.22}$$

and $\hat{\theta}_1 = \hat{\theta}_1(\hat{\theta}_2)$.

We now consider sufficient conditions under which conditional optimization leads to a reduction in decoding complexity of space-time codes. Assuming that perfect channel state information is available at the receiver, the received signal is given by

$$\mathbf{Y} = \mathbf{H}\mathbf{X} + \mathbf{W} \tag{3.23}$$

where $\mathbf{X}$ is the transmitted STBC codeword with code length T and entries that are information symbols drawn from an N-QAM constellation, $\mathbf{H}$ is the matrix of channel gains from the transmit to the receive antennas and $\boldsymbol{n}$ is i.i.d Gaussian noise with zero mean and covariance $2\sigma^2\mathbf{I}_{n_r T}$.

The received signal can be written as

$$\boldsymbol{r} = \boldsymbol{x}\mathcal{H} + \boldsymbol{n} \tag{3.24}$$

where $\boldsymbol{x}$ is the transmitted information symbol vector and $\mathcal{H}$ is the induced (equivalent) channel matrix.

The likelihood function of symbols $\boldsymbol{x}$ given the received signal $\boldsymbol{r}$ is given by

$$p(\boldsymbol{r}|\boldsymbol{x}) \propto \exp\left(-\frac{1}{2\sigma^2}\left\|\boldsymbol{r} - \boldsymbol{x}\mathcal{H}\right\|^2\right). \tag{3.25}$$

Taking the prior distribution of symbols $\boldsymbol{x}$ to be uniform on the constellation $\mathcal{C}_N$, we obtain the ML estimate:

$$\hat{\boldsymbol{x}} = \arg\max_{\boldsymbol{x}\in\mathcal{C}_N^K} p(\boldsymbol{r}|\boldsymbol{x}). \tag{3.26}$$

ML decoding is certainly achieved with $|\mathcal{C}|^K$ computations of likelihood (3.25), but if the symbols are taken from an N-QAM constellation then dramatic reductions in complexity are possible.

Theorem 3 *If the induced channel matrix $\mathcal{H}$ has m rows which are mutually orthogonal, for all channels $\mathbf{H}$, then exact ML decoding can be implemented with complexity $\mathcal{O}(N^{K-m})$.*

Remark 3 *It follows that in all cases the complexity of exact ML decoding is at most $\mathcal{O}(N^{K-1})$.*

Proof: Let $\mathcal{H}_1$ be the sub-matrix consisting of m mutually orthogonal rows of the induced channel matrix $\mathcal{H}$ and let $\mathcal{H}_2$ be the matrix consisting of the remaining rows. We can then rewrite (3.24) as

$$\boldsymbol{r} = \boldsymbol{x}_1\mathcal{H}_1 + \boldsymbol{x}_2\mathcal{H}_2 + \boldsymbol{n} \tag{3.27}$$

where $\boldsymbol{x}_1$ is the $1 \times m$ vector of complex symbols corresponding to the rows in $\mathcal{H}_1$ and $\boldsymbol{x}_2$ consists of the $K - m$ remaining symbols. The likelihood function associated with (3.27) is

$$p(\boldsymbol{r}|\boldsymbol{x}_1, \boldsymbol{x}_2) \propto \exp\left(-\frac{1}{2\sigma^2}\left\|\boldsymbol{r} - \boldsymbol{x}_1\mathcal{H}_1 - \boldsymbol{x}_2\mathcal{H}_2\right\|^2\right). \tag{3.28}$$

We have isolated $\boldsymbol{x}_1$, as our approach is to maximize the likelihood function (3.28) with respect to $\boldsymbol{x}_1$ given $\boldsymbol{x}_2$, and then maximize the resulting partially optimized likelihood function with respect to $\boldsymbol{x}_2$. Now since the rows of $\mathcal{H}_1$ are mutually orthogonal

$$\mathcal{H}_1\mathcal{H}_1^\dagger = D, \tag{3.29}$$

where $D = \text{diag}(d_1^2, \cdots, d_m^2)$, and d_j is the norm of the j^{th} row of $\mathcal{H}_1$. The likelihood function (3.28) can then be written as

$$\begin{aligned} p(\boldsymbol{r}|\boldsymbol{x}_1, \boldsymbol{x}_2) \propto & \exp\left(-\frac{1}{2\sigma^2}(\boldsymbol{r} - \boldsymbol{x}_2\mathcal{H}_2)\left(\mathbf{I} - \mathcal{H}_1^\dagger D^{-1}\mathcal{H}_1\right)(\boldsymbol{r} - \boldsymbol{x}_2\mathcal{H}_2)^\dagger\right) \\ & \times \exp\left(-\frac{1}{2\sigma^2}\sum_{j=1}^{m} d_j^2|x_j - \tilde{x}_j(\boldsymbol{x}_2)|^2\right), \end{aligned} \tag{3.30}$$

where

$$\tilde{\boldsymbol{x}}_1(\boldsymbol{x}_2) = (\boldsymbol{r} - \boldsymbol{x}_2\mathcal{H}_2)\mathcal{H}_1^\dagger D^{-1}. \tag{3.31}$$

Thus, given $\boldsymbol{x}_2$,

$$\begin{aligned} \hat{\boldsymbol{x}}_1(\boldsymbol{x}_2) &= (\text{Q}(\tilde{x}_1(\boldsymbol{x}_2)), \cdots, \text{Q}(\tilde{x}_m(\boldsymbol{x}_2))), \\ &\equiv \text{Q}(\tilde{\boldsymbol{x}}_1(\boldsymbol{x}_2)), \end{aligned} \tag{3.32}$$

maximizes (3.30). Substituting (3.32) into (3.30) we obtain the optimization problem for $\boldsymbol{x}_2$:

$$\hat{\boldsymbol{x}}_2 = \underset{\boldsymbol{x}_2 \in \mathbb{C}_N^{K-m}}{\arg\min} \left\|\boldsymbol{r} - \hat{\boldsymbol{x}}_1(\boldsymbol{x}_2)\mathcal{H}_1 - \boldsymbol{x}_2\mathcal{H}_2\right\|^2, \tag{3.33}$$

which can be substituted back into (3.32) to obtain the ML estimate of $\boldsymbol{x}_1$

$$\hat{\boldsymbol{x}}_1 = \hat{\boldsymbol{x}}_1(\hat{\boldsymbol{x}}_2). \tag{3.34}$$

Thus, equations (3.33) and (3.34) provide an algorithm for obtaining the ML estimate of $x_i, i = 1, \ldots, K$, which involves at most N^{K-m} evaluations of the right hand side of (3.33). ■

We see that for codes satisfying the conditions of Theorem 3, conditional optimization reduces the search for the ML estimate to optimization of the objective function in (3.33) over the symbols in $\boldsymbol{x}_2$. This reduced search can be carried out by any means, in parallel, sequentially, by tree search and/or using sphere decoding. We will further elucidate its relation to sphere decoding in Section 3.5. For non-square QAM see Remark 2.

Remark 4 *If $\boldsymbol{x}_1$ and $\boldsymbol{x}_2$ are vectors of real symbols, then the above analysis holds with the following modifications. Firstly, in Theorem 3 "mutual orthogonality" of the rows of $\mathcal{H}$ (see Equation* (3.29)*) is replaced by the condition*

$$\mathcal{H}_1\mathcal{H}_1^\dagger + \overline{\mathcal{H}_1\mathcal{H}_1^\dagger} = D. \tag{3.35}$$

Secondly, Equation (3.31) *is replaced by*

$$\tilde{\boldsymbol{x}}_1(\boldsymbol{x}_2) = \left(\boldsymbol{r}\mathcal{H}_1^\dagger + \overline{\boldsymbol{r}\mathcal{H}_1^\dagger} - \boldsymbol{x}_2(\mathcal{H}_2\mathcal{H}_1^\dagger + \overline{\mathcal{H}_2\mathcal{H}_1^\dagger})\right) D^{-1}. \tag{3.36}$$

(Here $\overline{\ }$ denotes complex conjugate.)

3.5 Relationship to Sphere Decoding

The idea of sphere decoding is to search only within a sphere or ellipsoid of a certain size defined by the induced covariance matrix and the SNR. Suppose for a given decoding we have determined that we need only search symbols that lie within the ellipsoidal region $\mathcal{S} \subset \mathbb{C}^K$, defined by the equation

$$\mathcal{S}: \quad \boldsymbol{x}\mathbf{R}^{-1}\boldsymbol{x}^{\dagger} < \rho, \tag{3.37}$$

where $\mathbf{R}$ is a *diagonal* positive definite Hermitian (symmetric, if $\boldsymbol{x}$ is real) matrix and $\rho > 0$. Having decided on a sphere the reduced decoding problem becomes

$$\hat{\boldsymbol{x}} = \arg\max_{\boldsymbol{x} \in \mathcal{C}^K \cap \mathcal{S}} p(\boldsymbol{r}|\boldsymbol{x}). \tag{3.38}$$

In Theorem 3 we split the code vector $\boldsymbol{x}$ into two parts, $\boldsymbol{x}_1$ associated with the m mutually orthogonal rows of $\mathcal{H}$, and $\boldsymbol{x}_2$ associated with the other $K - m$ rows of $\mathcal{H}$. Let $\boldsymbol{x}$ be a general vector in $\mathbb{C}^K$ and define $U_2 : \mathbb{C}^K \to \mathbb{C}^{K-m}$ by

$$\boldsymbol{x}U_2 = \boldsymbol{x}_2, \tag{3.39}$$

so that $\Pi_2 = U_2 U_2^{\dagger}$ is the orthogonal projector on the "$\boldsymbol{x}_2$" subspace. Similarly, we can define an orthogonal projection $\Pi_1 = U_1 U_1^{\dagger}$ onto the "$\boldsymbol{x}_1$" subspace. If $\boldsymbol{x} \in \mathcal{S}$, then $\boldsymbol{x}_2$ is contained in the region

$$\mathcal{S}_{\Pi_2} : \boldsymbol{x}_2 \left(U_2^{\dagger} \mathbf{R}^{-1} U_2 \right) \boldsymbol{x}_2^{\dagger} < \rho, \tag{3.40}$$

where $U_2^{\dagger}\mathbf{R}^{-1}U_2 \in \mathbb{C}^{(K-m)\times(K-m)}$.

The optimization problem for $\boldsymbol{x}_2$ thus reduces to

$$\hat{\boldsymbol{x}}_2 = \arg\min_{\boldsymbol{x}_2 \in \mathcal{C}^{K-m} \cap \mathcal{S}_{\Pi_2}} \left\| \boldsymbol{r} - \hat{\boldsymbol{x}}_1(\boldsymbol{x}_2)\mathcal{H}_1 - \boldsymbol{x}_2\mathcal{H}_2 \right\|^2. \tag{3.41}$$

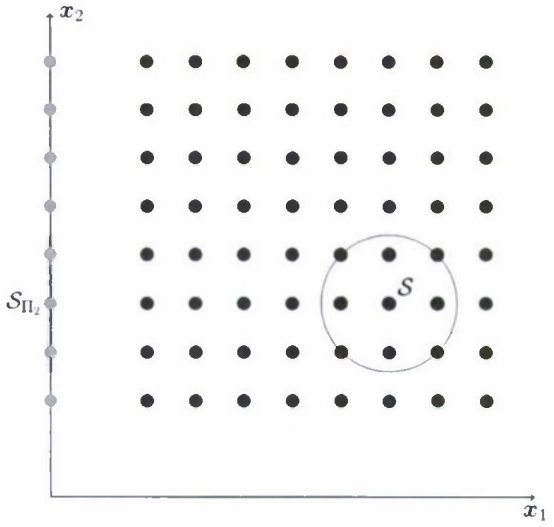

Figure 3.1: Relationship to sphere decoding

The situation is illustrated in Fig. 3.1, where the axes labeled $\boldsymbol{x}_1$ and $\boldsymbol{x}_2$ represent the two subspaces defined by the orthogonal projections Π_1 and Π_2. The grey points represent the projection of the full constellation $\mathcal{C}^K$ onto the Π_2 subspace. The projected constellation is searched over the projection of the sphere $\mathcal{S}$ onto the subspace Π_2, that is $\mathcal{S}_{\Pi_2}$.

Clearly, the method of conditional optimization can be naturally integrated with sphere decoding in a simple way leading to a sphere decoding algorithm with worst case complexity corresponding exactly to that of our direct algorithm in (3.33)–(3.34), that is $\mathcal{O}(|\mathcal{C}|^{K-m})$.

3.6 Fast Decoding of the Golden Code

It has been shown recently that the ML decoding complexity of the Golden Code is cubic in the size of the underlying QAM constellation for an arbitrary $N-$QAM constellation [46, 52]. In Chapter 4 we show that if a square QAM constellation is used then the complexity of exact ML decoding is further reduced to $\mathcal{O}(N^2\sqrt{N})$. Here we apply the conditional optimization approach to the Golden Code to obtain a simple approximate quadratic complexity decoding algorithm with essentially ML performance. For a large constellation, this is a significant reduction in complexity when compared to $\mathcal{O}(N^2\sqrt{N})$. The algorithm can be employed by mobile terminals with either one or two receive antennas and it is resilient to near singularity of the channel matrix. Dual use is an advantage, since there will likely be some IEEE 802.16 mobile terminals with one receive antenna and some with two antennas. The key to the quadratic algorithm is a maximization of the likelihood function with respect to one of the pair of signal points conditioned on the other. This choice is made by comparing the determinants of two covariance matrices (or equivalently, the norm of two channel vectors), and the underlying geometry of the Golden Code guarantees that one of these choices is good with high probability.

3.6.1 Model and Decoding Problem

The Golden Code is a 2×2 block space-time code that employs 2 transmit and 2 receive antennas and encodes four complex QAM symbols over two time slots yet achieves full diversity [22, 53, 54] and is incorporated in the IEEE 802.16 standard. As described in Section 1.5.1 the codewords in the Golden Code take the form

$$\begin{aligned}\mathbf{X} &= \begin{pmatrix}\alpha & 0\\ 0 & \bar{\alpha}\end{pmatrix}\begin{pmatrix}x_1+\tau x_2 & x_3+\tau x_4\\ i(x_3+\mu x_4) & x_1+\mu x_2\end{pmatrix}\\ &= \begin{pmatrix}\alpha & 0\\ 0 & \alpha\end{pmatrix}\left[\begin{pmatrix}x_1 & x_3\\ ix_3 & x_1\end{pmatrix}+\begin{pmatrix}\tau & 0\\ 0 & \mu\end{pmatrix}\begin{pmatrix}x_2 & x_4\\ ix_4 & x_2\end{pmatrix}\right]\end{aligned} \tag{3.42}$$

where $\{x\}_{i=1}^4 \in \mathcal{C} \subset \mathbb{Z}[i]$ are transmitted symbols, and $\mathcal{C}$ is a signal constellation taken to be 2^m-QAM. The parameters $\tau = (1+\sqrt{5})/2$ and $\mu = (1-\sqrt{5})/2$ are the Golden Ratio. The diagonal matrix $\mathrm{diag}[\alpha, \bar{\alpha}]$ where $\alpha = (1+i\mu)/\sqrt{5}, \bar{\alpha} = (1+i\tau)/\sqrt{5}$ serves to equalize transmitted signal power across the two transmit antennas.

Let (r_{11}, r_{12}) and (r_{21}, r_{22}) be the two received signal vectors at the first and second receive antennas and the components are the signals received over two consecutive time slots. The

received signal can be represented as

$$\begin{aligned}(r_{11}, r_{12}) &= (\alpha h_{11}, \bar{\alpha} h_{21}) \begin{pmatrix} x_1 & x_3 \\ ix_3 & x_1 \end{pmatrix} + (\tau h_{11}, \mu h_{21}) \begin{pmatrix} x_2 & x_4 \\ ix_4 & x_2 \end{pmatrix} + (n_{11}, n_{12}), \\ (r_{21}, r_{22}) &= (\alpha h_{12}, \bar{\alpha} h_{22}) \begin{pmatrix} x_1 & x_3 \\ ix_3 & x_1 \end{pmatrix} + (\tau h_{12}, \mu h_{22}) \begin{pmatrix} x_2 & x_4 \\ ix_4 & x_2 \end{pmatrix} + (n_{12}, n_{22}),\end{aligned} \tag{3.43}$$

where n_{ij} are complex Gaussian random variables with zero mean and variance $2\sigma^2$. Equation (3.43) can be rewritten as:

$$\begin{aligned}(r_{11}, r_{12}) &= (x_1, x_3) \begin{pmatrix} \alpha h_{11} & \bar{\alpha} h_{21} \\ i\bar{\alpha} h_{21} & \alpha h_{11} \end{pmatrix} + (x_2, x_4) \begin{pmatrix} \tau h_{11} & \mu h_{21} \\ i\mu h_{21} & \tau h_{11} \end{pmatrix} + (n_{11}, n_{12}), \\ (r_{21}, r_{22}) &= (x_1, x_3) \begin{pmatrix} \alpha h_{12} & \bar{\alpha} h_{22} \\ i\bar{\alpha} h_{22} & \alpha h_{12} \end{pmatrix} + (x_2, x_4) \begin{pmatrix} \tau h_{12} & \mu h_{22} \\ i\mu h_{22} & \tau h_{12} \end{pmatrix} + (n_{21}, n_{22}).\end{aligned} \tag{3.44}$$

Given that the channel gains h_{ij} are known at the receivers and each symbol is transmitted with equal probability, optimum decoding is provided by the maximum a posterior MAP/ML estimate as follows. We can rewrite (3.44) as

$$\boldsymbol{r} = \boldsymbol{c}\mathcal{H} + \boldsymbol{s}\mathcal{G} + \boldsymbol{n} \tag{3.45}$$

where

$$\begin{aligned}&\boldsymbol{r} = (r_{11}, r_{12}, r_{21}, r_{22}), \quad \boldsymbol{n} = (n_{11}, n_{12}, n_{21}, n_{22}), \quad \boldsymbol{c} = (x_1, x_3), \quad \boldsymbol{s} = (x_2, x_4), \\ &\mathcal{H} = \begin{pmatrix} \alpha h_{11} & \bar{\alpha} h_{21} & \alpha h_{12} & \bar{\alpha} h_{22} \\ i\bar{\alpha} h_{21} & \alpha h_{11} & i\bar{\alpha} h_{22} & \alpha h_{12} \end{pmatrix}, \quad \mathcal{G} = \begin{pmatrix} \alpha\tau h_{11} & \bar{\alpha}\mu h_{21} & \alpha\tau h_{12} & \bar{\alpha}\mu h_{22} \\ i\bar{\alpha}\mu h_{21} & \alpha\tau h_{11} & i\bar{\alpha}\mu h_{22} & \alpha\tau h_{12} \end{pmatrix}.\end{aligned} \tag{3.46}$$

The likelihood function of codewords $\boldsymbol{c}$ and $\boldsymbol{s}$ given the received signal $\boldsymbol{r}$ is

$$p(\boldsymbol{r}|\boldsymbol{c}, \boldsymbol{s}) \propto \exp\left(-\frac{1}{2\sigma^2} \|\boldsymbol{r} - \boldsymbol{c}\mathcal{H} - \boldsymbol{s}\mathcal{G}\|^2\right). \tag{3.47}$$

Taking the prior distribution of the symbols $\boldsymbol{c}$ and $\boldsymbol{s}$ to be uniform on the constellation $\mathcal{C}$, we obtain the maximum likelihood estimate:

$$(\hat{\boldsymbol{c}}, \hat{\boldsymbol{s}}) = \arg\max_{\boldsymbol{c}, \boldsymbol{s} \in \mathcal{C}^2} p(\boldsymbol{r}|\boldsymbol{c}, \boldsymbol{s}). \tag{3.48}$$

3.6.2 Quadratic Decoding of the Golden Code

In this section we show that decoding the Golden Code with essentially ML performance can be achieved with a simple algorithm which is quadratic in size of the underlying QAM signal constellation. Our approach is an extension of ideas used to derive the fast optimal algorithm for multiplexing orthogonal designs described in the Section 3.3.

Optimal Decoding: $\mathcal{O}(N^3)$

We begin by rewriting (3.44) as

$$\boldsymbol{r} = x_1\boldsymbol{h} + \boldsymbol{x}\widetilde{\mathcal{H}} + \boldsymbol{n}, \tag{3.49}$$

where $\boldsymbol{r}$ is defined in (3.46), $\boldsymbol{x} = (x_2, x_3, x_4)$, $\boldsymbol{h} = (\alpha h_{11}, \bar{\alpha} h_{21}, \alpha h_{12}, \bar{\alpha} h_{22})$ and

$$\widetilde{\mathcal{H}} = \begin{pmatrix} \alpha\tau h_{11} & \bar{\alpha}\mu h_{21} & \alpha\tau h_{12} & \bar{\alpha}\mu h_{22} \\ i\bar{\alpha} h_{21} & \alpha h_{11} & i\bar{\alpha} h_{22} & \alpha h_{12} \\ i\bar{\alpha}\mu h_{21} & \alpha\tau h_{11} & i\bar{\alpha}\mu h_{22} & \alpha\tau h_{12} \end{pmatrix}. \tag{3.50}$$

The likelihood funetion associated with (3.49) is

$$p(\boldsymbol{r}|x_1, x_2, x_3, x_4) \propto \exp\left(-\frac{1}{2\sigma^2}\left\|\boldsymbol{r} - x_1\boldsymbol{h} - \boldsymbol{x}\widetilde{\mathcal{H}}\right\|^2\right). \tag{3.51}$$

We have isolated x_1, as our approach is to maximize the likelihood with respect to x_1 given $\boldsymbol{x}$, and then maximize the resulting partially optimized likelihood with respect to $\boldsymbol{x}$. To this end, we rewrite (3.51) in the form

$$\begin{aligned} p(\boldsymbol{r}|x_1, \boldsymbol{x}) \propto \exp&\left(-\frac{1}{2\sigma^2}(\boldsymbol{r} - \boldsymbol{x}\widetilde{\mathcal{H}})\left(\mathbf{I}_4 - \frac{\boldsymbol{h}^\dagger\boldsymbol{h}}{\|\boldsymbol{h}\|^2}\right)(\boldsymbol{r} - \boldsymbol{x}\widetilde{\mathcal{H}})^\dagger\right) \\ &\times \exp\left(-\frac{\|\boldsymbol{h}\|^2}{2\sigma^2}\|x_1 - \tilde{x}_1(\boldsymbol{x})\|^2\right), \end{aligned} \tag{3.52}$$

where $\|\boldsymbol{h}\|^2$ is a Euclidean norm and

$$\tilde{x}_1(\boldsymbol{x}) = \frac{\boldsymbol{r}\boldsymbol{h}^\dagger - \boldsymbol{x}\widetilde{\mathcal{H}}\boldsymbol{h}^\dagger}{\|\boldsymbol{h}\|^2}. \tag{3.53}$$

Thus, given $\boldsymbol{x}$,

$$\hat{x}_1(\boldsymbol{x}) = \mathrm{Q}(\tilde{x}_1(\boldsymbol{x})), \tag{3.54}$$

maximizes (3.52).

Substituting (3.54) into (3.51) we obtain the optimization problem for $\boldsymbol{x}$:

$$\hat{\boldsymbol{x}} = \arg\min_{\boldsymbol{x}\in\mathcal{C}^3}\left\|\boldsymbol{r} - \boldsymbol{x}\widetilde{\mathcal{H}} - \hat{x}_1(\boldsymbol{x})\boldsymbol{h}\right\|^2. \tag{3.55}$$

The ML solution is then $(x_1, x_2, x_3, x_4) = (\hat{x}_1(\hat{\boldsymbol{x}}), \hat{\boldsymbol{x}})$. Thus (3.54) and (3.55) provide an algorithm for obtaining the ML estimate of $x_i, i = 1, \ldots, 4$, which involves at most N^3 evaluations of the right hand side of (3.55) since there are N^3 possibilities to choose the symbol set (x_2, x_3, x_4) and $\mathcal{O}(1)$ complexity for calculating the symbol x_1 from (3.53) and (3.54). Thus we have an algorithm with ML performance with a complexity $\mathcal{O}(N^3)$, where N is the size of the underlying QAM constellation.

Optimal Decoding: $\mathcal{O}(N^2\sqrt{N})$

See Section 4.4.1.

Essentially Optimal Quadratic Decoding: $\mathcal{O}(N^2)$

Consider the likelihood function given in (3.47). We can optimize (3.47) in two steps, i.e. first maximize with respect to $\boldsymbol{s}$ given $\boldsymbol{c}$ or vice versa. Suppose we maximize with respect to $\boldsymbol{s}$ given $\boldsymbol{c}$. We first write (3.47) as

$$\begin{aligned} p(\boldsymbol{r}|\boldsymbol{c},\boldsymbol{s}) \propto \exp\left(-\frac{1}{2\sigma^2}(\boldsymbol{r}-\boldsymbol{c}\mathcal{H})(\mathbf{I}_4 - \mathcal{G}^\dagger(\mathcal{G}\mathcal{G}^\dagger)^{-1}\mathcal{G})(\boldsymbol{r}-\boldsymbol{c}\mathcal{H})^\dagger\right) \\ \times \exp\left(-\frac{1}{2\sigma^2}(\boldsymbol{s}-\tilde{\boldsymbol{s}}(\boldsymbol{c}))\mathcal{G}\mathcal{G}^\dagger(\boldsymbol{s}-\tilde{\boldsymbol{s}}(\boldsymbol{c}))^\dagger\right) \end{aligned} \tag{3.56}$$

where

$$\tilde{\boldsymbol{s}}(\boldsymbol{c}) = (\boldsymbol{r}-\boldsymbol{c}\mathcal{H})\mathcal{G}^\dagger(\mathcal{G}\mathcal{G}^\dagger)^{-1}. \tag{3.57}$$

We now make what is essentially a zero forcing approximation, since $\mathcal{G}\mathcal{G}^\dagger$ is not generally a multiple of the identity. We take

$$\begin{aligned} \hat{\boldsymbol{s}}(\boldsymbol{c}) &= \mathrm{Q}\left(\tilde{\boldsymbol{s}}(\boldsymbol{c})\right) \\ &\equiv \left(\mathrm{Q}(\tilde{s}_1(\boldsymbol{c})), \mathrm{Q}(\tilde{s}_2(\boldsymbol{c}))\right), \end{aligned} \tag{3.58}$$

Substituting (3.58) into (3.47) we thus estimate $\boldsymbol{c}$ and $\boldsymbol{s}$ as follows:

$$\hat{\boldsymbol{c}} = \underset{\boldsymbol{c}\in\mathbb{C}^2}{\arg\min}\ \|\boldsymbol{r}-\boldsymbol{c}\mathcal{H}-\hat{\boldsymbol{s}}(\boldsymbol{c})\mathcal{G}\|^2, \tag{3.59}$$

$$\hat{\boldsymbol{s}} = \mathrm{Q}\left(\tilde{\boldsymbol{s}}(\hat{\boldsymbol{c}})\right), \tag{3.60}$$

where $\tilde{\boldsymbol{s}}(\boldsymbol{c})$ are given in (3.57).

Alternatively, if we reverse the roles of $\boldsymbol{c}$ and $\boldsymbol{s}$, we obtain the estimate

$$\hat{\boldsymbol{s}} = \underset{\boldsymbol{s}\in\mathbb{C}^2}{\arg\min}\ \|\boldsymbol{r}-\hat{\boldsymbol{c}}(\boldsymbol{s})\mathcal{H}-\boldsymbol{s}\mathcal{G}\|^2, \tag{3.61}$$

$$\hat{\boldsymbol{c}} = \mathrm{Q}\left(\tilde{\boldsymbol{c}}(\hat{\boldsymbol{s}})\right), \tag{3.62}$$

where

$$\tilde{\boldsymbol{c}}(\boldsymbol{s}) = (\boldsymbol{r}-\boldsymbol{s}\mathcal{G})\mathcal{H}^\dagger(\mathcal{H}\mathcal{H}^\dagger)^{-1}, \tag{3.63}$$

and

$$\hat{\boldsymbol{c}}(\boldsymbol{s}) = \mathrm{Q}\left(\tilde{\boldsymbol{c}}(\boldsymbol{s})\right). \tag{3.64}$$

Thus, we have two possible decoding solutions (3.59) and (3.61). Of course, if $\mathcal{H}\mathcal{H}^\dagger$ and $\mathcal{G}\mathcal{G}^\dagger$ were multiples of the 2×2 identity matrix, both optimizations (3.59) and (3.61) would be exact ML, and we would not need to make a choice. However, as we are making a zero forcing approximation, we need to choose the best alternative for each channel. In order to make the best choice, let's first consider the following covariance matrices

$$\mathcal{H}\mathcal{H}^\dagger = \begin{pmatrix} a & b \\ b^* & a \end{pmatrix}, \mathcal{G}\mathcal{G}^\dagger = \begin{pmatrix} \bar{a} & -b \\ -b^* & \bar{a} \end{pmatrix} \tag{3.65}$$

where

$$\begin{aligned} a &= |\alpha|^2\|\boldsymbol{h}_1\|^2 + |\bar{\alpha}|^2\|\boldsymbol{h}_2\|^2 \\ \bar{a} &= |\bar{\alpha}|^2\|\boldsymbol{h}_1\|^2 + |\alpha|^2\|\boldsymbol{h}_2\|^2 \\ b &= -i\alpha\alpha^*(h_{11}h_{21}^* + h_{12}h_{22}^*) + \bar{\alpha}\alpha^*(h_{21}h_{11}^* + h_{22}h_{12}^*) \end{aligned} \tag{3.66}$$

where $\|\boldsymbol{h}_i\|^2 = |h_{i1}|^2 + |h_{i2}|^2$. The accuracy of the quantization in (3.60) and (3.62), depends on both the determinant (which determines the SNR) and the condition number (which determines the accuracy of the zero forcing approximation) of $\mathcal{H}\mathcal{H}^\dagger$ or $\mathcal{G}\mathcal{G}^\dagger$. The following compares the determinant and the condition number of $\mathcal{H}\mathcal{H}^\dagger$ and $\mathcal{G}\mathcal{G}^\dagger$.

	$\mathcal{H}\mathcal{H}^\dagger$	$\mathcal{G}\mathcal{G}^\dagger$
Determinant	$a^2 - \lvert b\rvert^2$	$\bar{a}^2 - \lvert b\rvert^2$
Condition Number	$\gamma = \frac{a+\lvert b\rvert}{a-\lvert b\rvert}$	$\tilde{\gamma} = \frac{\bar{a}+\lvert b\rvert}{\bar{a}-\lvert b\rvert}$

Fortunately, it can be seen that for $\mathcal{H}\mathcal{H}^\dagger$ and $\mathcal{G}\mathcal{G}^\dagger$ the matrix with the largest determinant also has the smallest condition number. Thus, we have a clear choice: i.e. if

$$\det(\mathcal{G}\mathcal{G}^\dagger) \geq \det(\mathcal{H}\mathcal{H}^\dagger), \tag{3.67}$$

then we estimate $\boldsymbol{c}$ and $\boldsymbol{s}$ using (3.59), otherwise, use (3.61).

The condition (3.67) is equivalent to $\bar{a} \geq a$, which in turn reduces to

$$\|\boldsymbol{h}_1\|^2 \geq \|\boldsymbol{h}_2\|^2 . \tag{3.68}$$

The simulation results presented in Fig. 3.3 show use of our fast decoding algorithm involves little loss in performance compared to the optimal ML decoder. We gain some understanding of why this is by examining the joint behavior of the condition numbers for $\mathcal{H}\mathcal{H}^\dagger$ and $\mathcal{G}\mathcal{G}^\dagger$, γ and $\tilde{\gamma}$. We find empirically that for i.i.d. Gaussian channel coefficients, although the condition numbers γ and $\tilde{\gamma}$ can individually be large, the minimum of the two ($\min(\gamma, \tilde{\gamma})$) has a very high probability of being small. Fig. 3.2 shows the distribution of $\min(\gamma, \tilde{\gamma})$, for 10^6 realizations. The largest value of $\min(\gamma, \tilde{\gamma})$ obtained in the 10^6 realizations was approximately 17.5. This corresponds to a ratio of the lengths of the major and minor axes of the noise ellipse of $\sqrt{17.5} \approx 4.18$.

Note that the minimum condition number is not bounded above. If equality holds in (3.68) then there is a common condition number, and when the magnitudes of the channel gains are approximately equal, and their phases are aligned, then this condition number can be made arbitrarily large. This however is a very improbable event.

To sum up, the algorithm involves one of two possibilities:

If $\|\boldsymbol{h}_1\|^2 \geq \|\boldsymbol{h}_2\|^2$

$$\hat{\boldsymbol{c}} = \arg\min_{\boldsymbol{c}\in\mathbb{C}^2} \|\boldsymbol{r} - \boldsymbol{c}\mathcal{H} - \hat{\boldsymbol{s}}(\boldsymbol{c})\mathcal{G}\|^2 ,$$
$$\hat{\boldsymbol{s}} = \mathrm{Q}(\tilde{\boldsymbol{s}}(\hat{\boldsymbol{c}})),$$

otherwise,

$$\hat{\boldsymbol{s}} = \arg\min_{\boldsymbol{s}\in\mathbb{C}^2} \|\boldsymbol{r} - \hat{\boldsymbol{c}}(\boldsymbol{s})\mathcal{H} - \boldsymbol{s}\mathcal{G}\|^2 ,$$
$$\hat{\boldsymbol{c}} = \mathrm{Q}(\tilde{\boldsymbol{c}}(\hat{\boldsymbol{s}})),$$

where

$$\tilde{\boldsymbol{s}}(\boldsymbol{c}) = (\boldsymbol{r} - \boldsymbol{c}\mathcal{H})\mathcal{G}^\dagger(\mathcal{G}\mathcal{G}^\dagger)^{-1},$$
$$\tilde{\boldsymbol{c}}(\boldsymbol{s}) = (\boldsymbol{r} - \boldsymbol{s}\mathcal{G})\mathcal{H}^\dagger(\mathcal{H}\mathcal{H}^\dagger)^{-1}.$$

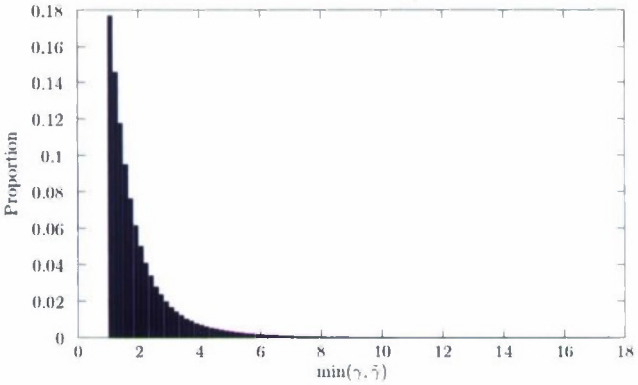

Figure 3.2: Empirical distribution of $\min(\gamma, \tilde{\gamma})$

This algorithm involves only N^2 evaluations of the argument of (3.59) or (3.61) compared to the $\mathcal{O}(N^3)$ ML algorithm. As the simulation result shows in Figure 3.3, the loss in performance compared to ML is negligible.

The algorithm works equally well when there is only one receive antenna. In this case the decoding problem becomes

$$\boldsymbol{r} = \boldsymbol{c}h + \boldsymbol{s}g + \boldsymbol{n}, \tag{3.69}$$

where $\boldsymbol{r} = (r_{11}, r_{12})$, $\boldsymbol{n} = (n_{11}, n_{12})$ and h, g are defined in (3.44). The algorithm applies with h, g in place of $\mathcal{H}, \mathcal{G}$.

3.6.3 Simulation Results

We compare the performance of the fast decoding algorithm (*Quadratic Decoder*) described in the last section with the ML decoder. The channel is assumed to be known at the receiver. The elements of the channel matrix are modelled as samples of independent complex Gaussian random variables with zero mean and variance 0.5 per real dimension. The noise is complex white Gaussian with zero mean and variance $2\sigma^2$. The signal to noise ratio at a receive antenna is defined as

$$\text{SNR(dB)} = 10 \log_{10} \left(\frac{P_s}{2\sigma^2} \right), \tag{3.70}$$

where P_s is the (average) signal power per symbol at a receive antenna which is defined as

$$P_s = E_s(\|\mathcal{H}\|^2 + \|\mathcal{G}\|^2), \tag{3.71}$$

and E_s is the average energy per symbol.

Figure 3.3, shows the symbol error rate for 4-QAM and 16-QAM as a function of SNR. The simulation shows that in both cases the performance of the *Quadratic Decoder* is essentially optimal (ML decoder).

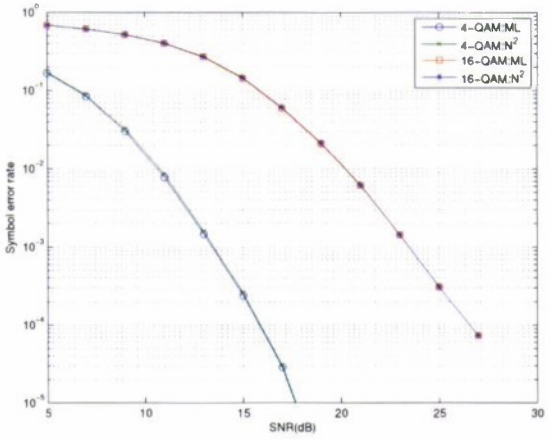

Figure 3.3: Performance comparison between the MAP/ML $\mathcal{O}(N^3)$ decoder and the quadratic decoder for 4-QAM and 16-QAM

3.7 Fast Decoding of 3×3 Perfect STBC

Oggier et al.[7] introduced the perfect space-time block codes which satisfy all of the following criteria: full-rate, full-diversity, non-vanishing determinant, good shaping and uniform average transmitted energy per antenna. These codes are constructed for $2 \times 2, 3 \times 3, 4 \times 4$ and 6×6 MIMO systems. An example of a 2×2 perfect STBC is the Golden Code [22] described in Section 3.6. The conventional ML decoder for perfect STBCs with an N-QAM or N-HEX constellation is based on an implementation of sphere decoding. Although there is no report on the decoding complexity for other perfect codes, it is expected that when the channel matrix is close to singular, the preprocessing stage of the sphere decoding algorithm will yield a plane of possibilities rather than a single initial estimate. When this occurs, the lattice point search degenerates to an exhaustive search.

In this Section we show that the approach described in Section 3.6 can be applied to obtain a fast decoding algorithm for 3×3 perfect STBCs which gives essentially ML performance with substantially reduced complexity. This approach can be also applied to other perfect STBCs to obtain low complexity decoding with essentially ML performance.

3.7.1 Model and Decoding Problem

Consider the codeword matrices of the perfect STBCs for 3×3 MIMO systems which we write in a form that will assist in the development of our algorithm. The perfect 3×3 STBC transmits nine complex (usually $N-$HEX constellation) information symbols $\{x_i\}_{i=1}^{9}$ over three time slots from three transmit antennas. The transmit codewords of the 3×3 perfect STBC can be

expressed as

$$\mathbf{X} = \sum_{i=0}^{2} B_{i+1} \begin{pmatrix} x_{3i+1} & x_{3i+2} & x_{3i+3} \\ jx_{3i+3} & x_{3i+1} & x_{3i+2} \\ jx_{3i+2} & jx_{3i+3} & x_{3i+1} \end{pmatrix}, \tag{3.72}$$

where the diagonal matrices B_i are

$$\begin{aligned} B_1 &= (1+j)I_3 + \Theta \\ B_2 &= (-1-2j)I_3 + j\Theta^2 \\ B_3 &= (-1-2j)I_3 + (1+j)\Theta + (1+j)\Theta^2 \end{aligned} \tag{3.73}$$

with $\Theta = \mathrm{diag}(\theta_1, \theta_2, \theta_3), \theta_i = 2\cos(2^i\pi/7), j = e^{2\pi i/3}$ and B_i satisfy

$$\mathrm{Tr}(B_j B_m^\dagger) = 7\delta_{jm}. \tag{3.74}$$

Assume that the channel state information is available at the receiver. Let h_{ij} be the channel gain from transmit antenna i to a receive antenna j, then the received signal is given by

$$\mathbf{Y} = \mathbf{HX} + \mathbf{W} \tag{3.75}$$

where

$$\mathbf{H} = \begin{pmatrix} h_{11} & h_{21} & h_{31} \\ h_{12} & h_{22} & h_{32} \\ h_{13} & h_{23} & h_{33} \end{pmatrix}. \tag{3.76}$$

Equation (3.75) can be rewritten as

$$\boldsymbol{r} = (x_1, x_2, x_3)\boldsymbol{\mathcal{H}}_1 + (x_4, x_5, x_6)\boldsymbol{\mathcal{H}}_2 + (x_7, x_8, x_9)\boldsymbol{\mathcal{H}}_3 + \boldsymbol{n} \tag{3.77}$$

where $\boldsymbol{r} = (\boldsymbol{r}_1, \boldsymbol{r}_2, \boldsymbol{r}_3)$ contains the three received signal vectors, $\boldsymbol{r}_i = (r_{i1}, r_{i2}, r_{i3})$ with the component r_{ij} representing the received signal at antenna i in time slot j. The noise $\boldsymbol{n}$ is i.i.d Gausian noise with zero mean and covariance $2\sigma^2 I_3$ and

$$\boldsymbol{\mathcal{H}}_1 = (H_1, G_1, C_1), \boldsymbol{\mathcal{H}}_2 = (H_2, G_2, C_2), \boldsymbol{\mathcal{H}}_3 = (H_3, G_3, C_3), \tag{3.78}$$

where H_i, G_i and C_i are induced channel matrices from the three transmit antennas to the first, second and the third receive antenna respectively. Explicitly

$$H_i = \begin{pmatrix} b_{i1}h_{11} & b_{i2}h_{21} & b_{i3}h_{31} \\ jb_{i3}h_{31} & b_{i1}h_{11} & b_{i2}h_{21} \\ jb_{i2}h_{21} & jb_{i3}h_{31} & b_{i1}h_{11} \end{pmatrix}, \tag{3.79}$$

and similarly for G_i and C_i. The induced channel matrices $\boldsymbol{\mathcal{H}}_1, \boldsymbol{\mathcal{H}}_2, \boldsymbol{\mathcal{H}}_3$ have the following property which is the basis of our fast decoding algorithm

$$\boldsymbol{\mathcal{H}}_1\boldsymbol{\mathcal{H}}_1^\dagger + \boldsymbol{\mathcal{H}}_2\boldsymbol{\mathcal{H}}_2^\dagger + \boldsymbol{\mathcal{H}}_3\boldsymbol{\mathcal{H}}_3^\dagger = 7\,\|\mathbf{H}\|_F^2\,\mathbf{I}_3. \tag{3.80}$$

That is $\sum_{i=1}^{K} \boldsymbol{\mathcal{H}}_i\boldsymbol{\mathcal{H}}_i^\dagger$ is a multiple of the identity. A similar property of the induced channel matrices holds for all of the perfect STBCs, including the Golden Code. In fact, our fast decoding method will apply to any STBC with structure giving rise to a relation of the form (3.80).

3.7.2 Low Complexity Decoding Algorithm

Let $\boldsymbol{c} = (x_1, x_2, x_3)$, $\boldsymbol{s} = (x_4, x_5, x_6)$, $\boldsymbol{y} = (x_7, x_8, x_9)$, we can rewrite (3.77) as

$$\boldsymbol{r} = \boldsymbol{c}\mathcal{H}_1 + \boldsymbol{s}\mathcal{H}_2 + \boldsymbol{y}\mathcal{H}_3 + \boldsymbol{n}. \tag{3.81}$$

The likelihood function associated with (3.81) is

$$p(\boldsymbol{r}|\boldsymbol{c}, \boldsymbol{s}, \boldsymbol{y},) \propto \exp\left(-\frac{1}{2\sigma^2}\left\|\boldsymbol{r} - \boldsymbol{c}\mathcal{H}_1 - \boldsymbol{s}\mathcal{H}_2 - \boldsymbol{y}\mathcal{H}_3\right\|^2\right). \tag{3.82}$$

Based on the conditional optimization described in Section 3.4, we first maximize (3.82) with respect to $\boldsymbol{s}$ and $\boldsymbol{y}$ given $\boldsymbol{c}$.

$$\begin{aligned} p(\boldsymbol{r}|\boldsymbol{c}, \boldsymbol{s}, \boldsymbol{y}) \propto & \exp\left(-\frac{1}{2\sigma^2}\boldsymbol{r}'\left(\mathbf{I}_9 - \mathcal{H}_1^\dagger(\mathcal{H}_1\mathcal{H}_1^\dagger)^{-1}\mathcal{H}_1\right)\boldsymbol{r}'^\dagger\right) \\ & \times \exp\left(-\frac{1}{2\sigma^2}\left(\boldsymbol{c} - \tilde{\boldsymbol{c}}(\boldsymbol{s}, \boldsymbol{y})\right)\mathcal{H}_1\mathcal{H}_1^\dagger\left(\boldsymbol{c} - \tilde{\boldsymbol{c}}(\boldsymbol{s}, \boldsymbol{y})\right)^\dagger\right) \end{aligned} \tag{3.83}$$

where $\boldsymbol{r}' = \boldsymbol{r} - \boldsymbol{s}\mathcal{H}_2 - \boldsymbol{y}\mathcal{H}_3$, and

$$\tilde{\boldsymbol{c}}(\boldsymbol{s}, \boldsymbol{y}) = (\boldsymbol{r} - \boldsymbol{s}\mathcal{H}_2 - \boldsymbol{y}\mathcal{H}_3)\mathcal{H}_1^\dagger(\mathcal{H}_1\mathcal{H}_1^\dagger)^{-1}. \tag{3.84}$$

We now make what is essentially a zero forcing approximation, since $\mathcal{H}_1\mathcal{H}_1^\dagger$ is not generally a multiple of the identity. We take

$$\hat{\boldsymbol{c}}(\boldsymbol{s}, \boldsymbol{y}) = \mathrm{Q}(\tilde{\boldsymbol{c}}(\boldsymbol{s}, \boldsymbol{y})) \equiv (\mathrm{Q}(\tilde{x}_1(\boldsymbol{s}, \boldsymbol{y})), \mathrm{Q}(\tilde{x}_2(\boldsymbol{s}, \boldsymbol{y})), \mathrm{Q}(\tilde{x}_3(\boldsymbol{s}, \boldsymbol{y}))). \tag{3.85}$$

Substituting (3.85) into (3.82) we thus estimate $\boldsymbol{c}$, $\boldsymbol{s}$ and $\boldsymbol{y}$ as follows:

$$\begin{aligned} (\hat{\boldsymbol{s}}, \hat{\boldsymbol{y}}) &= \arg\min_{\boldsymbol{s}, \boldsymbol{y} \in \mathcal{C}} \left\|\boldsymbol{r} - \hat{\boldsymbol{c}}(\boldsymbol{s}, \boldsymbol{y})\mathcal{H}_1 - \boldsymbol{s}\mathcal{H}_2 - \boldsymbol{y}\mathcal{H}_3\right\|^2, \\ \hat{\boldsymbol{c}} &= \mathrm{Q}(\tilde{\boldsymbol{c}}(\hat{\boldsymbol{s}}, \hat{\boldsymbol{y}})) \end{aligned} \tag{3.86}$$

where $\tilde{\boldsymbol{c}}(\boldsymbol{s}, \boldsymbol{y})$ is given in (3.84).

If we first maximize (3.82) with respect to $\boldsymbol{c}$ and $\boldsymbol{y}$ given $\boldsymbol{s}$ we obtain the estimate

$$\begin{aligned} (\hat{\boldsymbol{c}}, \hat{\boldsymbol{y}}) &= \arg\min_{\boldsymbol{c}, \boldsymbol{y} \in \mathcal{C}} \left\|\boldsymbol{r} - \boldsymbol{c}\mathcal{H}_1 - \hat{\boldsymbol{s}}(\boldsymbol{c}, \boldsymbol{y}) - \boldsymbol{y}\mathcal{H}_3\right\|^2, \\ \hat{\boldsymbol{s}} &= \mathrm{Q}(\tilde{\boldsymbol{s}}(\hat{\boldsymbol{c}}, \hat{\boldsymbol{y}})) \end{aligned} \tag{3.87}$$

where

$$\tilde{\boldsymbol{s}}(\boldsymbol{c}, \boldsymbol{y}) = (\boldsymbol{r} - \boldsymbol{c}\mathcal{H}_1 - \boldsymbol{y}\mathcal{H}_3)\mathcal{H}_2^\dagger(\mathcal{H}_2\mathcal{H}_2^\dagger)^{-1}. \tag{3.88}$$

Alternatively, if we maximize (3.82) with respect to $\boldsymbol{c}$ and $\boldsymbol{s}$ given $\boldsymbol{y}$ we obtain

$$\begin{aligned} (\hat{\boldsymbol{c}}, \hat{\boldsymbol{s}}) &= \arg\min_{\boldsymbol{c}, \boldsymbol{s} \in \mathcal{C}} \left\|\boldsymbol{r} - \boldsymbol{c}\mathcal{H}_1 - \boldsymbol{s}\mathcal{H}_2 - \hat{\boldsymbol{y}}(\boldsymbol{c}, \boldsymbol{s})\mathcal{H}_3\right\|^2, \\ \hat{\boldsymbol{y}} &= \mathrm{Q}(\tilde{\boldsymbol{y}}(\hat{\boldsymbol{c}}, \hat{\boldsymbol{s}})) \end{aligned} \tag{3.89}$$

where

$$\tilde{\boldsymbol{y}}(\boldsymbol{c}, \boldsymbol{s}) = (\boldsymbol{r} - \boldsymbol{c}\mathcal{H}_1 - \boldsymbol{s}\mathcal{H}_2)\mathcal{H}_3^\dagger(\mathcal{H}_3\mathcal{H}_3^\dagger)^{-1}. \tag{3.90}$$

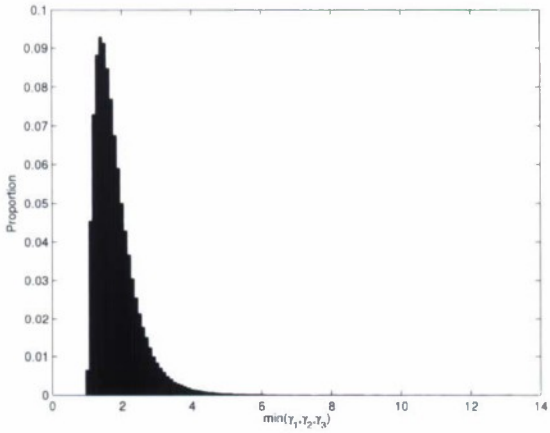

Figure 3.4: Empirical distribution of min($\gamma_1, \gamma_2, \gamma_3$)

Equations (3.86), (3.87) and (3.89) each provide an algorithm for obtaining the estimate of $x_i, i = 1, \ldots, 9$, each of which involves at most N^6 evaluations of the right hand side of one of (3.86), (3.87) and (3.89). Now, we have three possible decoding solutions. Of course if $\mathcal{H}_1\mathcal{H}_1^\dagger, \mathcal{H}_2\mathcal{H}_2^\dagger$ and $\mathcal{H}_3\mathcal{H}_3^\dagger$ were multiples of the identity matrix, all of the optimizations (3.86), (3.87) and (3.89) would have exact ML solutions and we would not need to make a choice. However, as we are making a zero forcing approximation, we need to choose the best alternative for each channel. One approach is to compute all three alternatives and take the alternative which maximizes the likelihood. The key to the current algorithm is that due to the structure of the code one of the three estimates is good, i.e. essentially ML, with very high probability. The accuracy of the quantization depends on both the determinant (which determines signal to noise ratio) and condition number (which determines the accuracy of the zero forcing approximation) of $\mathcal{H}_1\mathcal{H}_1^\dagger, \mathcal{H}_2\mathcal{H}_2^\dagger$ or $\mathcal{H}_3\mathcal{H}_3^\dagger$. Fig.3.4 shows the empirical distribution of $\min(\gamma_1, \gamma_2, \gamma_3)$ for i.i.d Gaussian channel coefficients, where $\gamma_1, \gamma_2, \gamma_3$ represent the condition numbers. This shows that although the condition numbers can individually be large, the minimum of the three has a very high probability of being small.

We can reduce the computation by a factor of three by deciding on one of the three estimates based on the channel. A possible criterion is to choose to quantize the variables corresponding to the $\mathcal{H}_j$ with the largest value of $\det(\mathcal{H}_j\mathcal{H}_j^\dagger)$. Another choice is to quantize the variable for which the corresponding matrix $\mathcal{H}_j\mathcal{H}_j^\dagger$ has the smallest condition number. For the Golden Code these two criteria are equivalent, but here they are not. We have found experimentally that the former criterion is just slightly better and obviates the need to compute all three estimates. The algorithm can be summarized as follows:

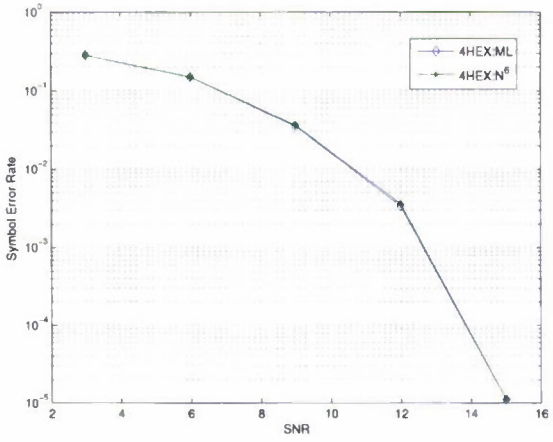

Figure 3.5: Performance of the $\mathcal{O}(N^6)$ decoder and the ML $\mathcal{O}(N^8)$ decoder

Let $\det(\mathcal{H}) = \max[\det(\mathcal{H}_1\mathcal{H}_1^\dagger), \det(\mathcal{H}_2\mathcal{H}_2^\dagger), \det(\mathcal{H}_3\mathcal{H}_3^\dagger)]$,

If $\det(\mathcal{H}_1\mathcal{H}_1^\dagger) = \det(\mathcal{H})$

$$(\hat{s}, \hat{y}) = \arg\min_{s,y\in\mathcal{C}} \|r - \hat{c}(s,y)\mathcal{H}_1 - s\mathcal{H}_2 - y\mathcal{H}_3\|^2$$
$$\hat{c} = \mathrm{Q}(\tilde{c}(\hat{s}, \hat{y}))$$

elseif $\det(\mathcal{H}_2\mathcal{H}_2^\dagger) = \det(\mathcal{H})$

$$(\hat{c}, \hat{y}) = \arg\min_{c,y\in\mathcal{C}} \|r - c\mathcal{H}_1 - \hat{s}(c,y)\mathcal{H}_2 - y\mathcal{H}_3\|^2$$
$$\hat{s} = \mathrm{Q}(\tilde{s}(\hat{c}, \hat{y}))$$

otherwise

$$(\hat{c}, \hat{s}) = \arg\min_{c,s\in\mathcal{C}} \|r - c\mathcal{H}_1 - s\mathcal{H}_2 - \hat{y}(c,s)\mathcal{H}_3\|^2$$
$$\hat{y} = \mathrm{Q}(\tilde{y}(\hat{c}, \hat{s}))$$

where $\tilde{c}$, $\tilde{s}$, $\tilde{y}$ are given in (3.84), (3.88), (3.90) respectively.

The perfect STBCs are constructed in terms of information symbols, either a QAM or HEX constellation. This means that the computational complexity of the quantization step is $O(1)$. Therefore our algorithm involves at most N^6 evaluations of the likelihood function. We compare the performance of the fast decoding algorithm described above with the ML decoder for a 3×3 perfect STBC. Figure 3.5 shows the symbol error rate as a function of SNR using a 4-HEX constellation for a Rayleigh fading channel model. The result shows that our fast decoder is essentially a ML decoder with complexity $\mathcal{O}(N^6)$.

Chapter 4: Fast Decodable Space-Time Block Codes: General Theory

In this chapter we consider how to write linear dispersion codes and in particular, the perfect STBCs, in a way that makes the decoding structure clear. It will become clear that the perfect STBCs can be considered as multiplexed quasi-orthogonal designs. Application of the conditional optimization approach developed in Chapter 3 lead to fast exact ML decoders.

Consider a MIMO communication system with n_t transmit antennas and n_r receive antennas. The transmitted signal matrix $\mathbf{X} \in \mathbb{C}^{n_t \times T}$ and the received signal matrix $\mathbf{Y} \in \mathbb{C}^{n_t \times T}$ are related by

$$\mathbf{Y} = \mathbf{HX} + \mathbf{W} \tag{4.1}$$

where $\mathbf{H} \in \mathbb{C}^{n_r \times n_t}$ denotes the channel matrix with entry h_{ij} representing the fading coefficient associated with the transmit antenna i and receive antenna j. The channel coefficients are i.i.d. circularly symmetric complex Gaussian random variables with zero mean and unit variance. $\mathbf{W} \in \mathbb{C}^{n_r \times T}$ denotes the complex additive white Gaussian noise with i.i.d. entries $\mathbf{W}_{ij} \sim \mathcal{CN}(0, 2\sigma^2)$. We assume quasi-static flat Rayleigh fading where the channel coefficients are fixed for the codeword duration i.e. for T symbol periods.

4.1 Linear Dispersion Codes

Let $\{x_k\}_{k=1}^{2K}$ be a set of real scalar symbols which are selected in pairs from some constellation. A linear dispersion (LD) code [34] is a space-time code in which codeword matrices are obtained as linear combinations of certain basis matrices according to

$$\mathbf{X} = \sum_{k=1}^{2K} x_k A_k, \tag{4.2}$$

where $\{A_k\}_{k=1}^{2K} \in \mathbb{C}^{n_t \times T}$ is a set of complex matrices. If the x_k roam over all of $\mathbb{R}$ this is the real linear span of the matrices A_k and as such is a real vector subspace of $\mathbb{C}^{n_r \times T}$. That is, a subspace of $\mathbb{C}^{n_r \times T}$ which is a vector space over $\mathbb{R}$. We denote this space by V.

Note that LD codes encompass all possible linear space-time codes. Substituting (4.2) into (4.1), the received signal vector $\boldsymbol{y}$ can be written as

$$\boldsymbol{y} = \boldsymbol{x}\mathcal{H} + \boldsymbol{n} \tag{4.3}$$

where $\boldsymbol{x} \in \mathbb{R}^{n_t}$ is the transmitted information symbol vector, and $\mathcal{H}$ is the induced channel matrix

$$\mathcal{H} = \begin{pmatrix} \boldsymbol{h}_1 A_1 & \boldsymbol{h}_2 A_1 & \dots & \boldsymbol{h}_{n_r} A_1 \\ \vdots & \vdots & \vdots & \vdots \\ \boldsymbol{h}_1 A_{2K} & \boldsymbol{h}_2 A_{2K} & \dots & \boldsymbol{h}_{n_r} A_{2K} \end{pmatrix} \tag{4.4}$$

where $\boldsymbol{h}_i = (h_{1i}, h_{2i}, \dots, h_{n_t i})$.

4.2 Algebraic Properties

In this section we look at some algebraic properties of an LD codes which leads to a fast ML decodable property. We begin by recalling the definition of an orthogonal design.

Definition 2 *If an LD code* (4.2) *is an* orthogonal design *then for all* $k, l = 1, \ldots, 2K$,

$$A_k A_l^\dagger + A_l A_k^\dagger = \alpha_k \delta_{k,l} I, \quad \alpha_k > 0. \tag{4.5}$$

There are many codes which are not themselves an orthogonal design but do have subcodes which are orthogonal designs. Following [9] we refer to these codes as having embedded orthogonality. More precisely:

Definition 3 *An LD code* (4.2) *is said to have* embedded orthogonality *of order* m *if some subset of size* m *of the matrices* A_k *satisfies* (4.5). *For such a code we can relabel the* A_k, *and write* (4.2) *as*

$$\mathbf{X} = \sum_{k=1}^{2m} x_k A_k + \sum_{k=2m+1}^{2K} x_k A_k \tag{4.6}$$

where $\{A_k\}_{k=1}^{2m}$ *satisfies the condition* (4.5).

Definition 4 *An LD code* (4.2) *is a* $(2K, d)$-Quasi-Orthogonal Design *(*$(2K, d)$*-QOD) if there is a partition of the set of integers* $\{1, \ldots, 2K\}$ *into* $2K/d$ *sets* $S_1, \ldots, S_{2K/d}$, *each of size* d, *such that*

1. *For each* $j \in S_\ell$ *and* $m \in S_{\ell'}$, *with* $\ell \neq \ell'$,

$$A_j A_m^\dagger + A_m A_j^\dagger = 0, \tag{4.7}$$

2. *For all* $\ell = 1, \ldots, 2K/d$

$$\sum_{j \in S_\ell} A_j A_j^\dagger = \alpha_\ell \mathbf{I}_M. \tag{4.8}$$

Note that a $(2K, 1)$-QOD is an orthogonal design.

Definition 5 *An LD code is said to have* embedded $(2m, d)$-quasi-orthogonality *if some subset of the matrices* A_k *of size* $2m$ *satisfies the conditions* (4.7) *and* (4.8). *For such a code we can relabel the* A_k *(and* x_k*), and write* (4.2) *as*

$$\mathbf{X} = \sum_{\ell=1}^{2m/d} \sum_{k=(\ell-1)d+1}^{\ell d} x_k A_k + \sum_{k=2m+1}^{2K} x_k A_k, \tag{4.9}$$

where $\{A_k\}_{k=1}^{2m}$ *satisfies the* $(2m, d)$*-QOD conditions with partition* $S_\ell = \{(\ell-1)d + 1, \ldots, \ell d\}$, *for* $\ell = 1, \ldots, 2m/d$.

4.3 Fast Maximum Likelihood Decoding

Consider the received signal given in (4.3). The likelihood function of symbols $\boldsymbol{x}$ given the received signal $\boldsymbol{y}$ is given by

$$p(\boldsymbol{y}|\boldsymbol{x}) \propto \exp\left\{-\frac{1}{2\sigma^2}\|\boldsymbol{y}-\boldsymbol{x}\mathcal{H}\|^2\right\}. \tag{4.10}$$

The maximum likelihood estimate of $\boldsymbol{x}$ is:

$$\hat{\boldsymbol{x}} = \arg\max_{\boldsymbol{x}} p(\boldsymbol{y}|\boldsymbol{x}). \tag{4.11}$$

If an LD code $\mathbf{X}$ in (4.2) is an orthogonal design then the ML decoding problem for $x_k, k = 1,\ldots,2K$ decouples into $2K$ real parallel sub-channels.

Theorem 4 *If a linear dispersion code of the form* (4.3) *has embedded orthogonality of order* m *then exact ML decoding can be implemented with complexity* $\mathcal{O}(N^{K-m})$ *for square* N*-QAM and with complexity* $\mathcal{O}(N^{K-m+1})$ *for a general constellation.*

Remark 5 *It follows that in all cases the complexity of ML decoding is at most* $\mathcal{O}(N^{K-1})$ *for square* N*-QAM.*

Proof: Suppose our code $\mathbf{X}$ has the form (4.6). Write $\boldsymbol{x}_1 = (x_1,\cdots,x_{2m})$ and $\boldsymbol{x}_2 = (x_{2m+1},\cdots,x_{2K})$, and decompose (4.3) as

$$\boldsymbol{y} = \boldsymbol{x}_1\mathcal{H}_1 + \boldsymbol{x}_2\mathcal{H}_2 + \boldsymbol{n}. \tag{4.12}$$

The likelihood function associated with (4.12) is

$$p(\boldsymbol{y}|\boldsymbol{x}_1,\boldsymbol{x}_2) \propto \exp\left\{-\frac{1}{2\sigma^2}\|\boldsymbol{y}-\boldsymbol{x}_1\mathcal{H}_1-\boldsymbol{x}_2\mathcal{H}_2\|^2\right\}. \tag{4.13}$$

We have isolated $\boldsymbol{x}_1$, as our approach is to maximize the likelihood function (4.13) with respect to $\boldsymbol{x}_1$ given $\boldsymbol{x}_2$, and then maximize the resulting partially optimized likelihood function with respect to $\boldsymbol{x}_2$.

Since the matrices $\{A_k, k = 1,\ldots,2m\}$ satisfy the condition (4.5),

$$\mathcal{H}_1\mathcal{H}_1^\dagger + \overline{\mathcal{H}_1\mathcal{H}_1^\dagger} = D, \tag{4.14}$$

where $D = \mathrm{diag}(\alpha_1,\cdots,\alpha_{2m})$, the likelihood function (4.13) can be written as

$$\begin{aligned} p(\boldsymbol{y}|\boldsymbol{x}_1,\boldsymbol{x}_2) \propto \exp\Big\{ &-\frac{1}{2\sigma^2}(\boldsymbol{y}-\boldsymbol{x}_2\mathcal{H}_2)(\boldsymbol{y}-\boldsymbol{x}_2\mathcal{H}_2)^\dagger \\ &+ \frac{1}{4\sigma^2}\sum_{j=1}^{2m}\alpha_j|\tilde{x}_j(\boldsymbol{x}_2)|^2\Big\}\prod_{j=1}^{2m}\exp\left\{-\frac{\alpha_j}{4\sigma^2}|x_j-\tilde{x}_j(\boldsymbol{x}_2)|^2\right\}, \end{aligned} \tag{4.15}$$

where

$$\tilde{\boldsymbol{x}}_1(\boldsymbol{x}_2) = \left(\boldsymbol{y}\mathcal{H}_1^\dagger + \overline{\boldsymbol{y}\mathcal{H}_1^\dagger} - \boldsymbol{x}_2(\mathcal{H}_2\mathcal{H}_1^\dagger + \overline{\mathcal{H}_2\mathcal{H}_1^\dagger})\right)D^{-1}. \tag{4.16}$$

Thus, given $\boldsymbol{x}_2$, the ML decoding problem for $\boldsymbol{x}_1$ decouples into m parallel sub-decoding problems. We have

$$\begin{aligned}\hat{\boldsymbol{x}}_1(\boldsymbol{x}_2) &= (\mathrm{Q}(\tilde{x}_1(\boldsymbol{x}_2)), \cdots, \mathrm{Q}(\tilde{x}_m(\boldsymbol{x}_2))) \\ &\equiv \mathrm{Q}(\tilde{\boldsymbol{x}}_1(\boldsymbol{x}_2)),\end{aligned} \tag{4.17}$$

where Q denotes the ML decoder for the sub-decoding problems. For square N-QAM the ML decoder Q is just quantization which has complexity $\mathcal{O}(1)$. For a general constellation Q will involve a search with linear complexity in the size of the constellation. Substituting (4.17) into (4.15) we obtain the optimization problem for $\boldsymbol{x}_2$:

$$\hat{\boldsymbol{x}}_2 = \arg\min_{\boldsymbol{x}_2} \|\boldsymbol{y} - \hat{\boldsymbol{x}}_1(\boldsymbol{x}_2)\boldsymbol{\mathcal{H}}_1 - \boldsymbol{x}_2\boldsymbol{\mathcal{H}}_2\|^2, \tag{4.18}$$

which can be substituted back into (4.17) to obtain the ML estimate of $\boldsymbol{x}_1$

$$\hat{\boldsymbol{x}}_1 = \hat{\boldsymbol{x}}_1(\hat{\boldsymbol{x}}_2). \tag{4.19}$$

Thus, (4.18) and (4.19) provide an algorithm for obtaining the ML estimate of $x_i, i = 1, \ldots, 2K$, which involves at most N^{K-m} evaluations of the right hand size of (4.18) for square N-QAM. For a general constellation we need to evaluate (4.18) N^{K-m} times and each evaluation involves $2m$ parallel searches through N alternatives to give an overall complexity of $\mathcal{O}(N^{K-m+1})$. ■

Theorem 5 *If an LD code* (4.2) *has embedded* $(2m, d)$*-quasi-orthogonality, then exact ML decoding can be implemented with complexity* $\mathcal{O}(N^{K-m+(d-1)/2})$ *for transmitted symbols taken from a square* N*-QAM constellation while for a general constellation the complexity is* $\mathcal{O}(N^{K-m+d})$.

Proof: Write $\boldsymbol{x}_\ell = (x_{(\ell-1)d+1}, \cdots, x_{\ell d}), \ell = 1, \cdots, 2m$ and $\boldsymbol{x}_{2m+1} = (x_{2m+1}, \cdots, x_{2K})$. Then we can rewrite (4.3) as

$$\boldsymbol{y} = \sum_{\ell=1}^{2m/d} \boldsymbol{x}_\ell \mathcal{H}_\ell + \boldsymbol{x}_{2m+1}\mathcal{H}_{m+1} + \boldsymbol{n}. \tag{4.20}$$

The likelihood function associated with (4.20) is

$$p(\boldsymbol{y}|\{\boldsymbol{x}_\ell\}, \boldsymbol{x}_{2m+1}) \propto \exp\left\{-\frac{1}{2\sigma^2}\left\|\boldsymbol{y} - \sum_{\ell=1}^{2m/d} \boldsymbol{x}_\ell\mathcal{H}_\ell - \boldsymbol{x}_{2m+1}\boldsymbol{\mathcal{H}}_{2m+1}\right\|^2\right\}. \tag{4.21}$$

Now since the matrices $\{A_k, k = 1, \cdots, 2m\}$ satisfy the condition (4.7) then, for $\ell \neq \ell'$,

$$\boldsymbol{\mathcal{H}}_\ell\boldsymbol{\mathcal{H}}_{\ell'}^\dagger + \overline{\boldsymbol{\mathcal{H}}_\ell\boldsymbol{\mathcal{H}}_{\ell'}^\dagger} = \begin{pmatrix} \mathbf{M}_d & \mathbf{0}_d \\ \mathbf{0}_d & \mathbf{M}_d \end{pmatrix}, \tag{4.22}$$

where $\mathbf{M}_d$ is a $d \times d$ matrix and $\mathbf{0}_d$ denotes a $d \times d$ matrix with all elements are zero, and so the likelihood function (4.21) can be written as

$$\begin{aligned} & p(\boldsymbol{y}|\{\boldsymbol{x}_\ell\}, \boldsymbol{x}_{2m+1}) \\ & \quad \propto \exp\Big\{ -\frac{1}{2\sigma^2}(\boldsymbol{y} - \boldsymbol{x}_{2m+1}\mathcal{H}_{2m+1})(\boldsymbol{y} - \boldsymbol{x}_{2m+1}\mathcal{H}_{2m+1})^\dagger \\ & \quad + \frac{1}{4\sigma^2}\sum_{\ell=1}^{2m/d} \tilde{\boldsymbol{x}}_\ell(\boldsymbol{x}_{2m+1})\left(\mathcal{H}_\ell\mathcal{H}_\ell^\dagger + \overline{\mathcal{H}_\ell\mathcal{H}_\ell^\dagger}\right)\tilde{\boldsymbol{x}}_\ell(\boldsymbol{x}_{2m+1})^{\mathsf{T}}\Big\} \\ & \quad \times \prod_{\ell=1}^{2m/d} \exp\Big\{(-\frac{1}{4\sigma^2}(\boldsymbol{x}_\ell - \tilde{\boldsymbol{x}}_\ell(\boldsymbol{x}_{2m+1}))(\mathcal{H}_\ell\mathcal{H}_\ell^\dagger + \overline{\mathcal{H}_\ell\mathcal{H}_\ell^\dagger})(\boldsymbol{x}_\ell - \tilde{\boldsymbol{x}}_\ell(\boldsymbol{x}_{2m+1}))^{\mathsf{T}}\Big\}, \end{aligned} \tag{4.23}$$

where, for $\ell = 1, \cdots, 2m/d$,

$$\begin{aligned} & \tilde{\boldsymbol{x}}_\ell(\boldsymbol{x}_{2m+1}) \\ & \quad = \left(\boldsymbol{y}\mathcal{H}_\ell^\dagger + \overline{\boldsymbol{y}\mathcal{H}_\ell^\dagger} - \boldsymbol{x}_{2m+1}(\mathcal{H}_{2m+1}\mathcal{H}_\ell^\dagger + \overline{\mathcal{H}_{2m+1}\mathcal{H}_\ell^\dagger})\right)\left(\mathcal{H}_\ell\mathcal{H}_\ell^\dagger + \overline{\mathcal{H}_\ell\mathcal{H}_\ell^\dagger}\right)^{-1}. \end{aligned} \tag{4.24}$$

Thus, given $\boldsymbol{x}_{2m+1}$, the ML decoding problem for $\{\boldsymbol{x}_\ell | \ell = 1, \cdots, 2m/d\}$ decouples into $2m/d$ independent sub-decoding problems. We have

$$\hat{\boldsymbol{x}}_\ell(\boldsymbol{x}_{2m+1}) = \arg\min_{\boldsymbol{x}_\ell} (\boldsymbol{x}_\ell - \tilde{\boldsymbol{x}}_\ell(\boldsymbol{x}_{2m+1}))\left(\mathcal{H}_\ell\mathcal{H}_\ell^\dagger + \overline{\mathcal{H}_\ell\mathcal{H}_\ell^\dagger}\right)(\boldsymbol{x}_\ell - \tilde{\boldsymbol{x}}_\ell(\boldsymbol{x}_{2m+1}))^{\mathsf{T}}. \tag{4.25}$$

For a square N-QAM constellation the complexity of the above $2m/d$ minimization is $\mathcal{O}(N^{(d-1)/2})$ using conditional optimization, while for a general constellation the complexity is $\mathcal{O}(N^d)$. Suhstituting (4.17) into (4.15) we obtain the optimization problem for $\boldsymbol{x}_{2m+1}$:

$$\hat{\boldsymbol{x}}_{2m+1} = \arg\min_{\boldsymbol{x}_{2m+1}} \left\| \boldsymbol{y} - \sum_{\ell=1}^{2m/d} \hat{\boldsymbol{x}}_\ell(\boldsymbol{x}_{2m+1})\mathcal{H}_\ell - \boldsymbol{x}_{2m+1}\mathcal{H}_{2m+1} \right\|^2, \tag{4.26}$$

which can he suhstituted back into (4.25) to obtain the ML estimate of $\boldsymbol{x}_\ell$

$$\hat{\boldsymbol{x}}_\ell = \hat{\boldsymbol{x}}_\ell(\hat{\boldsymbol{x}}_{2m+1}), \quad \ell = 1, \cdots, 2m/d. \tag{4.27}$$

Thus, (4.25) and (4.26) provide an algorithm for ohtaining the ML estimate of $x_i, i = 1, \cdots, 2K$, which involves at most N^{K-m} evaluations of the right hand size of (4.26) for square N-QAM, with each evaluation having complexity $\mathcal{O}(N^{(d-1)/2})$, giving an overall complexity of $\mathcal{O}(N^{K-m+(d-1)/2})$. For a general constellation we need to evaluate (4.26) N^{K-m} times with each evaluation involving $2m/d$ parallel searches through N^d alternatives giving an overall complexity of $\mathcal{O}(N^{K-m+d})$. ∎

Of course, we can apply this general theorem to reproduce the conclusions of Chapter 3 for multiplexed orthogonal [55] and quasi-orthogonal designs [56]. However, somewhat surprisingly, this theorem also applies to the perfect space-time hlock codes of Oggier et al. [7] which we will show below have the structure of multiplexed quasi-orthogonal designs.

4.4 Examples

4.4.1 The Golden Code

Reeall that the Golden Code eodewords take the form

$$\mathbf{X} = \frac{1}{\sqrt{5}} \begin{pmatrix} \alpha & 0 \\ 0 & \bar{\alpha} \end{pmatrix} \left[\begin{pmatrix} x_1 & x_3 \\ ix_3 & x_1 \end{pmatrix} + \begin{pmatrix} \tau & 0 \\ 0 & \mu \end{pmatrix} \begin{pmatrix} x_2 & x_4 \\ ix_4 & x_2 \end{pmatrix} \right] \tag{4.28}$$

where $\alpha = (1 + i\mu)$ and $\bar{\alpha} = (1 + i\tau)$. This ean be written in terms of a real LD eode as

$$\mathbf{X} = \sum_{k=1}^{8} s_k A_k \tag{4.29}$$

with $s_1 = x_{1R}, s_2 = x_{1I}, s_3 = x_{2R}, s_4 = x_{2I}, s_5 = x_{3R}, s_6 = x_{3I}, s_7 = x_{4R}, s_8 = x_{4I}$, where subseripts nR and nI represent real and imaginary parts of symbol x_n, and

$$\begin{aligned} A_1 &= \begin{pmatrix} \alpha & 0 \\ 0 & \bar{\alpha} \end{pmatrix}, A_2 = \begin{pmatrix} i\alpha & 0 \\ 0 & i\bar{\alpha} \end{pmatrix}, A_3 = \begin{pmatrix} \alpha\tau & 0 \\ 0 & \bar{\alpha}\mu \end{pmatrix}, A_4 = \begin{pmatrix} i\alpha\tau & 0 \\ 0 & i\bar{\alpha}\mu \end{pmatrix} \\ A_5 &= \begin{pmatrix} 0 & \alpha \\ i\bar{\alpha} & 0 \end{pmatrix}, A_6 = \begin{pmatrix} 0 & i\alpha \\ -\bar{\alpha} & 0 \end{pmatrix}, A_7 = \begin{pmatrix} 0 & \alpha\tau \\ i\bar{\alpha}\mu & 0 \end{pmatrix}, A_8 = \begin{pmatrix} 0 & i\alpha\tau \\ -\bar{\alpha}\mu & 0 \end{pmatrix}. \end{aligned} \tag{4.30}$$

We ean interpret the Golden Code as a multiplexed pair of (4,2)-QOD leading to a fast ML deeoder. To see this eonsider the matriees

$$\mathcal{T} = \begin{pmatrix} \tau & 0 \\ 0 & \mu \end{pmatrix} \quad \text{and} \quad \mathcal{Z} = \begin{pmatrix} 0 & 1 \\ i & 0 \end{pmatrix} \tag{4.31}$$

and note that $\mathcal{Z}^8 = \mathbf{I}_2$. From $\mathcal{T}$ we ean construct a pair of diagonal matriees

$$\begin{aligned} B_1 &= (1 + i)\mathbf{I}_2 - i\mathcal{T} \\ B_2 &= -i\mathbf{I}_2 + \mathcal{T}, \end{aligned} \tag{4.32}$$

whieh satisfy

$$\mathrm{Tr}(B_j B_m^{\dagger}) = 5\delta_{jm}. \tag{4.33}$$

Note that $A_1 = B_1, A_2 = B_1\mathcal{Z}^2 = iB_1, A_3 = B_2, A_4 = B_2\mathcal{Z}^2 = iB_2, A_{k+4} = A_k\mathcal{Z}, k = 1, \ldots, 4$. It ean be verified that the subsets $\{A_k\}_{k=1}^4$ and $\{A_k\}_{k=5}^8$ satisfy the $(4, 2)$-QOD eonditions (4.7) and (4.8) with partition $\{1, 3\}, \{2, 4\}$ and $\{5, 7\}, \{6, 8\}$ respeetively. Therefore the Golden Code is the multiplexing of a pair of (4,2)-QOD with multiplexing matrix $\mathcal{Z}$,

$$\mathbf{X} = \mathbf{X}_1(x_{1R}, x_{2R}, x_{1I}, x_{2I}) + \mathbf{X}_2(x_{3R}, x_{4R}, x_{3I}, x_{4I})\mathcal{Z} \tag{4.34}$$

where

$$\mathbf{X}_i(a_1, a_2, a_3, a_4) = \sum_{k=1}^{4} a_k A_k. \tag{4.35}$$

The received signal can be written as

$$\boldsymbol{r} = \boldsymbol{x}_1\mathcal{H}_1 + \boldsymbol{x}_2\mathcal{H}_2 + \boldsymbol{n}, \tag{4.36}$$

where $\boldsymbol{x}_1 = (x_{1R}, x_{2R}, x_{1I}, x_{2I}), \boldsymbol{x}_2 = (x_{3R}, x_{4R}, x_{3I}, x_{4I})$ and also

$$\mathcal{H}_1\mathcal{H}_1^\dagger + \overline{\mathcal{H}_1\mathcal{H}_1^\dagger} = \begin{pmatrix} a & b & 0 & 0 \\ b & c & 0 & 0 \\ 0 & 0 & a & b \\ 0 & 0 & b & c \end{pmatrix} = \mathcal{H}_2\mathcal{H}_2^\dagger + \overline{\mathcal{H}_2\mathcal{H}_2^\dagger} \tag{4.37}$$

where a, b, c are some constants. Theorem 5 implies that the Golden Code has ML decoding complexity $\mathcal{O}(N^2\sqrt{N})$ (see [57, 52]) for square N-QAM constellations using the decoding algorithm of the last Section.

4.4.2 3×3 Perfect STBC

The perfect 3×3 STBC transmits nine complex (usually N-HEX constellation) information symbols over three time slots from three antennas. The codeword of the 3×3 perfect STBC can be expressed as

$$\mathbf{X} = \sum_{i=0}^{2} B_{i+1} \begin{pmatrix} x_{3i+1} & x_{3i+2} & x_{3i+3} \\ jx_{3i+3} & x_{3i+1} & x_{3i+2} \\ jx_{3i+2} & jx_{3i+3} & x_{3i+1} \end{pmatrix}, \tag{4.38}$$

where the diagonal matrices B_i are

$$\begin{aligned} B_1 &= (1+j)I_3 + \Theta \\ B_2 &= (-1-2j)I_3 + j\Theta^2 \\ B_3 &= (-1-2j)I_3 + (1+j)\Theta + (1+j)\Theta^2 \end{aligned} \tag{4.39}$$

with $\Theta = \mathrm{diag}(\theta_1, \theta_2, \theta_3), \theta_i = 2\cos(2^i\pi/7), j = e^{2\pi i/3}$ and B_i satisfy

$$\mathrm{Tr}(B_j B_m^\dagger) = 7\delta_{jm}. \tag{4.40}$$

Similarly, let

$$\begin{aligned} \boldsymbol{x}_1 &= (x_{1R}, x_{4R}, x_{7R}, x_{1I}, x_{4I}, x_{7I}), \\ \boldsymbol{x}_2 &= (x_{2R}, x_{5R}, x_{8R}, x_{2I}, x_{5I}, x_{8I}), \\ \boldsymbol{x}_3 &= (x_{3R}, x_{6R}, x_{9R}, x_{3I}, x_{6I}, x_{9I}), \end{aligned}$$

then the 3×3 perfect STBC (4.38) can be written as three (6,3)-QOD multiplexed as follows

$$\mathbf{X} = \mathbf{X}_1(\boldsymbol{x}_1) + \mathbf{X}_2(\boldsymbol{x}_2)\mathcal{Z} + \mathbf{X}_3(\boldsymbol{x}_3)\mathcal{Z}^2 \tag{4.41}$$

where

$$\mathbf{X}_i(s_1, s_2, s_3, s_4, s_5, s_6) = \sum_{k=1}^{6} s_k A_k, \tag{4.42}$$

$$\mathcal{Z} = \begin{pmatrix} 0 & 1 & 0 \\ 0 & 0 & 1 \\ j & 0 & 0 \end{pmatrix}, \tag{4.43}$$

and

$$A_1 = B_1, A_2 + B_2, A_3 = B_3, A_4 = iB_1, A_5 = iB_2, A_6 = iB_3. \tag{4.44}$$

In this ease the received signal is given by

$$\boldsymbol{r} = \boldsymbol{x}_1\mathcal{H}_1 + \boldsymbol{x}_2\mathcal{H}_2 + \boldsymbol{x}_3\mathcal{H}_3 + \boldsymbol{n} \tag{4.45}$$

and

$$\begin{aligned} \mathcal{H}_1\mathcal{H}_1^\dagger + \overline{\mathcal{H}_1\mathcal{H}_1^\dagger} &= \mathcal{H}_2\mathcal{H}_2^\dagger + \overline{\mathcal{H}_2\mathcal{H}_2^\dagger} = \mathcal{H}_3\mathcal{H}_3^\dagger + \overline{\mathcal{H}_3\mathcal{H}_3^\dagger} \\ &= \begin{pmatrix} \mathbf{M}_3 & \mathbf{0}_3 \\ \mathbf{0}_3 & \mathbf{M}_3 \end{pmatrix}. \end{aligned} \tag{4.46}$$

Theorem 5 implies that the 3×3 perfeet STBC has ML decoding complexity $\mathcal{O}(N^7)$ for square QAM constellations.

4.4.3 4×4 Perfect STBC

The 4×4 perfeet STBC transmits 16 complex (N-QAM eonstellation) information symbols $\{x_i\}_{i=1}^{16}$ over four times slots from four antennas. The eodewords ean be expressed as

$$\mathbf{X} = \sum_{i=0}^{3} B_{i+1} \begin{pmatrix} x_{4i+1} & x_{4i+2} & x_{4i+3} & x_{4i+4} \\ ix_{4i+4} & x_{4i+1} & x_{4i+2} & x_{4i+3} \\ ix_{4i+3} & ix_{4i+4} & x_{4i+1} & x_{4i+2} \\ ix_{4i+2} & ix_{4i+3} & ix_{4i+4} & x_{4i+1} \end{pmatrix}, \tag{4.47}$$

where

$$\begin{aligned} B_1 &= (1-3i)I_4 + i\Theta^2 \\ B_2 &= (1-3i)\Theta + i\Theta^3 \\ B_3 &= -iI_4 + (-3+4i)\Theta + (1-i)\Theta^3 \\ B_4 &= (-1+i)I_4 - 3\Theta + \Theta^2 + \Theta^3 \end{aligned}$$

with $\Theta = \mathrm{diag}(\theta_1, \theta_2, \theta_3, \theta_4), \theta_i = 2\cos(2^i\pi/15)$, and

$$\mathrm{Tr}(B_j B_m^\dagger) = 15\delta_{jm}. \tag{4.48}$$

Write

$$\begin{aligned} \boldsymbol{x}_1 &= (x_{1R}, x_{5R}, x_{9R}, x_{13R}, x_{1I}, x_{5I}, x_{9I}, x_{13I}), \\ \boldsymbol{x}_2 &= (x_{2R}, x_{6R}, x_{10R}, x_{14R}, x_{2I}, x_{6I}, x_{10I}, x_{14I}), \\ \boldsymbol{x}_3 &= (x_{3R}, x_{7R}, x_{11R}, x_{15R}, x_{3I}, x_{7I}, x_{11I}, x_{15I}), \\ \boldsymbol{x}_4 &= (x_{4R}, x_{8R}, x_{12R}, x_{16R}, x_{4I}, x_{8I}, x_{12I}, x_{16I}). \end{aligned}$$

The 4×4 perfect STBC (4.47) can be written as four $(8, 4)$-QOD multiplexed as follows

$$\mathbf{X} = \mathbf{X}_1(\boldsymbol{x}_1) + \mathbf{X}_2(\boldsymbol{x}_2)\mathcal{Z} + \mathbf{X}_3(\boldsymbol{x}_3)\mathcal{Z}^2 + \mathbf{X}_4(\boldsymbol{x}_4)\mathcal{Z}^3, \tag{4.49}$$

where

$$\mathbf{X}_i(s_1, s_2, s_3, s_4, s_5, s_6, s_7, s_8) = \sum_{k=1}^{8} s_k A_k, \tag{4.50}$$

$$\mathcal{Z} = \begin{pmatrix} 0 & 1 & 0 & 0 \\ 0 & 0 & 1 & 0 \\ 0 & 0 & 0 & 1 \\ i & 0 & 0 & 0 \end{pmatrix} \tag{4.51}$$

and

$$A_1 = B_1, A_2 = B_2, A_3 = B_3, A_4 = B_4, A_5 = iB_1, A_6 = iB_2, A_7 = iB_3, A_8 = iB_4.$$

The received signal is

$$\boldsymbol{r} = \boldsymbol{x}_1\mathcal{H}_1 + \boldsymbol{x}_2\mathcal{H}_2 + \boldsymbol{x}_3\mathcal{H}_3 + \boldsymbol{x}_4\mathcal{H}_4 + \boldsymbol{n} \tag{4.52}$$

and

$$\begin{aligned} \mathcal{H}_1\mathcal{H}_1^\dagger + \overline{\mathcal{H}_1\mathcal{H}_1^\dagger} = \mathcal{H}_2\mathcal{H}_2^\dagger + \overline{\mathcal{H}_2\mathcal{H}_2^\dagger} = \mathcal{H}_3\mathcal{H}_3^\dagger + \overline{\mathcal{H}_3\mathcal{H}_3^\dagger} = \mathcal{H}_4\mathcal{H}_4^\dagger + \overline{\mathcal{H}_4\mathcal{H}_4^\dagger} \\ = \begin{pmatrix} \mathbf{M}_4 & \mathbf{0}_4 \\ \mathbf{0}_4 & \mathbf{M}_4 \end{pmatrix}, \end{aligned} \tag{4.53}$$

Theorem 5 implies that the 4×4 perfect STBC has ML decoding complexity $O(N^{13}\sqrt{N})$ for square QAM.

Chapter 5: Space-Polarization-Time System

The performance of MIMO systems is highly dependent on the availability of a rich scattering environment (e.g. densely urban and indoor) as well as sufficient antenna spacing to achieve multiplexing or diversity gain. In rural and remote environments the wide open space and flat or smooth undulating terrain give rise to LOS conditions dominating between the transmitter and the receiver and consequently to a loss of diversity. In order to achieve significant multiplexing or diversity gain, many wavelengths spacing between antenna elements at the base station, and up to a wavelength at a mobile unit are required [58]. As the polarization of transmitted signals is mostly preserved by the LOS environment, the use of dual-polarized antennas (polarization diversity) is a promising cost and space effective alternative, where two spatially separated uni-polarized antennas are replaced by a single antenna structure employing orthogonal polarization. In this chapter we investigate the performance of various transmission schemes for coding onto a dual polarimetric antenna.

We begin with a brief overview of electromagnetic polarization and polarimetic transmission systems by following [59].

5.1 Polarization

Polarization is a property of the electromagnetic plane wave solutions of Maxwell's equations. In an infinite medium in which there are no sources, Maxwell's equations have so-called plane wave solutions of the form

$$\boldsymbol{E}(\boldsymbol{x},t) = \boldsymbol{\mathcal{E}} e^{i(\boldsymbol{k}\cdot\boldsymbol{x}-\omega t)}, \tag{5.1}$$

$$\boldsymbol{B}(\boldsymbol{x},t) = \boldsymbol{\mathcal{B}} e^{i(\boldsymbol{k}\cdot\boldsymbol{x}-\omega t)}, \tag{5.2}$$

where t denotes time, $\boldsymbol{x} \in \mathbb{R}^3$ denotes a point in space and $\boldsymbol{\mathcal{E}}$ and $\boldsymbol{\mathcal{B}} \in \mathbb{C}^3$. The (angular) frequency of the plain wave is ω and $\boldsymbol{k}$ is called the wave vector of the plane wave. In order to be solutions of Maxwell's equations the following relations must hold

$$\boldsymbol{k}\cdot\boldsymbol{k} = \mu\epsilon\frac{\omega^2}{c^2}, \tag{5.3}$$

$$\hat{\boldsymbol{k}}\cdot\boldsymbol{\mathcal{E}} = 0, \tag{5.4}$$

$$\hat{\boldsymbol{k}}\cdot\boldsymbol{\mathcal{B}} = 0, \tag{5.5}$$

$$\boldsymbol{\mathcal{B}} = \sqrt{\mu\epsilon}\,\hat{\boldsymbol{k}}\times\boldsymbol{\mathcal{E}}. \tag{5.6}$$

Equations (5.1) and (5.2) are a complex solution to Maxwell's equations. Physical solutions are given by both the real and imaginary components of this solution. The unit vector $\hat{\boldsymbol{k}}$ determines the direction of propagation of the plane wave. Equations (5.4) and (5.5) imply that the $\boldsymbol{E}$ and $\boldsymbol{B}$ are in the plane perpendicular to the direction of propagation $\hat{\boldsymbol{k}}$. Furthermore, equation (5.6) implies that E and B are perpendicular to each other.

The concept of polarization of a plane wave is related to the nature of the vector $\boldsymbol{\mathcal{E}}$. Suppose that ϵ_1 and $\epsilon_2 \in \mathbb{R}^3$ are orthogonal real unit vectors which are both orthogonal to $\hat{\boldsymbol{k}}$, the direction of propagation. Since $\boldsymbol{\mathcal{E}}$ is orthogonal to $\hat{\boldsymbol{k}}$, it is a complex linear combination of ϵ_1 and ϵ_2

$$\boldsymbol{\mathcal{E}} = E_1\epsilon_1 + E_2\epsilon_2, \tag{5.7}$$

where E_1 and E_2 are complex numbers. If the complex phases of E_1 and E_2 are equal, so that $E_1 = |E_1|e^{i\phi}$ and $E_2 = |E_2|e^{i\phi}$, then the real electric field is

$$\boldsymbol{E}(\boldsymbol{x}, t) = \sqrt{|E_1|^2 + |E_2|^2}\, \boldsymbol{e} \cos(\boldsymbol{k} \cdot \boldsymbol{x} - \omega t + \phi), \tag{5.8}$$

where $\boldsymbol{e}$ is the unit vector

$$\boldsymbol{e} = (|E_1|\boldsymbol{\epsilon}_1 + |E_2|\boldsymbol{\epsilon}_2) / (\sqrt{|E_1|^2 + |E_2|^2}). \tag{5.9}$$

We see that in this case the electric field oscillates between $\pm\sqrt{|E_1|^2 + |E_2|^2}\, \boldsymbol{e}$ always remaining parallel to $\boldsymbol{e}$. In this case the plane wave is said to be *linearly polarized* in direction $\boldsymbol{e}$. In situations where the plane wave propagates parallel to the surface to the Earth, waves linearly polarized in a direction perpendicular to the Earth's surface are called *vertically polarized* and those linearly polarized in a direction parallel to the Earth's surface are called *horizontally polarized*.

Another important type of polarization occurs when $|E_1| = |E_2|$ and the phase of E_1 is different from that of E_2 by $\pm\pi/2$, so that $E_2 = \pm iE_1$. The real electric field then has the form

$$\boldsymbol{E}(\boldsymbol{x}, t) = |E_1| \left(\boldsymbol{\epsilon}_1 \cos(\boldsymbol{k} \cdot \boldsymbol{x} - \omega t + \phi) \mp \boldsymbol{\epsilon}_2 \sin(\boldsymbol{k} \cdot \boldsymbol{x} - \omega t + \phi)\right). \tag{5.10}$$

Notice that here $\boldsymbol{E}$ just rotates around a circle of radius $|E_1|$ with angular frequency ω radians/sec. Such waves are called *circularly* polarized. The two possibilities $\mp$ in Equation (5.10) correspond to the $\boldsymbol{E}$ rotating in opposite directions around the circle. These two possibilities are referred to as being *left-handed* and *right-handed* circularly polarized depending on the convention chosen. Finally, we note that a plane wave which is not linearly or circularly polarized is said to be *elliptically* polarized.

5.2 Polarimetric Transmission Systems

The vector potential for a sinusoidally oscillating source (antenna), that is, a source consisting of localized charges and current with charge and current densities of the form

$$\rho(\boldsymbol{x}, t) = \rho(\boldsymbol{x}) e^{i\omega t} \tag{5.11}$$

$$\boldsymbol{J}(\boldsymbol{x}, t) = \boldsymbol{J}(\boldsymbol{x}) e^{i\omega t} \tag{5.12}$$

which is small compared to the wavelength is

$$\boldsymbol{A}(\boldsymbol{x}, t) = -ik\boldsymbol{p} \frac{e^{i(kr - \omega t)}}{r} \tag{5.13}$$

where for free space $k = \omega/c$ and r is the distance between the transmitter and the receiver. Here $\boldsymbol{p}$ is a possibly complex valued *electric dipole moment* of the source

$$\boldsymbol{p} = \int \boldsymbol{x}' \rho(\boldsymbol{x}')\, d\boldsymbol{x}'. \tag{5.14}$$

The corresponding electric and magnetic fields are

$$\boldsymbol{B} = \nabla \times \mathbf{A} = k^2(\boldsymbol{n} \times \boldsymbol{p})\frac{e^{i(kr-\omega t)}}{r}\left(1 - \frac{1}{ikr}\right) \tag{5.15}$$

$$\boldsymbol{E} = \frac{i}{k}\nabla \times \boldsymbol{B} = \frac{e^{i(kr-\omega t)}}{r}\left(k^2(\boldsymbol{n} \times \boldsymbol{p}) \times \boldsymbol{n} + (3\boldsymbol{n}(\boldsymbol{n} \cdot \boldsymbol{p}) - \boldsymbol{p})\left(\frac{1}{r^2} - \frac{ik}{r}\right)\right). \tag{5.16}$$

where $\boldsymbol{x} = r\boldsymbol{n}$. In the far field or radiation zone ($kr \gg 1$) this reduces to the limiting form

$$\boldsymbol{B} = k^2(\boldsymbol{n} \times \boldsymbol{p})\frac{e^{i(kr-\omega t)}}{r} \tag{5.17}$$

$$\boldsymbol{E} = k^2\left((\boldsymbol{n} \times \boldsymbol{p}) \times \boldsymbol{n}\right)\frac{e^{i(kr-\omega t)}}{r}. \tag{5.18}$$

The electric field can be rewritten as

$$\boldsymbol{E} = k^2\left(\boldsymbol{p} - (\boldsymbol{p} \cdot \boldsymbol{n})\boldsymbol{n}\right)\frac{e^{i(kr-\omega t)}}{r}. \tag{5.19}$$

Notice that $\boldsymbol{p} - (\boldsymbol{p} \cdot \boldsymbol{n})\boldsymbol{n}$ is the projection of the dipole moment $\boldsymbol{p}$ onto the plane perpendicular to $\boldsymbol{n}$. At a point $\boldsymbol{x} = r\boldsymbol{n}$ in space the electric and magnetic fields look locally like an outgoing plane wave with polarization vector $\boldsymbol{\mathcal{E}} = \boldsymbol{p} - (\boldsymbol{p} \cdot \boldsymbol{n})\boldsymbol{n}$.

For antennas which are small compared to a wavelength, which is often the case in mobile wireless communication systems, we can imagine having three feeds into the antenna configured in such a way that we have complete control over the dipole moment $\boldsymbol{p}$ of the antenna. For a larger antennas, or for concreteness in the case of small antennas, we consider so-called triad antennas. A triad antenna is composed of three orthogonal dipoles oriented along euclidean directions as shown in Figure 5.1. At the transmitter a triad antenna can generate an arbitrary oscillating dipole moment and consequently an arbitrary polarized electric field at the receiver, subject only to the constraints imposed by the physics of the electromagnetic field. A triad antenna at the receiver allows the receiver to measure the electric field as shown in Figure 5.2.

The use of triad antennas allows us to think of this MIMO system in an unusual way. Instead of thinking of the individual component antennas and the symbols coded onto them at the transmitter and read off at the receiver, we can think directly of coding onto a physical dipole moment vector at the transmitter and measuring the resulting electric field at the receiver.

Figure 5.1: Schematic of a triad antenna

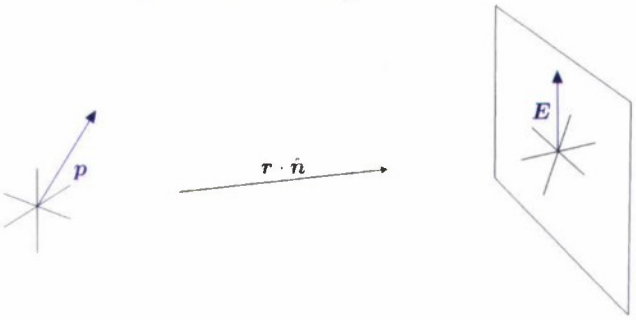

Figure 5.2: A triad antenna system. Electric field (E) at the receiver is perpendicular to the direction of propagation

A special case of the triad antenna is the more usual dual polarimetric antenna. A dual-polarized antenna consists of two co-located polarized antennas, typically *horizontal/vertical* ($0°/90°$) or *slanted* ($+45°/-45°$) as shown in Figure 5.3. The signals, say x_1 and x_2, are transmitted on the two different polarizations, and r_1 and r_2 are the signals received on the corresponding polarization. Note that, although there is one physical transmit and one physical receive antenna, the underlying channel is a two-input two-output channel since each polarization mode is treated as a separate physical channel.

Figure 5.3: Schematic of a dual-polarized antenna

5.3 Space-Polarization-Time System: Alamouti Signaling

Nabar et al. [58] have studied the performance of a system with one dual-polarized transmit and one dual-polarized received antenna with Alamouti signaling and spatial multiplexing. Deng et al. [60] have extended these results to the case of two dual-polarized transmit and one dual-polarized received antenna with Alamouti signaling and proposed a particular hybrid

transmission scheme. In this section we further analyze Deng et al's system and investigate the performance of two Alamouti multiplexing in the presence of polarization diversity and compare with the performance achieved using a uni-polarized scheme and the hybrid scheme of Deng et al. We analyze and predict the performance of the systems with different transmission schemes by applying the parameter λ developed in Chapter 2. The parameter λ measures the "*quaternionic angle*" between the two Alamouti channels.

5.4 MIMO Channel Model

Consider a MIMO wireless communication system with n_t transmit and n_r receive antennas. The channel is assumed to have quasi-static fading represented by a $n_r \times n_t$ matrix $\mathbf{H}$ with entries which are complex Gaussian random variables. The channel matrix can be decomposed into the sum of an average (LOS) component and a variable (scattered) component as

$$\mathbf{H} = \sqrt{\frac{K}{1+K}}\overline{\mathbf{H}} + \sqrt{\frac{1}{1+K}} R_r^{1/2} \widetilde{\mathbf{H}} R_t^{1/2} \tag{5.20}$$

where $E\{\mathbf{H}\} = \sqrt{\frac{K}{1+K}}\overline{\mathbf{H}}$ is the channel mean. The factor $\sqrt{\frac{K}{1+K}}$ and $\sqrt{\frac{1}{1+K}}$ are energy normalization factors and are related to the Riecan $K-$factor, with K being referred to as the $K-$factor. Note that $K = 0$ corresponds to the case of a pure Rayleigh fading channel and $K = \infty$ corresponds to the case of a pure LOS channel. $K = 10$ is used to represent the typical suburban environment of a personal communication system (PCS), with not very high building density and partial LOS [60]. The elements of the matrix $\widetilde{\mathbf{H}}$ are zero-mean circularly symmetric complex Gaussian random variables and unit variance. $R_t = R_t^{1/2} R_t^{1/2\dagger}$ and $R_r = R_r^{1/2} R_r^{1/2\dagger}$ are transmit and receive correlation matrices. The LOS component $\overline{\mathbf{H}}$ is modelled as

$$\overline{\mathbf{H}} = \beta \boldsymbol{a}_r \boldsymbol{a}_t^{\dagger} \tag{5.21}$$

where $\boldsymbol{a}_t$ and $\boldsymbol{a}_r$ are transmit and receive steering vectors and β is a complex gain. If the transmit and receive antennas are uniform linear arrays with spacing d then

$$\begin{aligned} \boldsymbol{a}_t &= (1, e^{-i\pi d \cos\theta_t}, \ldots, e^{-i\pi(n_t-1)d\cos\theta_t})^{\mathrm{T}} \\ \boldsymbol{a}_r &= (1, e^{-i\pi d \cos\theta_r}, \ldots, e^{-i\pi(n_r-1)d\cos\theta_r})^{\mathrm{T}} \end{aligned} \tag{5.22}$$

are the transmit and receive steering vectors respectively. We take $\overline{\mathbf{H}}$ to be normalized such that

$$\mathrm{Tr}(\overline{\mathbf{H}}^{\dagger}\mathbf{H}) = n_t n_r, \tag{5.23}$$

so that $|\beta| = 1$.

5.5 Dual-Polarized Channel Model

Consider a system with one dual-polarized transmit and one dual-polarized receive antenna. The 2×2 channel matrix

$$\mathbf{H} = \begin{pmatrix} h_{\mathrm{vv}} & h_{\mathrm{hv}} \\ h_{\mathrm{vh}} & h_{\mathrm{hh}} \end{pmatrix}, \tag{5.24}$$

is a polarization matrix where h_{vv} and h_{hh} represent path gain from vertical transmit to vertical receive antenna and from the horizontal transmit to the horizontal receive antenna, respectively. Similarly, h_{hv} and h_{vh} represent path gain from the horizontal transmit to the vertical receive antenna and vice versa. The elements of the matrix $\widetilde{\mathbf{H}}$, which are denoted as $\widetilde{h}_{ij}(i,j = \mathrm{v}, \mathrm{h})$ are zero-mean circularly symmetric complex Gaussian random variables whose variances depend on the propagation conditions and the antenna characteristics. We use the model given in [58], that is

$$\begin{aligned} E\{|\widetilde{h}_{vv}|^2\} &= E\{|\widetilde{h}_{hh}|^2\} = 1 \\ E\{|\widetilde{h}_{vh}|^2\} &= E\{|\widetilde{h}_{hv}|^2\} = \gamma, \end{aligned} \tag{5.25}$$

where $0 < \gamma \leq 1$ describes the cross polarization discrimination (XPD) or separation of orthogonal polarization for the variable component of the channel. γ is a composite of the properties of the antennas and the scattering environment (coupling between elements due to scattering). Good discrimination of orthogonal polarization corresponds to a small value of γ and vice versa. The elements of the matrix $\overline{\mathbf{H}}$, which are denoted as $\overline{h}_{ij}, (i,j = \mathrm{vh})$, are fixed complex numbers satisfying

$$|\overline{h}_{vv}|^2 = |\overline{h}_{hh}|^2 = 1, |\overline{h}_{vh}|^2 = |\overline{h}_{hv}|^2 = \gamma_f, \tag{5.26}$$

where $0 \leq \gamma_f \leq 1$ is related to the XPD for the LOS component. For pure LOS conditions, γ_f is solely a function of the antennas' ability to separate the orthogonal polarization.

It was stated in [58] that the experimental data collected in [61] and [62] shows that the elements of $\mathbf{H}$ are, in general, correlated. The correlation coefficients are therefore defined as

$$t = \frac{E\{\widetilde{h}_{vv}\widetilde{h}^*_{hv}\}}{\sqrt{\gamma}} = \frac{E\{\widetilde{h}_{vh}\widetilde{h}^*_{hh}\}}{\sqrt{\gamma_f}}, r = \frac{E\{\widetilde{h}_{vv}\widetilde{h}^*_{vh}\}}{\sqrt{\gamma}} = \frac{E\{\widetilde{h}_{hv}\widetilde{h}^*_{hh}\}}{\sqrt{\gamma_f}}, \tag{5.27}$$

where t is referred to as the transmit correlation coefficient, and r is the receive correlation coefficient. The experimental data [58] also reveals that the correlation between the diagonal element matrix $\widetilde{h}_{vv}$ and $\widetilde{h}_{hh}$ and the off-diagonal elements $\widetilde{h}_{vh}$ and $\widetilde{h}_{hv}$ is typically very small. Therefore, for simplicity, we assume that

$$E\{\widetilde{h}_{vv}\widetilde{h}^*_{hh}\} = E\{\widetilde{h}_{hv}\widetilde{h}^*_{vh}\} = 0. \tag{5.28}$$

Consider a two user system with two dual-polarized transmit and one dual-polarized receive antenna, where each user employs the Alamouti STBC over a dual-polarized transmit antenna. The equivalent polarization matrices from the first user to the first and second receive antenna, can be represented as

$$\mathcal{H}_1 = \begin{pmatrix} h_{vv} & h_{hv} \\ -h^*_{vh} & h^*_{vv} \end{pmatrix}, \quad \text{and} \quad \mathcal{H}_2 = \begin{pmatrix} h_{vh} & h_{hh} \\ -h^*_{hh} & h^*_{vh} \end{pmatrix}. \tag{5.29}$$

Similarly, the equivalent channel matrices for the second user to the first and second receive antenna are

$$\mathcal{G}_1 = \begin{pmatrix} g_{vv} & g_{hv} \\ -g^*_{vh} & g^*_{vv} \end{pmatrix}, \quad \text{and} \quad \mathcal{G}_2 = \begin{pmatrix} g_{vh} & g_{hh} \\ -g^*_{hh} & g^*_{vh} \end{pmatrix}. \tag{5.30}$$

We consider three different transmission schemes. The first is a uni-polarized system as described in Section 2, i.e. four vertically polarized transmit and two vertically polarized receive antennas, all spatially separated as shown in Figure 5.4.

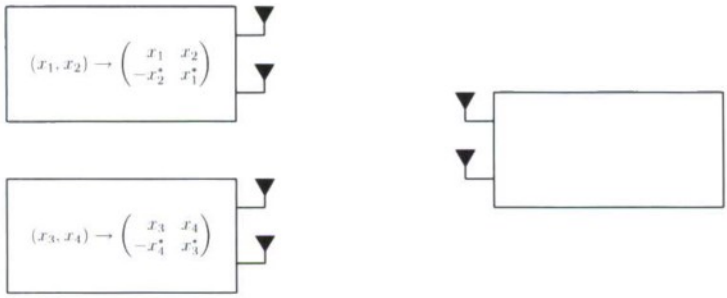

Figure 5.4: Scheme 1:Uni-polarized

The LOS components of the equivalent channel matrices are modelled as

$$\overline{\mathcal{H}}_1 = \begin{pmatrix} 1 & \mu_1 \\ -\mu_1^* & 1 \end{pmatrix}, \overline{\mathcal{H}}_2 = \begin{pmatrix} \mu_2 & \mu_3 \\ -\mu_3^* & \mu_2^* \end{pmatrix}, \overline{\mathcal{G}}_1 = \begin{pmatrix} \mu_4 & \mu_5 \\ -\mu_5^* & \mu_4^* \end{pmatrix}, \overline{\mathcal{G}}_2 = \begin{pmatrix} \mu_6 & \mu_7 \\ -\mu_7^* & \mu_6^* \end{pmatrix}, \quad (5.31)$$

where $\mu_1, \mu_2, \ldots, \mu_7$ are arbitrarily chosen unimodular complex numbers that represent the different LOS paths. Note that in this case $\gamma = 1$.

The second scheme consists of two dual-polarized transmit and one dual-polarized receive antenna and employs Alamouti STBC on each pair of dual-polarized transmit antennas as shown in Figure 5.5.

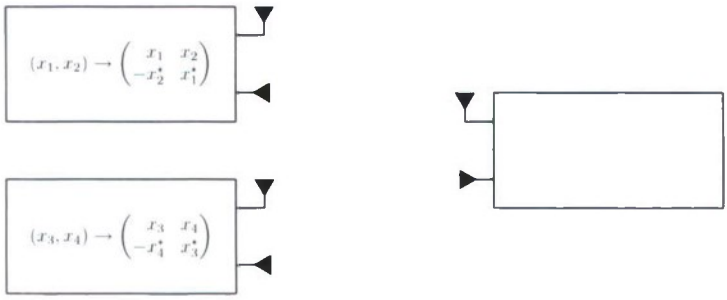

Figure 5.5: Scheme 2:Dual-polarized

This scheme will be referred to as the dual-polarized system and the equivalent LOS component channels are modelled as

$$\overline{\mathcal{H}}_1 = \begin{pmatrix} 1 & \sqrt{\gamma_f} \\ -\sqrt{\gamma_f} & 1 \end{pmatrix}, \overline{\mathcal{H}}_2 = \begin{pmatrix} \sqrt{\gamma_f} & 1 \\ -1 & \sqrt{\gamma_f} \end{pmatrix}, \overline{\mathcal{G}}_1 = \begin{pmatrix} \mu & \sqrt{\gamma_f}\mu \\ -\sqrt{\gamma_f}\mu^* & \mu^* \end{pmatrix}, \overline{\mathcal{G}}_2 = \begin{pmatrix} \sqrt{\gamma_f}\mu & \mu \\ -\mu^* & \sqrt{\gamma_f}\mu^* \end{pmatrix}, \quad (5.32)$$

where μ is again a unimodular eomplex number. Under the assumption that the reeeiver is in the far field of the transmit antenna, then $\mu = \exp(-\frac{2\pi i}{\lambda}\mathbf{n} \cdot \mathbf{\Delta})$, where λ is the earrier wavelength, $\mathbf{n}$ is the unit veetor in the direetion of the reeeiver and $\mathbf{\Delta}$ is the position of the seeond antenna relative to the first antenna. Furthermore, since the two orthogonal eomponents of eaeh of the dual polarized antennas are eo-loeated, their relative path differenee is zero.

The third seheme is that proposed by Deng et al. [60]. It also consists of two dual-polarized transmit antennas and one dual-polarized reeeive antenna, but employs Alamouti STBC on the same polarization aeross the two transmit antennas as shown in figure 5.6.

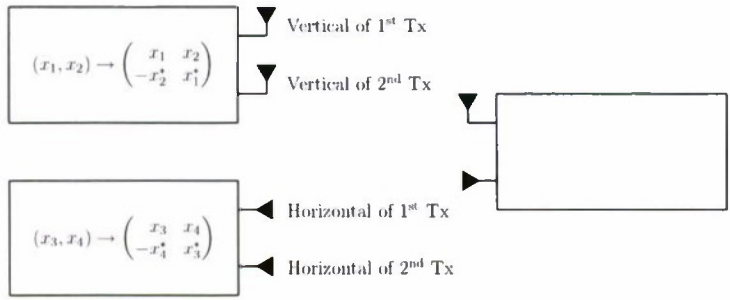

Figure 5.6: Scheme 3:Dual-polarized hybrid

In this ease the equivalent LOS ehannel matriees are modelled as follows

$$\overline{\mathcal{H}}_1=\begin{pmatrix} 1 & \mu \\ -\mu^* & 1 \end{pmatrix}, \overline{\mathcal{H}}_2=\begin{pmatrix} \sqrt{\gamma_f} & \sqrt{\gamma_f}\mu \\ -\sqrt{\gamma_f}\mu^* & \sqrt{\gamma_f} \end{pmatrix}, \overline{\mathcal{G}}_1=\begin{pmatrix} \sqrt{\gamma_f} & \sqrt{\gamma_f}\mu \\ -\sqrt{\gamma_f}\mu^* & \sqrt{\gamma_f} \end{pmatrix}, \overline{\mathcal{G}}_2=\begin{pmatrix} 1 & \mu \\ -\mu^* & 1 \end{pmatrix}, \quad (5.33)$$

where μ is as defined above.

5.6 Analysis and Simulation

We now analyse the three transmission sehemes deseribed above by applying the parameter λ obtained in Chapter 2. We eonsider both the Rayleigh fading ehannel and the Rieean ehannel where $K = 10$. In the simulation results reported here, the data symbols were taken from an 8-PSK eonstellation and deeoded with the algorithm given in (2.42) and (2.49). For the polarization sehemes we set the XPD parameters to $\gamma = 0.4$ and $\gamma_f = 0.3$ and for correlated ehannels, the transmit and reeeive eorrelation eoeffieients, as defined in (5.27), were ehosen to be $t = 0.5$ and $r = 0.3$.

Figure 5.7 illustrates how the angles between the ehannel matriees $|\lambda|^2$ are distributed for an uneorrelated Rayleigh fading ehannel, for the three different transmission sehemes. Figure 5.8 shows the symbol error rate ohtained under the same ehannel eonditions. Figure 5.9 and Figure 5.10 show the eorresponding results for the ease of an uneorrelated Rieean ehannel when $K = 10$. It is elear that the presenee of the LOS eomponent eauses the means of the $|\lambda|^2$ distrihutions to shift and the distributions to heeome more eoneentrated around the mean. The effect is quite pronounced even for relatively small values of K. This behavior holds generally and leads to the eonelusion that, when present, the angle hetween LOS paths is the dominant factor in the performanee of various sehemes.

Figure 5.11 shows the $|\lambda|^2$ distributions for three different LOS paths for correlated channels. Figure 5.12 shows the corresponding results with the XPD parameter set to $\gamma_f = 0.1$ rather than 0.3. Note that each row represents a different LOS path and each column represents different transmission schemes. It is evident that the $|\lambda|^2$ distributions for the unipolarized and dual-polarized schemes have considerable variability as the relative phases in the LOS components vary. However, what stands out is the stability of the $|\lambda|^2$ distribution for the dual-polarized hybrid transmission scheme. The distribution, and hence the performance of this scheme, is insensitive to the relative phases of the LOS components of the channel.

We can understand this behavior by considering the angles between the LOS components of the channels which we denote by λ_{LOS}. From (2.33) and (5.20), we have

$$\lambda_{\text{LOS}} = \frac{\bar{\mathcal{H}}^{\dagger}\bar{\mathcal{G}}}{|\bar{\mathcal{H}}|\,\|\bar{\mathcal{G}}\|}. \tag{5.34}$$

For the dual-polarized hybrid system

$$|\lambda_{\text{LOS}}| = \frac{2\sqrt{\gamma_f}}{1+\gamma_f}, \tag{5.35}$$

and for the dual-polarized system we have

$$|\lambda_{\text{LOS}}| = \sqrt{\cos^2\phi + \frac{4\gamma_f}{(1+\gamma_f)^2}\sin^2\phi}, \tag{5.36}$$

where $\phi = \angle\mu$.

We immediately note from (5.35), that $|\lambda_{\text{LOS}}|$ for the dual-polarized hybrid scheme depends only on γ_f. This explains why the dual-polarized hybrid scheme is robust to changes in the relative path lengths between the two dual polarized transmitters, as observed in Figures 5.11 and 5.12.

We note that for the dual-polarized scheme

$$\frac{2\sqrt{\gamma_f}}{1+\gamma_f} \leq |\lambda_{\text{LOS}}| \leq 1. \tag{5.37}$$

We have demonstrated that the performance parameter λ obtained in Chapter 2 can be used to analyze and predict the performance of different transmission schemes involving polarization diversity and the Alamouti codes. The results show that the performance is dominated by the "angle" between the component Alamouti channels. In designing transmission schemes that involve multiplexing Alamouti coded transmissions, one should aim for multiplexing schemes which keep the channel volume away from zero (see Section 2.8 on channel volume). This is the case for the dual-polarized hybrid scheme analysed here, which has a normalised channel volume dominated by the LOS channel volume

$$V_{\text{LOS}} = (1-\gamma_f)^2/(1+\gamma_f)^2. \tag{5.38}$$

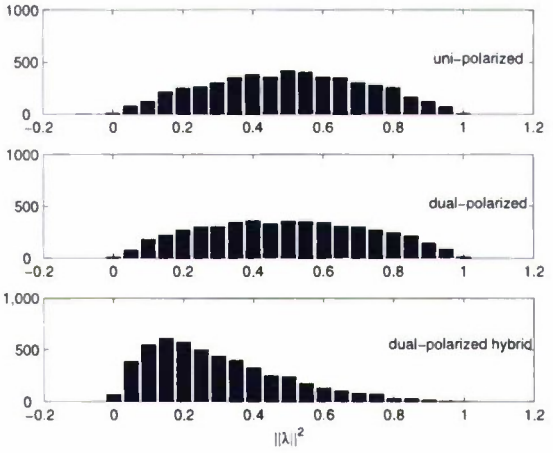

Figure 5.7: Distribution of $|\lambda|^2$ for three different transmission schemes over an uncorrelated Rayleigh channel

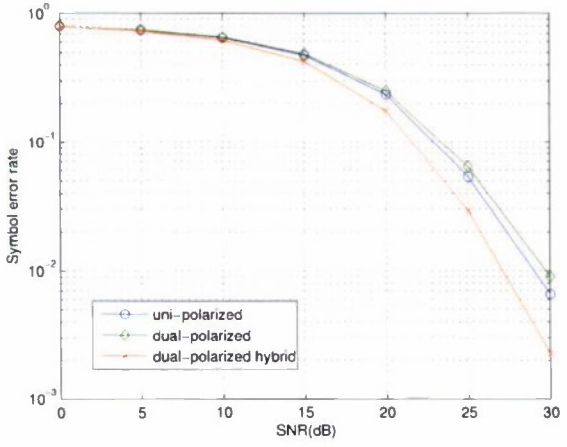

Figure 5.8: Performance of three different transmission schemes over an uncorrelated Rayleigh channel

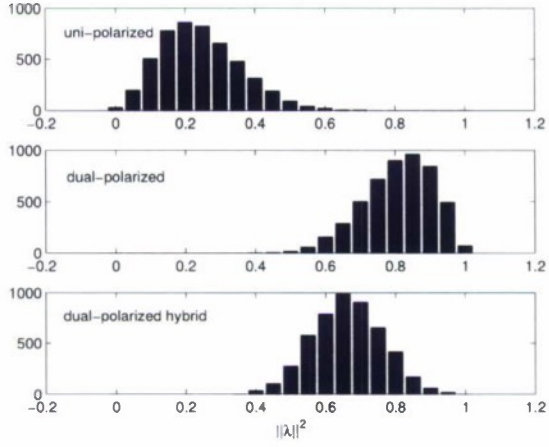

Figure 5.9: Distribution of $|\lambda|^2$ for different transmission schemes over an uncorrelated Ricean channel

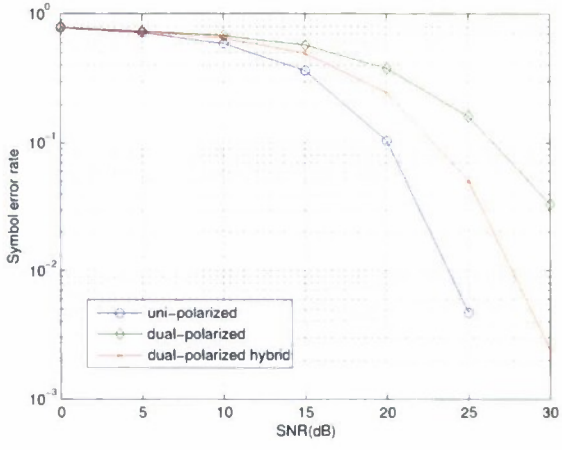

Figure 5.10: Performance of three different transmission schemes over an uncorrelated Ricean channel

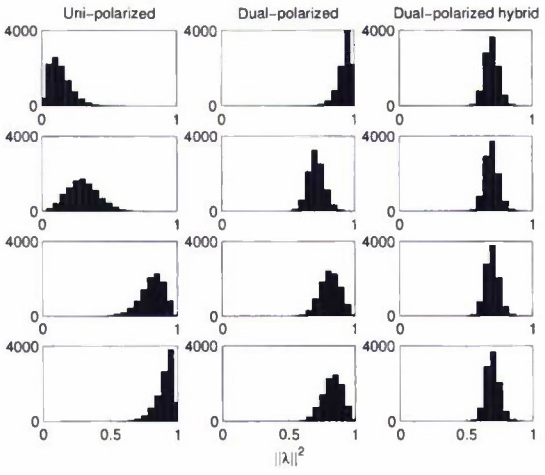

Figure 5.11: Distribution of $|\lambda|^2$ for three different LOSs, $\gamma_f = 0.3$

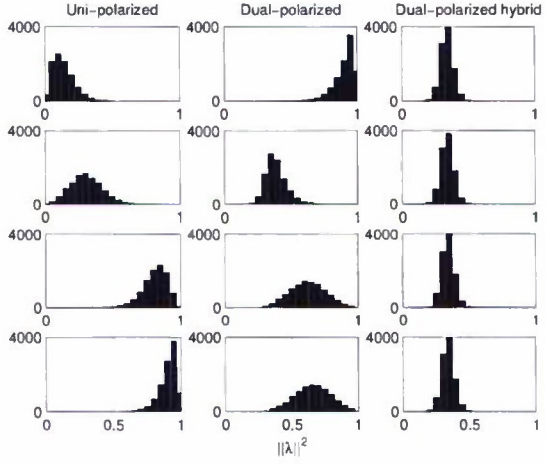

Figure 5.12: Distribution of $|\lambda|^2$ for three different LOSs, $\gamma_f = 0.1$

5.7 Polarization-Time System: The Golden Code

In the last section, we investigated the performance of three different transmission schemes using Alamouti STBCs across a pair of dual-polarized antennas at the transmitter. The results indicate that the performance is dominated by the LOS component and that polarization diversity along with an appropriate transmission scheme can provide stability of performance across changes in environmental conditions.

Typical of uni-polarized space-time systems, the performance of the Golden Code degrades considerably as the LOS component increases due to the loss of diversity. Figure 5.13 shows the simulated performance of 4-QAM and 16-QAM modulation in various channel conditions (pure scattering $K = 0$, Riccan $K = 10$ and pure LOS $K = \infty$ in uncorrelated channel). These simulation results show that the performance degrades as the $K-$ factor increases. In this chapter we consider the effect of LOS on the performance of the Golden Code and introduce a possible remedy with the use of dual-polarized antennas. We analyse the performance of the Golden Code in terms of angle between the channels corresponding to the two receivers, which allows us to predict the performance without necessarily needing to resort to simulations. Analysis and simulation results show that with the introduction of polarization diversity the performance of the Golden Code can be made consistently good across both rich scattering and LOS conditions.

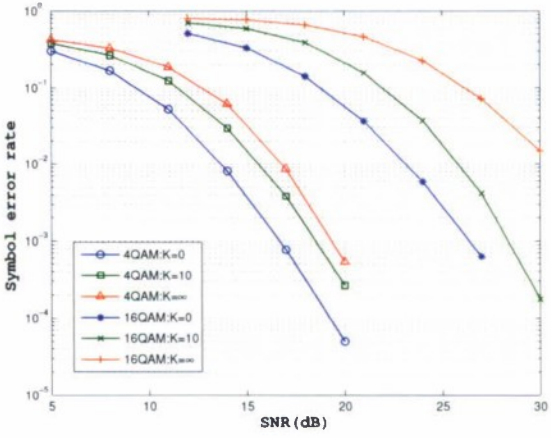

Figure 5.13: Performance of the Golden Code for uncorrelated uni-polarized channels from pure scattering to pure LOS

5.8 The Effect of LOS on the Performance

Codewords in the Golden Code take the form

$$\mathbf{X} = \begin{pmatrix} \alpha & 0 \\ 0 & \bar{\alpha} \end{pmatrix} \begin{pmatrix} x_1 + x_2\tau & x_3 + x_4\tau \\ i(x_3 + x_4\mu) & x_1 + x_2\mu \end{pmatrix} \tag{5.39}$$

where $\alpha = (1 + i\mu)/\sqrt{5}, \bar{\alpha} = (1 + i\tau)/\sqrt{5}$ and $\{x\}_{i=1}^{4} \in \mathcal{C} \subset \mathbb{Z}[i]$ are transmitted symbols, where $\mathcal{C}$ is a signal constellation taken to be $2^m - QAM$ and m bits per symbol. The parameters τ and μ are the real roots of the polynomial $x^2 - x - 1$, that is, the Golden ratio $\tau = (1 + \sqrt{5})/2$ and its algebraic conjugate $\mu = -1/\tau = (1 - \sqrt{5})/2$. The diagonal matrix $\mathrm{diag}(\alpha, \bar{\alpha})$ serves to equalize transmitted signal power across the two transmit antennas.

Let $\boldsymbol{r}_1 = (r_{11}, r_{12})$ and $\boldsymbol{r}_2 = (r_{21}, r_{22})$ be the two received signal vectors at the first and the second receiver and the components are the signals received over two consecutive time slots. For convenience, in what follows we will use the rescaled channel gains, $h_{1j} = \alpha h_{ij}$ and $h_{2j} = \alpha h_{2j}$ $\boldsymbol{c} = (x_1, x_3)$ and $\boldsymbol{s} = (x_2, x_4)$, so the received signals can be written as

$$\begin{aligned} \boldsymbol{r}_1 &= \boldsymbol{c}h + \boldsymbol{s}\tilde{h} + \boldsymbol{n}_1 \\ \boldsymbol{r}_2 &= \boldsymbol{c}g + \boldsymbol{s}\tilde{g} + \boldsymbol{n}_2 \end{aligned} \tag{5.40}$$

where

$$\begin{aligned} h &= \begin{pmatrix} h_{11} & h_{21} \\ ih_{21} & h_{11} \end{pmatrix}, \quad \tilde{h} = \begin{pmatrix} h_{11}\tau & h_{21}\mu \\ ih_{21}\mu & h_{11}\tau \end{pmatrix}, \\ g &= \begin{pmatrix} h_{12} & h_{22} \\ ih_{22} & h_{12} \end{pmatrix}, \quad \tilde{g} = \begin{pmatrix} h_{12}\tau & h_{22}\mu \\ ih_{22}\mu & h_{12}\tau \end{pmatrix}, \end{aligned} \tag{5.41}$$

where h_{ij} is the channel gain from transmit antenna i to the receive antenna j.

Given that the channel gains are known at the receivers and each symbol is transmitted with equal probability, optimal decoding is provided by the maximum a posterior/maximum likelihood (MAP/ML) estimate as follows. Let $\boldsymbol{r} = (\boldsymbol{r}_1, \boldsymbol{r}_2), \mathcal{H} = (h, \tilde{h})^{\mathrm{T}}$ and $\mathcal{G} = (g, \tilde{g})^{\mathrm{T}}$ and rewrite (5.40) as

$$\boldsymbol{r} = \boldsymbol{x}\mathbf{A} + \boldsymbol{n}, \tag{5.42}$$

where $\mathbf{A} = (\mathcal{H}, \mathcal{G})$ and $\boldsymbol{x} = (\boldsymbol{c}, \boldsymbol{s})$. The likelihood function of $\boldsymbol{x}$ given the received signal $\boldsymbol{r}$ is given by

$$p(\boldsymbol{r}|\boldsymbol{x}) \propto \exp\left(-\frac{1}{2\sigma^2}(\boldsymbol{x} - \tilde{\boldsymbol{x}})\mathbf{A}\mathbf{A}^{\dagger}(\boldsymbol{x} - \tilde{\boldsymbol{x}})^{\dagger}\right) \tag{5.43}$$

where

$$\tilde{\boldsymbol{x}} = \boldsymbol{r}\mathbf{A}^{\dagger}(\mathbf{A}\mathbf{A}^{\dagger})^{-1}. \tag{5.44}$$

Taking the prior distribution of $\boldsymbol{x}$ to be uniform on the constellation $\mathcal{C}$, we obtain the MAP/ML estimate:

$$\hat{\boldsymbol{x}} = \arg\max_{\boldsymbol{x} \in \mathcal{C}^4} p(\boldsymbol{r}|\boldsymbol{x}). \tag{5.45}$$

The performance of (5.45) in decoding $\boldsymbol{x}$ is determined by the determinant of $\mathbf{A}\mathbf{A}^{\dagger}$ or equivalently $\mathbf{A}^{\dagger}\mathbf{A}$. Since

$$\mathbf{A}^{\dagger}\mathbf{A} = \begin{pmatrix} \|\mathcal{H}\|_{\tau}^2 \mathbf{I}_2 & \mathcal{H}^{\dagger}\mathcal{G} \\ \mathcal{G}^{\dagger}\mathcal{H} & \|\mathcal{G}\|_{\tau}^2 \mathbf{I}_2 \end{pmatrix} \tag{5.46}$$

where

$$\begin{aligned} \|\mathcal{H}\|_{\tau}^2 &= (1 + \tau^2)|h_{11}|^2 + (1 + \mu^2)|h_{21}|^2, \\ \|\mathcal{G}\|_{\tau}^2 &= (1 + \tau^2)|h_{12}|^2 + (1 + \mu^2)|h_{22}|^2, \end{aligned} \tag{5.47}$$

we have

$$\det(\mathbf{A}^{\dagger}\mathbf{A}) = \|\mathcal{H}\|_{\tau}^{4} \|\mathcal{G}\|_{\tau}^{4} (1 - |\lambda|^2)^2 \tag{5.48}$$

where

$$\lambda = \frac{\mathcal{H}^{\dagger}\mathcal{G}}{\|\mathcal{H}\|_{\tau} \|\mathcal{G}\|_{\tau}}. \tag{5.49}$$

The parameter λ is an inner product of two unit cyclotomic vectors and it represents the differences (angle) between the channel components $\mathcal{H}$ and $\mathcal{G}$. A similar measure to this parameter which represents the angle between two Alamouti users was given in Section 2.4, [48] and was used to predict the performance of various Alamouti transmission schemes involving dual-polarized antennas (see [40] for details). Good performance corresponds to small values of $|\lambda|^2$ and vice versa.

Consider the capacity of the equivalent channel matrix $\mathbf{A}$ which is given by [9],

$$\begin{aligned} C(\mathbf{A}) &= \frac{1}{2} E\left[\log\left(\det\left(\mathbf{I}_4 + \frac{E_s}{4\sigma^2}\mathbf{A}^{\dagger}\mathbf{A}\right)\right)\right] \\ &= \frac{1}{2} E\left[\log \prod_{i=1}^{2}\left(1 + \frac{E_s}{4\sigma^2} e_i\right)^2\right] \end{aligned} \tag{5.50}$$

where E_s is an average transmitted signal power and e_i are eigenvalues of $\mathbf{A}^{\dagger}\mathbf{A}$ with multiplicity 2 and are

$$e_{1,2} = \frac{\|\mathcal{H}\|_{\tau}^2 \|\mathcal{G}\|_{\tau}^2}{2}\left[1 \pm \sqrt{1 - \frac{4\|\mathcal{H}\|_{\tau}^2 \|\mathcal{G}\|_{\tau}^2}{\|\mathcal{H}\|_{\tau}^2 + \|\mathcal{G}\|_{\tau}^2}(1 - |\lambda|^2)}\right]. \tag{5.51}$$

This implies that the capacity of the channel depends on the parameter λ. If $|\lambda|^2 = 0$ then we have

$$e_1 = \|\mathcal{H}\|_{\tau}^2 \quad \text{and} \quad e_2 = \|\mathcal{G}\|_{\tau}^2 \tag{5.52}$$

and the corresponding capacity

$$C_{|\lambda|^2=0}(\mathbf{A}) = 2E\left[\log\left(\left(1 + \frac{E_s}{4\sigma^2}\|\mathcal{H}\|_{\tau}^2\right)\left(1 + \frac{E_s}{4\sigma^2}\|\mathcal{G}\|_{\tau}^2\right)\right)\right]. \tag{5.53}$$

If $|\lambda|^2 = 1$ then the channel is rank deficient, that is

$$e_1 = \|\mathcal{H}\|_{\tau}^2 + \|\mathcal{G}\|_{\tau}^2 \quad \text{and} \quad e_2 = 0, \tag{5.54}$$

and the corresponding capacity is

$$C_{|\lambda|^2=1}(\mathbf{A}) = 2E\left[\log\left(1 + \frac{E_s}{4\sigma^2}\left(\|\mathcal{H}\|_{\tau}^2 + \|\mathcal{G}\|_{\tau}^2\right)\right)\right]. \tag{5.55}$$

Consider the case of a pure scattering channel, i.e. $K = 0$, then the values of $|\lambda|^2$ is uniformly distributed between $[0, 1]$ and can be explicitly written as

$$|\lambda|_{K=0}^2 = \frac{|(\hat{h}, \hat{g})_{\tau}|^2}{\left\|\hat{\mathcal{H}}\right\|_{\tau}^2 \left\|\hat{\mathcal{G}}\right\|_{\tau}^2} \tag{5.56}$$

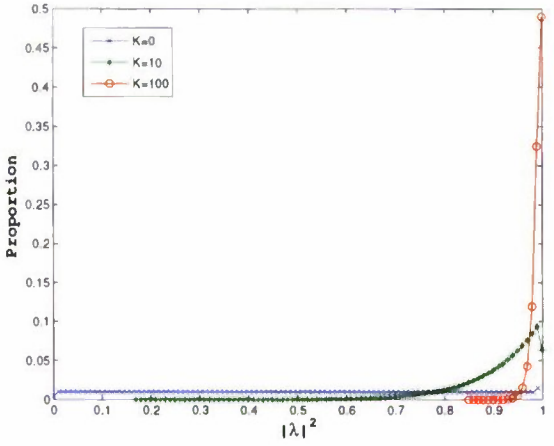

Figure 5.14: Distribution of $|\lambda|^2$ for uncorrelated uni-polarized channels

where

$$\begin{aligned}(\hat{h},\hat{g})_\tau &= (1+\tau^2)\hat{h}_{11}^*\hat{h}_{12} + (1+\mu^2)\hat{h}_{21}^*\hat{h}_{22},\\ \left\|\hat{\mathcal{H}}\right\|_\tau^2 &= (1+\tau^2)|\hat{h}_{11}|^2 + (1+\mu^2)|\hat{h}_{21}|^2,\\ \left\|\hat{\mathcal{G}}\right\|_\tau^2 &= (1+\tau^2)|\hat{h}_{12}|^2 + (1+\mu^2)|\hat{h}_{22}|^2.\end{aligned} \tag{5.57}$$

It is also clear from (5.56) that in the pure scattering environment, the channel becomes rank deficient, i.e. $|\lambda|^2_{K=0} = 1$, only if $\hat{h}_{11}\hat{h}_{22} = \hat{h}_{21}\hat{h}_{12}$ or equivalently $\det(\mathbf{H}) = 0$. As K increases $\overline{\mathbf{H}}$ dominates the behaviour of the system and when $K = \infty$, which corresponds to pure LOS channels, we have

$$\overline{\mathcal{H}} = \begin{pmatrix} 1 & e^{i\pi\cos\theta_T} \\ ie^{i\pi\cos\theta_T} & 1 \\ \tau & \mu e^{i\pi\cos\theta_T} \\ i\mu e^{i\pi\cos\theta_T} & \tau \end{pmatrix}, \quad \overline{\mathcal{G}} = \begin{pmatrix} e^{-i\pi\cos\theta_R} & e^{i\pi(\cos\theta_T-\cos\theta_R)} \\ ie^{i\pi(\cos\theta_T-\cos\theta_R)} & e^{-i\pi\cos\theta_R} \\ \tau e^{-i\pi\cos\theta_R} & \mu e^{i\pi(\cos\theta_T-\cos\theta_R)} \\ i\mu e^{i\pi(\cos\theta_T-\cos\theta_R)} & \tau e^{-i\pi\cos\theta_R} \end{pmatrix}.$$

Substituting these values into (2.33), we obtain

$$|\lambda|^2_{LOS} = 1, \tag{5.58}$$

i.e. the channel is rank-deficient hence resulting in the performance degradation.

Figure 5.13 shows the results of simulated performance of the Golden Code with 4-QAM and 16-QAM modulation in various channel conditions (pure scattering ($K = 0$), Ricean ($K = 10$) and pure LOS ($K = \infty$) in uncorrelated channels). Figure 5.14 shows the empirical distribution of $|\lambda|^2$ for $K = 0, 10$ and 100. Clearly, as the K-factor increases the mean of the distribution of $|\lambda|^2$ shifts toward $|\lambda|^2 = 1$. Thus, as expected, the distribution of $|\lambda|^2$

indicates that the performance degrades as K increases. The distribution of $|\lambda|^2$ agrees with the simulation results.

5.9 Golden Code and Polarization Diversity

Consider Golden Code signaling using one dual-polarized transmit and one dual-polarized receive antenna. Based on the channel model given by Nabar et al.[58] as described in Section 5.5, the LOS component can be explicitly written as

$$\overline{\mathcal{H}} = \begin{pmatrix} 1 & \sqrt{\gamma_f} \\ i\sqrt{\gamma_f} & 1 \\ \tau & \sqrt{\gamma_f}\mu \\ i\sqrt{\gamma_f}\mu & \tau \end{pmatrix}, \quad \overline{\mathcal{G}} = \begin{pmatrix} \sqrt{\gamma_f} & 1 \\ i & \sqrt{\gamma_f} \\ \sqrt{\gamma_f}\tau & \mu \\ i\mu & \sqrt{\gamma_f}\tau \end{pmatrix}. \tag{5.59}$$

Substituting this into (5.34), we find

$$|\lambda|^2_{LOS} = \frac{(2+\tau^2+\mu^2)^2\gamma_f}{[(1+\tau^2)+(1+\mu^2)\gamma_f][(1+\tau^2)\gamma_f+(1+\mu^2)]}. \tag{5.60}$$

If $\gamma_f < 1$, then $|\lambda|^2_{LOS} < 1$. As (5.60) shows, the antenna's cross-polarization discrimination (γ_f) will determine the mean performance of the system. For a pure LOS condition, the performance depends solely on the antenna's ability to separate the orthogonal polarization. Therefore as the $K-$ factor increases the effect of polarization diversity is to reduce the probability that the channel will be rank-deficient, thus resulting in a diversity gain.

We can predict the performance of the Golden Code in the presence of polarization diversity based on the distribution of the parameter $|\lambda|^2$. Figure 5.15 shows the distribution of $|\lambda|^2$ for $K = 0, 10, 100$ when dual-polarized antennas are used. Compared to the case of uni-polarized antennas in Figure 5.14, the mean of the $|\lambda|^2$ for $K > 0$ is now shifted away from the value 1. The simulation results in Figure 5.16 demonstrate the benefit of dual-polarized antennas in the high K environments as predicted in Figure 5.15. Note that for pure LOS conditions ($K = \infty$) the channel is fixed, therefore the probability of error decays exponentially with SNR and so no diversity order can be defined.

Figure 5.17 shows the distribution of $|\lambda|^2$ in a correlated environment, with $t = 0.5, r = 0.3$. We can see from the distribution that for a pure Rayleigh channel ($K = 0$), $|\lambda|^2$ is no longer uniformly distributed but biased toward 1. Hence the performance will degrade compared to an un-correlated environment. Figure 5.18 demonstrates that, for $K > 0$, the better the separation of orthogonal polarization (smaller γ_f), the better the improvement in performance.

5.10 Summary

We investigated the performance of three different transmission schemes for using Alamouti STBCs across a pair of spatially separated dual-polarized transmit antennas. The results indicate that the performance is dominated by the LOS component and that polarization diversity along with an appropriate transmission scheme can provide stability of performance across changes in environmental conditions. We went on to investigate the performance of the Golden Code using polarization in various environmental conditions from rich scattering to pure line

of sight. Our analysis leads to a performance parameter which represents the angle between the channels to the two receivers and can be used to predict performance. We have analysed how the performance of the Golden Code degrades as the environmental K-factor increases. When the Golden Code is used to code across orthogonal polarizations of a dual-polarized transmit antenna, rather than across spatially separated antennas, we have shown that polarization diversity can lead to consistently good performance across environmental conditions from rich scattering to pure line of sight. The simulation results agree with our analysis. We note that the approach is not restricted to the Golden Code but can be applied to most STBCs.

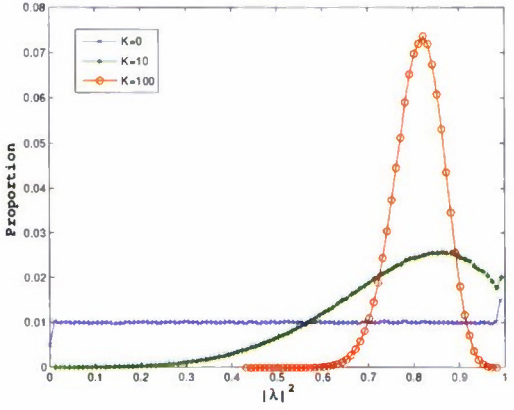

Figure 5.15: Distribution of $|\lambda|^2$ for uncorrelated channels with polarized antennas, $\gamma_f = 0.4$

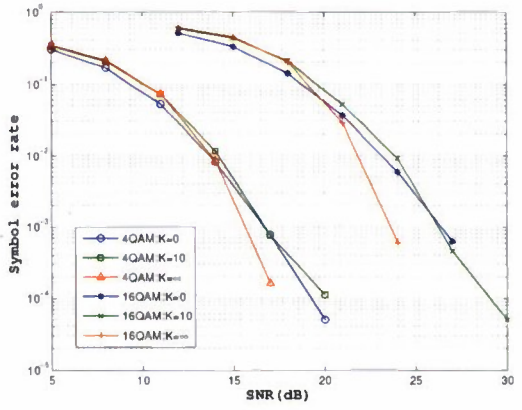

Figure 5.16: Performance of the Golden Code for uncorrelated channels with polarized antennas, $\gamma_f = 0.4$

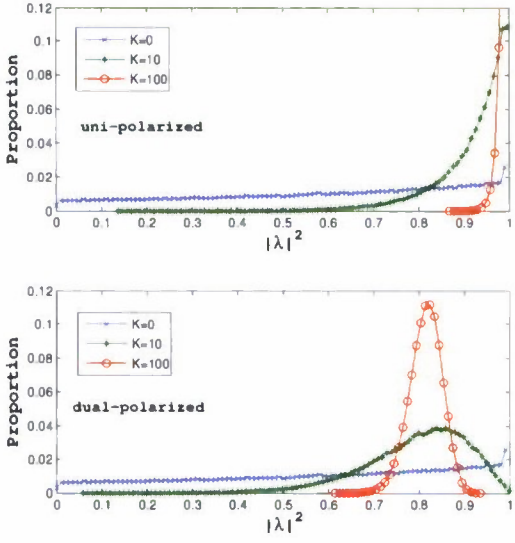

Figure 5.17: Distribution of $|\lambda|^2$ for correlated channels, $t = 0.5, r = 0.3, \gamma_f = 0.4$

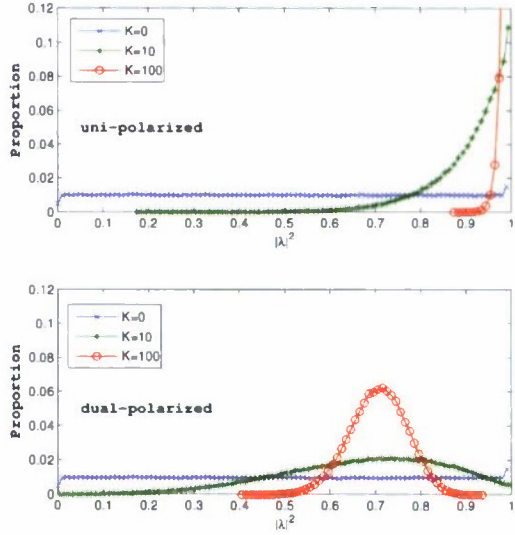

Figure 5.18: Distribution of $|\lambda|^2$ for uncorrelated channels, $\gamma_f = 0.3$

Chapter 6: Fully Polarimetric MIMO

In the previous chapter we investigated the performance of a MIMO system using the Golden Code with a dual-polarized antenna system and found that the performance can be made consistently good across environmental conditions from rich scattering to pure LOS. However, we assumed that the planes of the dual polarized transmit and receive antennas remained aligned. The simulation results for dual-polarized systems show that the performance degrades considerably if we allowed three dimensional (3-D) rotation of the transmit and/or receive antennas.

If we are to profitably use the performance stability introduced by polarimetric antennas for mobile terminals then we need to address the stability in transmission and/or reception under the 3-D rotation of the antennas in the MIMO system. To this end we investigate the use of triad antenna at the transmitter and receiver. A triad is composed of three orthogonal dipoles oriented along orthogonal directions as described in Section 5.2. We derive the channel model and show that the capacity is invariant under arbitrary rotation of the transmitter and/or receiver, since the channel matrix is always a 3×3 matrix of rank 2. We propose a 3×3 STBC suitable for this system which achieves full-rate and furthermore has a fast decoding algorithm. We give the simulation results for the performance of the triad system using the proposed 3×3 STBC with and without antenna rotation. We then compare the results with a dual-polarized system transmitting Golden Code codewords.

6.1 System Channel Models

Consider a MIMO wireless communication system with three transmit and three receive antennas. We assume a quasi-static fading channel, represented by a 3×3 matrix $\mathbf{H}$ with entries which are complex Gaussian random variables. For each symbol interval, $\boldsymbol{p} = (p_1, p_2, p_3)^{\mathrm{T}}$ denotes a vector of transmitted complex symbols. The received signal vector $\boldsymbol{y} = (y_1, y_2, y_3)^{\mathrm{T}}$ can be expressed as

$$\boldsymbol{y} = \mathbf{H}\boldsymbol{p} + \boldsymbol{w}, \tag{6.1}$$

where $\boldsymbol{w}$ denotes complex Gaussian noise with covariance $E\{\boldsymbol{w}\boldsymbol{w}^{\dagger}\} = \sigma^2 I_3$.

The channel matrix $\mathbf{H}$ can be written as the sum of an average (LOS) component $\overline{\mathbf{H}}$ and a variable Rayleigh fading component $\widetilde{\mathbf{H}}$,

$$\mathbf{H} = \sqrt{\frac{K}{1+K}}\overline{\mathbf{H}} + \sqrt{\frac{1}{1+K}} R_r^{1/2} \widetilde{\mathbf{H}} R_t^{1/2}, \tag{6.2}$$

where $E\{\mathbf{H}\} = \sqrt{K/(1+K)}\,\overline{\mathbf{H}}$ is the channel mean. $\widetilde{\mathbf{H}}$ is a complex Gaussian random matrix with independent zero-mean and unit variance entries, i.e. $\tilde{h}_{ij} \in \mathcal{CN}(0,1)$. $\overline{\mathbf{H}}$ and $\widetilde{\mathbf{H}}$ are weighted by the Ricean K-factor. Note that $K = 0$ corresponds to the case of pure Rayleigh channel. As K increases, $\overline{\mathbf{H}}$ dominates the behavior of the system and $K = \infty$ corresponds to a pure LOS channel. $R_t = R_t^{1/2} R_t^{1/2\dagger}$ and $R_r = R_r^{1/2} R_r^{1/2\dagger}$ are the transmit and receive correlation matrices respectively.

Consider a system with a triad antenna at both the transmitter and receiver. A triad is composed of three orthogonal dipoles oriented along Euclidean directions $\boldsymbol{e}_1$, $\boldsymbol{e}_2$, and $\boldsymbol{e}_3$ as shown in Figure 5.1. At the transmitter a triad antenna can generate an arbitrary dipole moment $\boldsymbol{p}$.

As shown in Section 5.2 the far field electric field generated by the triad is

$$\mathbf{E} = k^2 \frac{e^{ikr}}{r}(I_3 - \boldsymbol{n}\boldsymbol{n}^\dagger)\boldsymbol{p}. \tag{6.3}$$

The term $I_3 - \boldsymbol{n}\boldsymbol{n}^\dagger$ is a 3×3 projection matrix with rank 2 and it constrains the oscillation direction of the electric field to be perpendicular to its propagation direction as shown in Figure 5.2. In spherical coordinates, the propagation direction can be represented as

$$\boldsymbol{n} = \begin{pmatrix} \sin\theta\cos\phi \\ \sin\theta\sin\phi \\ \cos\theta \end{pmatrix}, \tag{6.4}$$

where $0 \leq \theta \leq \pi, 0 \leq \phi \leq 2\pi$. The use of triad antennas allows us to think of this MIMO system in an unusual way. Instead of thinking of the individual component antennas and the symbols coded onto them at the transmitter and read off at the receiver, we can think directly of coding onto a physical dipole moment vector at the transmitter and measuring the resulting electric field at the receiver with the LOS channel given by the matrix

$$\mathcal{H} = k^2 \frac{e^{ikr}}{r}(I_3 - \boldsymbol{n}\boldsymbol{n}^\dagger). \tag{6.5}$$

It is difficult to build co-located antennas without having some form of mutual coupling. To model this coupling between the three components of the triad antenna we introduce mixing operators $\mathcal{M}_t$ for the transmitter and $\mathcal{M}_r$ for the receiver so that the LOS channel becomes $\mathcal{M}_r^\dagger \mathcal{H} \mathcal{M}_t$. The mixing operators $\mathcal{M}_t$ and $\mathcal{M}_r$ are defined as

$$\mathcal{M}_t = \mathcal{M}_r = \frac{1}{\sqrt{N}} \begin{pmatrix} 1 & \rho_{12} & \rho_{13} \\ \rho_{12} & 1 & \rho_{23} \\ \rho_{13} & \rho_{23} & 1 \end{pmatrix}, \tag{6.6}$$

where $0 \leq \rho_{ij} \leq 1$ is a coupling between components i and j and is directly related to the cross coupling between the antenna elements comprising the triad, and N is a normalisation term given by

$$N = \max(1 + \rho_{12}^2 + \rho_{13}^2, 1 + \rho_{12}^2 + \rho_{23}^2, 1 + \rho_{13}^2 + \rho_{23}^2). \tag{6.7}$$

Assuming that the receiver is at position $r\boldsymbol{n}$ relative to the transmitter and denoting the three orthogonal axes of the triad transmitter and receiver (initially assumed to be aligned) by $\boldsymbol{e}_1$, $\boldsymbol{e}_2$, $\boldsymbol{e}_3$, the LOS component $\overline{\mathbf{H}}$ then consists of elements given by

$$(\overline{\mathbf{H}})_{ij} = \boldsymbol{e}_i^\dagger \mathcal{H} \boldsymbol{e}_j, \quad i, j = 1, 2, 3. \tag{6.8}$$

The elements of $\widetilde{\mathbf{H}}$ depend on the propagation conditions and the antenna characteristics and satisfy [58],

$$\begin{aligned} &E\{|\tilde{h}_{ii}|^2\} = 1, \quad \text{and} \\ &E\{|\tilde{h}_{ij}|^2\} = E\{|\tilde{h}_{ji}|^2\} = \gamma, \quad i, j = 1, 2, 3, \end{aligned} \tag{6.9}$$

where $0 < \gamma \leq 1$ describes attenuated cross coupling for polarization multiplexing. In a rich scattering environment γ tends to be close to 1 (for ranges beyond 1.6 km, γ is always close to 1) [58]. Here we assume that $\gamma = 1$, i.e. the scattering changes the polarization states randomly, hence in a pure scattering environment, a polarimetric antenna system is equivalent to a uni-polarized antenna system. The correlation matrices R_t and R_r are modelled as

$$R_t = \begin{pmatrix} 1 & t & t \\ t & 1 & t \\ t & t & 1 \end{pmatrix}, \quad R_r = \begin{pmatrix} 1 & r & r \\ r & 1 & r \\ r & r & 1 \end{pmatrix}, \tag{6.10}$$

where t and r are transmit and receive correlation coefficients respectively.

For a dual-polarized antenna consisting of co-located vertically and horizontally polarized antennas, consider a system with one dual-polarized transmit and one dual-polarized receive antenna. The LOS channel matrix $\overline{\mathbf{H}}_d$ is given by

$$\overline{\mathbf{H}}_d = P^{\dagger} \overline{\mathbf{H}} P, \tag{6.11}$$

where $P = \begin{pmatrix} 1 & 0 & 0 \\ 0 & 1 & 0 \\ 0 & 0 & 0 \end{pmatrix}$ and $\overline{\mathbf{H}}$ is as defined in (6.5). Similarly, $\widetilde{\mathbf{H}}_d$ is modelled as described for triad antennas and the correlation matrices are defined as

$$R_t = \begin{pmatrix} 1 & t \\ t & 1 \end{pmatrix}, \quad R_r = \begin{pmatrix} 1 & r \\ r & 1 \end{pmatrix}.$$

6.2 The Effect of Antenna Rotation

Consider the case of pure LOS ($K = \infty$). If the channel is known at the receiver, then the capacity is given by [2]

$$C(\mathbf{H}) = E_{\mathbf{H}} \left[\log_2 \det \left(I_3 + \frac{E_s}{3\sigma^2} \overline{\mathbf{H}}\, \overline{\mathbf{H}}^{\dagger} \right) \right], \tag{6.12}$$

where E_s is the average transmitted signal power. From (6.5) and (6.8) it follows that $\overline{\mathbf{H}}\,\overline{\mathbf{H}}^{\dagger}$ is a 3×3 rank 2 matrix with equal eigenvalues, and so the capacity (6.12) can be written as

$$C(\mathbf{H}) = E_{\mathbf{H}} \left[2 \log_2 (1 + \frac{E_s}{3\sigma^2} \lambda) \right], \tag{6.13}$$

where λ is the eigenvalue of $\overline{\mathbf{H}}\,\overline{\mathbf{H}}^{\dagger}$.

Assume that the transmit and receive triad antennas have been rotated or equivalently, the transmitted and receive signals have been rotated. The rotated signal can be represented as

$$\begin{aligned} \boldsymbol{p}' &= R\boldsymbol{p} = p_1 R\boldsymbol{e}_1 + p_2 R\boldsymbol{e}_2 + p_3 R\boldsymbol{e}_3, \\ \boldsymbol{y}' &= S\boldsymbol{y} = y_1 S\boldsymbol{e}_1 + y_2 S\boldsymbol{e}_2 + y_3 S\boldsymbol{e}_3, \end{aligned} \tag{6.14}$$

where S and R are 3×3 real orthogonal rotation matrices. The elements of the corresponding channel matrix $\overline{\mathbf{H}}'$ become

$$(\overline{\mathbf{H}}')_{ij} = \boldsymbol{e}_i^{\dagger} S^{\dagger} \mathcal{H} R \boldsymbol{e}_j, \quad i, j = 1, 2, 3. \tag{6.15}$$

Since S and R are orthogonal, $S^\dagger \mathcal{H} R$ has the same singular values as $\mathcal{H}$, i.e. $\overline{\mathbf{H}}'$ is still a 3×3 rank 2 matrix, therefore the capacity is invariant under the rotation of the transmit and receive antennas,

$$C(\mathbf{H}') = C(\mathbf{H}). \tag{6.16}$$

This is not the case when dual-polarized antennas are employed at the transmitter and receiver. In that case the change in orientation (3-D rotation) of the dual-polarized transmit and receive antennas will not preserve the capacity of the rotated channels. Moreover, a transmitter or receiver can be rotated such that the channel matrix becomes rank deficient (in fact, rank 1). For example, consider a rotated channel matrix,

$$\overline{\mathbf{H}}'_d = \begin{pmatrix} e_1^\dagger S^\dagger \mathcal{H} R e_1 & e_1^\dagger S^\dagger \mathcal{H} R e_2 \\ e_2^\dagger S^\dagger \mathcal{H} R e_1 & e_2^\dagger S^\dagger \mathcal{H} R e_2 \end{pmatrix}. \tag{6.17}$$

If a dual-polarized receive antenna is rotated such that one of the branches is parallel to the direction of propagation $\boldsymbol{n}$, i.e.

$$S e_1 = \boldsymbol{n}, \quad \text{and} \quad S e_2 = \boldsymbol{e}_2, \tag{6.18}$$

then (6.17) becomes

$$\overline{\mathbf{H}}'_d = \begin{pmatrix} \boldsymbol{n}^\dagger \mathcal{H} e_1 & \boldsymbol{n}^\dagger \mathcal{H} e_2 \\ e_2^\dagger \mathcal{H} e_1 & e_2^\dagger \mathcal{H} e_2 \end{pmatrix}. \tag{6.19}$$

Substituting (6.18) into (6.8), we obtain $\boldsymbol{n}^\dagger \mathcal{H} = 0$, and we have a rank 1 channel matrix $\overline{\mathbf{H}}'_d$.

However, if the dual-polarized receive antenna is rotated in a plane, then the capacity is invariant under rotation [63]. That is, under a rotation of the receive antenna, (6.11) becomes

$$\overline{\mathbf{H}}'_d = P^\dagger S^\dagger \overline{\mathbf{H}} P. \tag{6.20}$$

If $PS = SP$ (i.e. P and S commute), then the capacity is invariant under the rotations, and we obtain,

$$\overline{\mathbf{H}}'_d = S^\dagger \overline{\mathbf{H}}_d. \tag{6.21}$$

Note that P and S commute if and only if S fixes the plane defined by P, i.e. if S is a rotation around the normal to the plane defined by P.

The above analysis shows that in a LOS environment, a system with a triad antenna at both ends of the link can provide robustness (preserve capacity) to any orientation of the transmit and/or receive antennas, which is not the case for dual-polarized antennas. We will see that this robustness extends to the hybrid LOS and rich scattering environments described by (6.2).

6.3 The Full Rate STBC for a Triad Antenna

In this section we introduce a STBC which, in LOS environments, provides full-rate for the triad antenna system discussed above. We emphasize that, although our system consists of one physical transmit and one physical receive antenna, the underlying channel has three-inputs and three-outputs. The proposed code is a 3×3 STBC which transmits six complex information

symbols $\{x_i\}_{i=1}^{6}, x_i \in \mathbb{Z}[i]$ over three time slots from three effective transmit antennas. The codewords can be expressed as

$$\mathbf{X}=B_1\begin{pmatrix} x_1 & x_2 & x_3 \\ jx_3 & x_1 & x_2 \\ jx_2 & jx_3 & x_1 \end{pmatrix} + B_2\begin{pmatrix} x_4 & x_5 & x_6 \\ jx_6 & x_4 & x_5 \\ jx_5 & jx_6 & x_4 \end{pmatrix}, \tag{6.22}$$

where the diagonal matrices B_i are

$$B_1 = (1+j)I_3 + \Theta,$$
$$B_2 = (-1-2j)I_3 + j\Theta^2,$$

with $\Theta = \mathrm{diag}(\theta_1, \theta_2, \theta_3), \theta_i = 2\cos(2^i\pi/7), j = e^{2\pi i/3}$. This is a sub-code of the 3×3 perfect STBC introduced by Oggier et al. [7] which transmits nine complex information symbols over three time slots from three transmit antennas. However, this sub-code still provides rate 2 and can be decoded with essentially maximum likelihood performance using an algorithm introduced in [47] with complexity $\mathcal{O}(N^3)$, where N is the size of the underlying signal constellation.

6.4 Simulation Results

We simulated the performance of the triad and dual-polarized antenna systems allowing receiver rotation. The simulation included pure LOS ($K = \infty$), Ricean ($K = 10$) and Rayleigh ($K = 0$) channels. The system was initialized so that the polarization of the receiver and the transmitter were aligned, i.e. we set $\boldsymbol{n} = \boldsymbol{e}_3$. The receiver was then subject to a random rotation drawn from the uniform distribution. The counterclockwise rotation about an arbitrary unit vector (v_1, v_2, v_3), by an arbitrary angle α, is given by

$$S = \begin{pmatrix} v_1^2 + (1-v_1^2)c & v_1v_2(1-c) - v_1s & v_1v_3(1-c) + v_2s \\ v_1v_2(1-c) + v_3s & v_2^2 + (1-v_2^2)c & v_2v_3(1-c) - v_1s \\ v_1v_3(1-c) - v_2s & v_2v_3(1-c) + v_1s & v_3^2 + (1-v_3^2)c \end{pmatrix},$$

where $c = \cos\alpha$ and $s = \sin\alpha$. We assume the mutual coupling between the three elements is the same both at the transmitter and the receiver. That is the mixing operators are chosen as follows:

$$\mathcal{M}_t = \mathcal{M}_r = \frac{1}{\sqrt{1+2\rho^2}}\begin{pmatrix} 1 & \rho & \rho \\ \rho & 1 & \rho \\ \rho & \rho & 1 \end{pmatrix}.$$

For a triad antenna system, the transmit codewords are the 3×3 STBC given in (6.22) and the information symbols are taken from a 16-QAM constellation. As shown in Figure 6.1, the performance of the system is stable under the rotation of the receiver across LOS, Ricean and pure scattering conditions. The Golden Code [22] with information symbols taken from the 16-QAM constellation provides a baseline for evaluating coded dual-polarized system performance. The performance degradation under 3-D rotation shown in Figure 6.2 is consistent with the analysis given in Section 6.2.

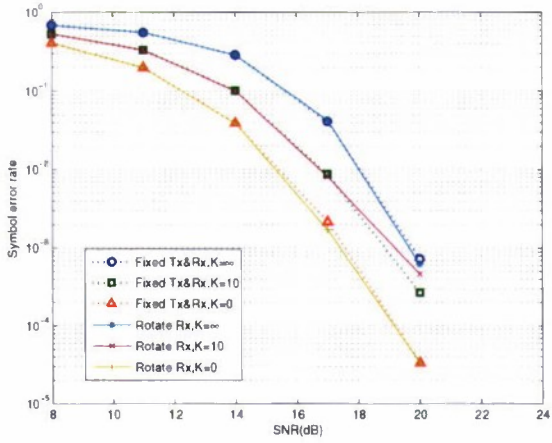

Figure 6.1: Performance of the triad system with and without receiver rotation for uncorrelated channels, $\rho = 0.3$

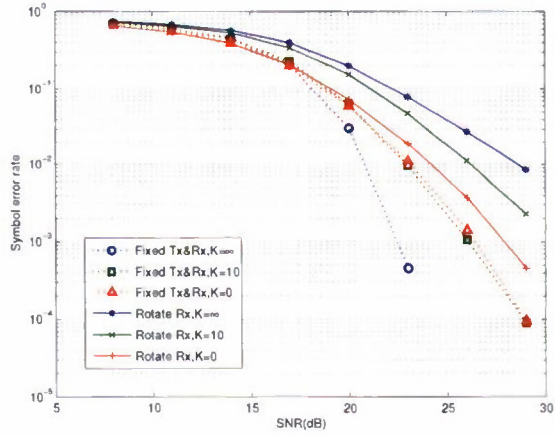

Figure 6.2: Performance of the dual-polarized system with and without receiver rotation for uncorrelated channels, $\rho = 0.3$

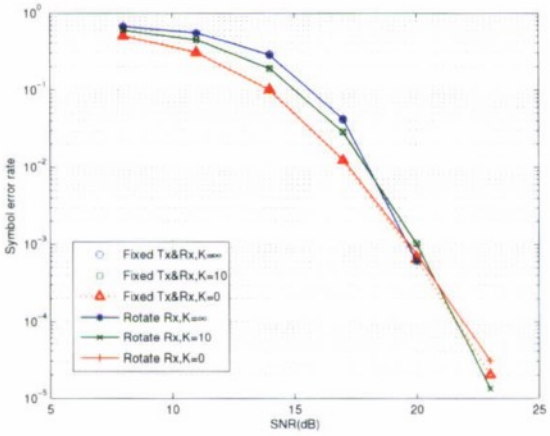

Figure 6.3: Performance of the triad system with and without receiver rotation for correlated channels, $t = r = 0.5$ and $\rho = 0.3$

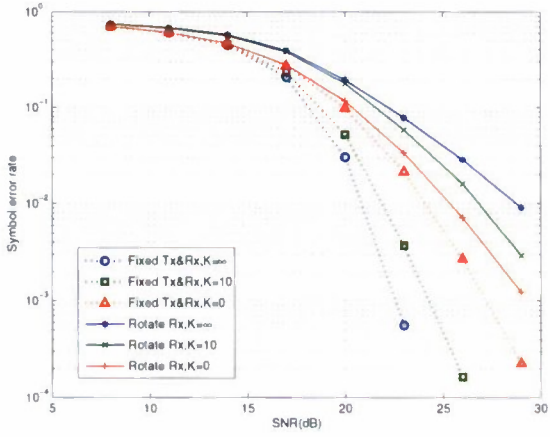

Figure 6.4: Performance of the dual-polarized system with and without receiver rotation for correlated channels, $t = r = 0.5$ and $\rho = 0.3$

Figures 6.3 and 6.4 show the performance of triad and dual-polarized systems respectively, in a correlated environment, with $t = r = 0.5$ and $\rho = 0.3$. In this case, the performance of the triad system is not only robust to the rotation of the antenna but is also robust to the propagation environment. In comparison, the dual-polarized system loses robustness to changing propagation environments.

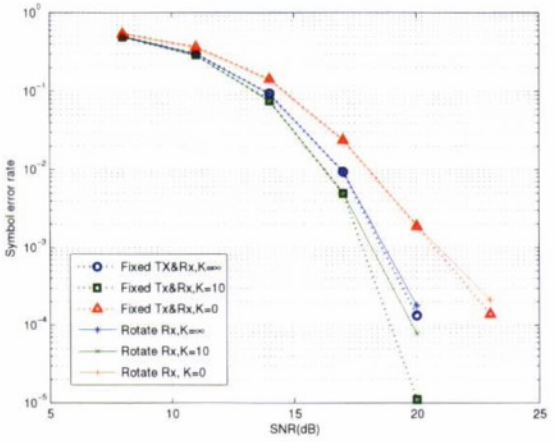

Figure 6.5: Performance of the triad system with and without receiver rotation in correlated channels, $t = r = 0.6$ and $\rho = 0.1$

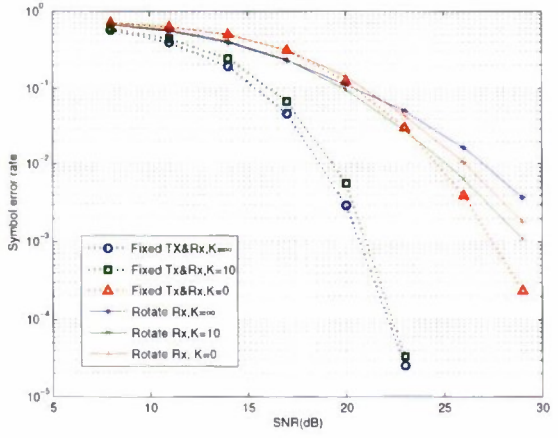

Figure 6.6: Performance of the dual-polarized system with and without receiver rotation in correlated channels, $t = r = 0.6$ and $\rho = 0.1$

If the polarimetric antennas have good cross polarization discrimination (XPD) (small value of ρ), even in highly correlated channels as shown in Figure 6.5 and Figure 6.6, where $t = r = 0.6$ and $\rho = 0.1$, the triad system is still robust across all conditions, while the performance of the dual-polarized system degrades severely under rotation of the antenna.

As shown in the simulation results, the use of triad antenna at the transmitter and the receiver ean provide resilienee to arbitrary rotations of the transmit and receive antennas as well as stahility in performance across propagation conditions. In the next section we consider the multi-user downlink where both the base station and each user is equipped with a triad antenna.

6.5 Fully Polarimetric Multi-user Downlink

In this seetion we investigate multi-user deteetion on a fully polarimetrie downlink. In partieular, we investigate a system whieh uses a Code Division Multiple Aeeess (CDMA) transmitting scheme in which each user is assigned a two dimensional suhspace and the transmitted information symbol for each user is coded across this subspace. The received signal for each user after despreading is equivalent to the deeoding problem of a single user with a spaee-time bloek code system. We demonstrate that the transmitted information symbols can he chosen to have the strueture of a STBC with full rate, full diversity and low complexity deeoding.

6.5.1 Multi-user Downlink Model

Consider the downlink of an M user MIMO multi-user system where the base station is equipped with a triad transmit antenna and eaeh user has a triad receive antenna. We eonsider CDMA as the multiplexing scheme, i.e. eaeh user is assigned a three dimensional subspaee of $\mathbb{C}^T$, that is, a matrix $A_m \in \mathbb{C}^{3\times T}$, sueh that

$$A_m A_\ell^\dagger = \delta_{m\ell} I_3, \quad \ell = 1, \ldots, M. \tag{6.23}$$

In order to makc this work for M users we must have $T \geq 3M$.

Let S_m be an information symbol matrix for user m with elements being $s_i, i = 1 \ldots, 9$, where $s_i \in \mathbb{C}$,

$$S_m = \begin{pmatrix} s_1 & s_2 & s_3 \\ s_4 & s_5 & s_6 \\ s_7 & s_8 & s_9 \end{pmatrix}. \tag{6.24}$$

In a pure seattering environment, in the case that $\mathbf{H} = \widetilde{\mathbf{H}}$ is a full rank ehannel matrix, this provides 3 timcs the rate that eould be achieved using single-transmit and single reeeive antennas [64, 65]. However in a LOS environment, $\mathbf{H} = \overline{\mathbf{H}}$ as described in (6.5) for a fully polarimetrie antenna systems, is a rank 2 channel matrix, and the rate is only twiee that of a single antenna system.

The signal transmitted from the triad at the base station is

$$\mathbf{X} = \sum_{m=1}^{M} S_m A_m \in \mathbb{C}^{3\times T}. \tag{6.25}$$

We ean write the spreading matrix of the ℓ^{th} user A_ℓ as $(\boldsymbol{a}_1^{\ell\mathrm{T}}, \boldsymbol{a}_2^{\ell\mathrm{T}}, \boldsymbol{a}_3^{\ell\mathrm{T}})^{\mathrm{T}}$ where a sequenee $\boldsymbol{a}_i^\ell \in \mathbb{C}^{1\times T}$ and $\boldsymbol{a}_i^\ell \boldsymbol{a}_j^{\ell\dagger} = \delta_{ij}$, then the transmitted signal (6.25) can be rewritten as

$$\mathbf{X} = \sum_{m=1}^{M} \begin{pmatrix} s_1^m \boldsymbol{a}_1^m + s_2^m \boldsymbol{a}_2^m + s_3^m \boldsymbol{a}_3^m \\ s_4^m \boldsymbol{a}_1^m + s_5^m \boldsymbol{a}_2^m + s_6^m \boldsymbol{a}_3^m \\ s_7^m \boldsymbol{a}_1^m + s_8^m \boldsymbol{a}_2^m + s_9^m \boldsymbol{a}_3^m \end{pmatrix}. \tag{6.26}$$

At each transmitter element, the transmitted signal is an element of the subspace of $\mathbb{C}^{3\times T}$ assigned to the m^{th} user. Therefore, the transmitted signal for the scheme is equivalent to that of spatial multiplexing over three time slots, that is, the number of time slots corresponds to the dimension of the subspace allocated to the user.

We note that Doostnejad et al., [66] study a space-time multiplexing structure for MIMO downlink channels in which they modulated the information symbols by a two dimensional spreading matrix which is reminiscent of the class of linear dispersion codes discussed in [18].

Assuming that perfect CSI is known at the receiver of each user, the received signal of the ℓ^{th} user is

$$\begin{aligned}\mathbf{Y}_\ell &= \mathbf{H}_\ell \mathbf{X} + \mathbf{W}, \\ &= \sum_{m=1, m\neq\ell}^{M} \mathbf{H}_\ell S_m A_m + \mathbf{W},\end{aligned} \tag{6.27}$$

where $\mathbf{W}$ is the complex Gaussian noise matrix with entries, $\mathbf{W}_{ij} \in \mathcal{CN}(0, \sigma^2)$ and $\mathbf{H}_\ell \in \mathbb{C}^{3\times 3}$ is the channel matrix of the ℓ^{th} user.

Multiplying (6.27) by $A^\dagger$, the ℓ^{th} received signal is despread,

$$\boldsymbol{y}_\ell = \mathbf{Y}_\ell A_\ell^\dagger = \mathbf{H}_\ell S_\ell + \boldsymbol{n}_\ell, \tag{6.28}$$

where the noise $\boldsymbol{n}_\ell = \mathbf{W} A_\ell^\dagger$ is the projection of the noise onto the user's subspace and is still white. Equation (6.28) shows that, after despreading, the decoding problem of each user is equivalent to that of a single user with STBC even though the two dimensions are polarization and the spreading subspace components, rather than space and time. This suggests that choosing the structure of the information symbol matrix S is equivalent to choosing an STBC. In the following sections, we consider a suitable choice for both the spreading matrix and the symbol matrices which are compatible with the triad structure and admit a fast decoding algorithm.

6.5.2 Symbols Matrix for Multi-user with Triad System

As shown in Section 6.5.1, the decoding problem at the receiver for each user after despreading is equivalent to that of decoding for a single user who is using an STBC. For the case of a single user system with triad transmit and receive antennas we have previously proposed the use of a polarization-time code [67]. This code has full rate (under LOS conditions), full diversity and is fast decodable. It is a sub-code of the 3×3 perfect STBC introduced by Oggier et al. [7]. The proposed code transmits six complex information symbols $\{x_i\}_{i=1}^{6}$ (usually N-HEX constellation) where x_i is an Eisenstein integer, $x_i \in \{a + \omega b | a, b \in \mathbb{Z}, \omega = e^{2\pi i/3}\}$ over three time slots from three effective transmit antennas. The symbols matrix for this code has the following structure

$$\mathbf{S} = \sum_{i=0}^{1} B_{i+1} \begin{pmatrix} s_{3i+1} & s_{3i+2} & s_{3i+3} \\ \omega s_{3i+3} & s_{3i+1} & s_{3i+2} \\ \omega s_{3i+2} & \omega s_{3i+3} & s_{3i+1} \end{pmatrix}, \tag{6.29}$$

where the diagonal matrices B_i are

$$\begin{aligned} B_1 &= (1+\omega) I_3 + \Theta, \\ B_2 &= (-1-2\omega) I_3 + \omega \Theta^2, \end{aligned}$$

with $\Theta = \text{diag}(\theta_1, \theta_2, \theta_3), \theta_i = 2\cos(2^i\pi/7), \omega = e^{2\pi i/3}$.

For each user, the despread procedure reduces the problem to an equivalent decoding problem of a single user with STBC. As shown in [67] this code (6.29) provides rate 2 across environmental conditions ranging from pure scattering to pure LOS environment, as well as resilience to arbitrary rotations of the transmit and receive antennas. The code can be decoded with essentially maximum likelihood performance using an algorithm introduced in [47] with complexity $O(N^3)$.

6.5.3 Decoding

As we have seen the signal received by the ℓ^{th} user after despreading has the form

$$\boldsymbol{y} = \mathbf{H}S + \boldsymbol{n}, \tag{6.30}$$

which can be rewritten as

$$\boldsymbol{y} = (\boldsymbol{y}_1, \boldsymbol{y}_2, \boldsymbol{y}_3) = (s_1, s_2, s_3)\boldsymbol{\mathcal{H}}_1 + (s_4, s_5, s_6)\boldsymbol{\mathcal{H}}_2 + \boldsymbol{n}, \tag{6.31}$$

where $\boldsymbol{y}_i = (y_{i1}, y_{i2}, y_{i3})$ and

$$\boldsymbol{\mathcal{H}}_1 = (\mathcal{H}_1, \mathcal{G}_1, \mathcal{C}_1), \quad \boldsymbol{\mathcal{H}}_2 = (\mathcal{H}_2, \mathcal{G}_2, \mathcal{C}_2), \tag{6.32}$$

where

$$\mathcal{H}_i = \begin{pmatrix} b_{i1}h_{11} & b_{i2}h_{21} & b_{i3}h_{31} \\ wb_{i3}h_{31} & b_{i1}h_{11} & b_{i2}h_{21} \\ wb_{i2}h_{21} & wb_{i3}h_{31} & b_{i1}h_{11} \end{pmatrix}, \tag{6.33}$$

and similarly for $\mathcal{G}_i$ and $\mathcal{C}_i$ for the second and third receive antenna respectively. Let $\boldsymbol{c} = (s_1, s_2, s_3)$ and $\boldsymbol{d} = (s_4, s_5, s_6)$. We can write (6.31) as

$$\boldsymbol{y} = \boldsymbol{c}\boldsymbol{\mathcal{H}}_1 + \boldsymbol{d}\boldsymbol{\mathcal{H}}_2 + \boldsymbol{n}. \tag{6.34}$$

The likelihood function associated with (6.34) is

$$p(\boldsymbol{y}|\boldsymbol{c}, \boldsymbol{d}) \propto \exp\left(-\frac{1}{2\sigma^2}\left\|\boldsymbol{y} - \boldsymbol{c}\boldsymbol{\mathcal{H}}_1 - \boldsymbol{d}\boldsymbol{\mathcal{H}}_2\right\|^2\right). \tag{6.35}$$

Based on the conditional optimization described in [46], the decoding algorithm can be summarized as follows:

If $\det(\boldsymbol{\mathcal{H}}_2\boldsymbol{\mathcal{H}}_2^\dagger) \geq \det(\boldsymbol{\mathcal{H}}_1\boldsymbol{\mathcal{H}}_1^\dagger)$

$$\hat{\boldsymbol{c}} = \arg\min_{\boldsymbol{c}} \left\|\boldsymbol{y} - \boldsymbol{c}\boldsymbol{\mathcal{H}}_1 - \hat{\boldsymbol{d}}(\boldsymbol{c})\boldsymbol{\mathcal{H}}_2\right\|^2,$$

$$\hat{\boldsymbol{d}} = \text{Q}(\tilde{\boldsymbol{d}}(\hat{\boldsymbol{c}})),$$

otherwise,

$$\hat{\boldsymbol{d}} = \arg\min_{\boldsymbol{d}} \left\|\boldsymbol{y} - \hat{\boldsymbol{c}}(\boldsymbol{d})\boldsymbol{\mathcal{H}}_1 - \boldsymbol{d}\boldsymbol{\mathcal{H}}_2\right\|^2, \tag{6.36}$$

$$\hat{\boldsymbol{c}} = \text{Q}(\tilde{\boldsymbol{c}}(\hat{\boldsymbol{d}})),$$

where

$$\tilde{\boldsymbol{d}}(\boldsymbol{c}) = (\boldsymbol{y} - \boldsymbol{c}\mathcal{H}_1)\mathcal{H}_2^\dagger(\mathcal{H}_2\mathcal{H}_2^\dagger)^{-1}, \tag{6.37}$$

$$\tilde{\boldsymbol{c}}(\boldsymbol{d}) = (\boldsymbol{y} - \boldsymbol{d}\mathcal{H}_2)\mathcal{H}_1^\dagger(\mathcal{H}_1\mathcal{H}_1^\dagger)^{-1}. \tag{6.38}$$

Here $\mathrm{Q}(\boldsymbol{c}) = (\mathrm{Q}(c_1), \cdots, \mathrm{Q}(c_3))$, where Q is the quantizer for the HEX constellation.

6.5.4 Spreading Matrix of Length 3^m

Finally, we need appropriate spreading sequences for this triad based multi-user scheme. As such we would like to have spreading sequences with a length which is a power of three, rather than the usual power of two. Fortunately, spreading sequences of length 3^m, which are analogous to the Walsh-Hadamard sequences, can be constructed as follows (See, for example [68]).

Begin with the $\mathbb{Z}_3^m$ consisting of m-tuples of elements from $\mathbb{Z}_3$, i.e. the integers modulo 3. For each $\boldsymbol{b} \in \mathbb{Z}_3^m$, we construct a function on $\mathbb{Z}_3^m$ with value at $\boldsymbol{a} \in \mathbb{Z}_3^m$ given by

$$f_{\boldsymbol{b}}(\boldsymbol{a}) = \omega^{\boldsymbol{b}\cdot\boldsymbol{a}} \tag{6.39}$$

for all $\boldsymbol{a} \in \mathbb{Z}_3^M$, where $\omega = \exp(2\pi i/3)$ is a cube root of unity and $\cdot$ denotes the usual dot product on $\mathbb{Z}_p^m$. The functions $f_{\boldsymbol{b}}$ take values in the set $\{1, \omega, \omega^2\}$. This set of functions is orthogonal, i.e.

$$\begin{aligned}(f_{\boldsymbol{b}}, f_{\boldsymbol{b}'}) &\equiv \sum_{\boldsymbol{a}\in\mathbb{Z}_p^m} f_{\boldsymbol{b}}(\boldsymbol{a})\overline{f_{\boldsymbol{b}'}(\boldsymbol{a})} \\ &= \sum_{\boldsymbol{a}\in\mathbb{Z}_p^m} \omega^{(\boldsymbol{b}-\boldsymbol{b}')\cdot\boldsymbol{a}} \\ &= 3^m\delta_{\boldsymbol{b},\boldsymbol{b}'}.\end{aligned} \tag{6.40}$$

Choosing an ordering for the elements of $\mathbb{Z}_p^m$ we can write these functions as sequences and stack them in a matrix. For example for $m = 2$, we obtain a 9×9 orthogonal matrix as follows

$$H_2 = \begin{pmatrix} 1 & 1 & 1 & 1 & 1 & 1 & 1 & 1 & 1 \\ 1 & \omega & \omega^2 & 1 & \omega & \omega^2 & 1 & \omega & \omega^2 \\ 1 & \omega^2 & \omega & 1 & \omega^2 & \omega & 1 & \omega^2 & \omega \\ 1 & 1 & 1 & \omega & \omega & \omega & \omega^2 & \omega^2 & \omega^2 \\ 1 & \omega & \omega^2 & \omega & \omega^2 & 1 & \omega^2 & 1 & \omega \\ 1 & \omega^2 & \omega & \omega & 1 & \omega^2 & \omega^2 & \omega & 1 \\ 1 & 1 & 1 & \omega^2 & \omega^2 & \omega^2 & \omega & \omega & \omega \\ 1 & \omega & \omega^2 & \omega^2 & 1 & \omega & \omega & \omega^2 & 1 \\ 1 & \omega^2 & \omega & \omega^2 & \omega & 1 & \omega & 1 & \omega^2 \end{pmatrix}. \tag{6.41}$$

In general H_m is unitary, i.e.

$$H_m H_m^\dagger = H_m^\dagger H_m = 3^m I_{3^m}. \tag{6.42}$$

The spreading matrices A_k for our scheme, for a maximum of 3^m users, consist of sets of mutually exclusive rows from the matrix H_{m+1}.

6.5.5 Inhomogeneous Multi-user Downlink MIMO

The MIMO CDMA scheme described in the previous section can be generalized to the inhomogeneous MIMO downlink where the base station is equipped with n_t transmit antennas but each user can be equipped with a different number of receive antennas. Note that the base station is equipped with a fixed number of transmit antennas no matter how many users there are. Hong et al [69] proposed a scheme which allows different number of receive antennas, however, the base station requires the number of transmit antennas to be the sum of all users' receive antennas in order to support such a capability.

We give an example of two transmit antennas, uni-polarized (vertically or horizontally polarized), spatially separated at the base station and each user can be equipped with either one or two receive antennas. The code structure for the user is chosen to be the structure of Alamouti signaling [14] or the 2×2 full rate, full diversity algebraic STBC such as the Golden Code [22], Silver code [27] etc. or even just spatial multiplexing. Let us use the Golden Code for the dual antenna users.

The user with a single receive antenna, Alamouti scheme is chosen,

$$S = \begin{pmatrix} s_1 & s_2 \\ -s_2^* & s_1^* \end{pmatrix}. \tag{6.43}$$

For the users with two receive antennas, the Golden Code structure is chosen,

$$S = \begin{pmatrix} \alpha(s_1 + \tau s_2) & \alpha(s_3 + \tau s_4) \\ i\bar{\alpha}(s_3 + \mu s_4) & \bar{\alpha}(s_1 + \mu s_2) \end{pmatrix}, \tag{6.44}$$

where $\alpha = (1 + i\mu)/\sqrt{5}, \bar{\alpha} = (1 + i\tau)/\sqrt{5}, \tau = (1 + \sqrt{5})/2$ and $\mu = (1 - \sqrt{5})/2$.

For M users, the spreading matrix for each user is a two dimensional subspace matrix, i.e. $A_m \in \mathbb{C}^{2\times T}$ where $T = 2M$ is the length of the sequence. The transmitted signal at the base station is given by

$$\mathbf{X} = \sum_{m=1}^{M} \begin{pmatrix} s_1^m \boldsymbol{a}_1^m + s_2^m \boldsymbol{a}_2^m \\ s_3^m \boldsymbol{a}_1^m + s_4 \boldsymbol{a}_2^m \end{pmatrix}. \tag{6.45}$$

If the ℓ^{th} user has a single antenna then their received signal is given by

$$\boldsymbol{y} = (h_{11}, h_{21}) \begin{pmatrix} s_1 \boldsymbol{a}_1 + s_2 \boldsymbol{a}_2 \\ -\bar{s}_2 \boldsymbol{a}_1 + \bar{s}_1 \boldsymbol{a}_2 \end{pmatrix} + (h_{11}, h_{21}) \sum_{m=1, m\neq \ell}^{M} S_m A_m + \boldsymbol{n}, \tag{6.46}$$

where $\boldsymbol{y}$ is the $1 \times T$ received signal vector. After despreading, this becomes

$$\boldsymbol{y}' = (h_{11}, h_{21}) \begin{pmatrix} s_1 & s_2 \\ -\bar{s}_2 & \bar{s}_1 \end{pmatrix} + \boldsymbol{n}', \tag{6.47}$$

where $\boldsymbol{y}' = \boldsymbol{y}(\boldsymbol{a}_1, \boldsymbol{a}_2)^\dagger$ and $\boldsymbol{n}' = \boldsymbol{n}(\boldsymbol{a}_1, \boldsymbol{a}_2)^\dagger$. Equation (6.47) is the well known Alamouti decoding problem.

Similarly, if the ℓ^{th} user is equipped with 2 receive antennas, after despreading the decoding problem becomes

$$\begin{aligned} \boldsymbol{y}' &= \boldsymbol{y}(\boldsymbol{a}_1, \boldsymbol{a}_2)^\dagger \\ &= \begin{pmatrix} h_{11} & h_{21} \\ h_{12} & h_{22} \end{pmatrix} \begin{pmatrix} \alpha(s_1 + \tau s_2) & \alpha(s_3 + \tau s_4) \\ i\bar{\alpha}(s_3 + \mu s_4) & \bar{\alpha}(s_1 + \mu s_2) \end{pmatrix} + \boldsymbol{n}', \end{aligned} \tag{6.48}$$

where $\boldsymbol{y}$ is the $2 \times T$ received vector. This is the decoding problem of the Golden Code for a single user which can be decoded with an essentially ML decoder with quadratic complexity given in [46].

6.6 Summary

We have quantified the performance gains that result from the introduction of a triad antenna at both the transmitter and receiver in a MIMO communication system. We have shown that, in a LOS environment, the capacity of the channel is invariant to the rotation of the transmitter and/or receiver. Simulation results show that system performance is stable across a full range of propagation environments from LOS to pure Rayleigh scattering. An advantage of the triad system over the baseline provided by dual-polarization was shown to be a resilience to arbitrary rotations of the transmit and receive antennas. The practicality of coded transmission for the triad system was shown through design of a full rate 3×3 STBC that provides full rate in LOS conditions and admits low-complexity decoding.

We have extended the triad system to a multi-user scenario in which we considered a CDMA transmitting scheme for the multi-user downlink in a system where both the base station and each user is equipped with a triad antenna. The information symbols for each user are spread over their assigned spreading matrix of orthogonal sequences. The received signal for each user after despreading is equivalent to the decoding problem of a single user using a 3×3 STBC. This allows the information symbols for each user to be coded on an STBC which achieves full-rate, full-diversity and has a fast decoding algorithm.

References

[1] G. J. Foschini and M. J. Gans, "On limits of wireless communication in a fading environment when using multiple antennas," *Wireless Personal Communications*, pp. 311–335, March 1998.

[2] E. Telatar, "Capacity of multi-antenna Gaussian channels," *European Transactions on Communications*, vol. 10, pp. 585–596, 1999.

[3] B. Daneshrad, "MIMO: The next revolution in wireless data communications," in *RFDESIGN Defense Electronics*.

[4] J. D. Gibson, ed, *The Mobile Communications Handbook, 2nd edition*. IEEE Press, 1999.

[5] A. M. D. Turkmani, A. A. Arowojulu, P. A. Jefford, and C. J. Kellett, "An experimental evaluation of the performance of two-branch space and polarisation diversity schemes at 1800 MHz," in *Proc. IEEE Trans. on Vehicular Technology*, pp. 290–294, May 1995.

[6] R. G. Vaughan, "Polarization diversity in mobile communications," in *Proc. IEEE Trans. on Vehicular Technology*, pp. 177–186, Aug. 1990.

[7] F. Oggier, G. Rekaya, J.-C. Belfiore, and E. Viterbo, "Perfect space-time block codes," *IEEE Trans. Inform. Theory*, vol. 52, pp. 3885–3902, Sept. 2006.

[8] H. Jafarkhani, *Space-Time Codeing: Theory and Practice*. Cambridge University Press, 2005.

[9] A. Hottinen, O. Tirkkonen, and R. Wichman, *Multi-antenna Transcive Techniques for 3G and Beyond*. Wiley & Sons Ltd., UK, 2003.

[10] V. Tarokh, N. Seshadri, and A. R. Calderbank, "Space-time codes for high data rate wireless communications: Performance criteria and code construction," *IEEE Trans. Inform. Theory*, vol. 44, pp. 744–765, 1998.

[11] D. Chizhik, G. Foschini, M. Gans, and R. Valenzuela, "Keyholes, correlations and capacities of multielement transmit and receive antennas," *IEEE Trans. Wireless Commun.*, vol. 1, pp. 361–368, Apr. 2002.

[12] D. Gesbert, H. Bolcskei, D. Gore, and A. Paulraj, "Outdoor MIMO wireless channels: Models and performance prediction," *IEEE Trans. Commun.*, vol. 50, pp. 1926–1934, Dec 2002.

[13] L. Zheng and D. N. Tse, "Diversity and multiplexing: A fundamental tradeoff in multiple-antenna channels," *IEEE Trans. Inform. Theory*, vol. 49, pp. 1073–1096, May 2003.

[14] S. Alamouti, "Space-block coding: A simple transmitter diversity technique for wireless communications,," *IEEE J. Select. Areas Commun.*, vol. 16, pp. 1451–1458, 1998.

[15] "Space-time block coded transmit antenna diversity for WCDMA," in *Texas Instruments Inc., dallas, TX, SMG2 Doc. 581/98*, 1998.

[16] TIA 45.5 Subcommittee, "The cdma 2000 candidate submission (draft)," in *TIA, Arlington, VA*, June 2,1998.

[17] S. N. Diggavi, N. Al Dhahir, A. Stamoulis, and A. R. Calderbank, "Great expectations: The value of spacial diversity to wireless networks," *Proc. IEEE*, pp. 219–270, Feb. 2004.

[18] B. Hassibi and B. Hochwald, "High-rate linear space-time codes," in *Proc. IEEE International Conference on Acoustics, Speech, and Signal Processing*, pp. 2461–2464, May 2001.

[19] V. Tarokh, H. Jafarkhani, and A. R. Calderbank, "Space-time block codes from orthogonal designs," *IEEE Trans. Inform. Theory*, vol. 45, pp. 1456–1467, July 1999.

[20] H. Wang and X.-G. Xia, "Upper bounds for rates of space-time block codes from complex orthogonal designs," *IEEE Trans. Inform. Theory*, vol. 49, no. 10, pp. 2788–2796, 2003.

[21] H. Jafarkhani, "A quasi-orthogonal space-time block code," *IEEE Trans. Commun.*, vol. 49, pp. 1–4, 2001.

[22] J.-C. Belfiore, G. Rekaya, and E. Viterbo, "The Golden code: A 2x2 full-rate space-time code with nonvanishing determinants," *IEEE Trans. Inform. Theory*, vol. 51, pp. 1432–1436, 2005.

[23] *IEEE 802.16e-2005:IEEE Standard for Local and Metropoliton Area Networks- Part 16: Air Interface for Fixed and Mobile Broadband Wireless Access Systems- Amendment2: Physical Layer and Medium Access Control Layers for Combined Fixed and Mobile Operation in Licensed Bands.* Feb, 2006.

[24] S. J. Lee, et. al, "A space-time code with full diversity and rate 2 for 2 transmit antenna transmission," in *IEEE 802.16 Session #34, 2004, Contribution IEEE C 802.16e-04/434r2*, 2004.

[25] R. Akhtar, "Cyclotomic euclidean number fields." Senior thesis. Harvard University, 1995.

[26] J. W. S. Cassels, *An Introduction to Diophantine Approximation*. Cambridge University Press, 1957.

[27] A. Hottinen and O. Tirkkonen, "Precoder designs for high rate space-time block codes," in *Proc. Conference on Information Sciences and Systems*, (Princeton, NJ), Mar. 2004.

[28] O. Tirkkonen and R. Kashaev, "Combined information and performance optimization of linear MIMO modulation," in *Proc. IEEE ISIT*, (Lausanne, Switzerland), July 2002.

[29] C. Hollanti, J. Lahtonen, K. Ranto, R. Vehkalahti, and E. Viterbo, "On the algebraic structure of the Silver code: A 2×2 perfect space time block code," in *Proc.IEEE Information Theory Workshop (ITW'08)*, pp. 91–94, May 2008.

[30] S. Sezginer and H. Sari, "A full-rate full-diversity 2x2 space-time code for mobile WiMAX system," in *Proc. IEEE International Conference on Signal Processing and Communications*, (Dubai), Nov. 2007.

[31] P. Rahici and N. Al-Dhahir, "A new information lossless STBC for 2 transmit antennas with reduced-complexity ML decoding," in *Proc. IEEE on Vehicular Technology*, Sept. 2007.

[32] A. F. Naguib, N. Seshadri, and A. R. Calderbank, "Applications of space-time block codes and interference suppression for high capacity and high data rate wireless systems," in *Proc. Thirty-Second Asilomar Conference on Signals, Systems and Computers*, pp. 1803–1810, Nov. 1998.

[33] S. Sandhu and A. Paulraj, "Space-time block codes: a capacity perspective," *IEEE Commun. Lett.*, vol. 4, no. 12, pp. 384–386, 2000.

[34] B. Hassibi and B. Hochwald, "High-rate codes that are linear in space and time," *IEEE Trans. Inform. Theory*, vol. 48, pp. 1804–1824, July 2002.

[35] D. Tse and P. Viswanath, *Fundamentals of Wireless Communication*. Cambridge University Press, 2005.

[36] A. R. Calderbank and A. F. Naguib, "Orthogonal designs and third generation wireless communication," in *Surveys in Combinatorics 2001* (J. Hirschfeld, ed.), London Math. Soc. Lecture Note Series 288, pp. pp.75–107, Cambridge Univ. Press, 2001.

[37] A. F. Naguib and N. Seshadri, "Combined interference cancellation and ML decoding of space-time block codes," in *Proc.Comm. Theory Miniconference,held in conjunction with Globecomm'98*, (Sydney, Australia), pp. 7–15, 1998.

[38] J. O. Berger, *Statistical Decision Theory and Bayesian Analysis*. Springer Verlag, 1985.

[39] J. R. Silvester, "Determinants of block matrices," *Maths Gazette 84*, pp. 460–467, 2000.

[40] S. Sirianunpiboon, A. R. Calderbank, and S. D. Howard, "Diversity gains across line of sight and rich scattering environments from space-polarization-time codes," in *Proc. IEEE ITW on Information Theory for Wireless Networks*, (Bergen, Norway), July 2007.

[41] R. A. Horn and C. R. Johnson, *Matrix Analysis*. Cambridge University Press, 1985.

[42] G. J. Foschini, "Layered space-time architecture for wireless communication in a fading environment when using multi-element antennas," *Bell Labs Technical Journal*, vol. 1, pp. 41–59, 1996.

[43] O. Damen, A. Chkeif, and J.-C. Belfiore, "Lattice code decoder for space-time codes," *IEEE Commun. Lett.*, vol. 4, pp. 161–163, May 2000.

[44] B. Hassibi and H. Vikalo, "On the sphere-decoding algorithm I. Expected complexity," *IEEE Trans. Inform. Theory*, vol. 53, pp. 2806–2818, August 2005.

[45] J. Jaldén and B. Ottersten, "On the complexity of the sphere decoding in digital communications," *IEEE Trans. Signal Processing*, vol. 53, pp. 1474–1484, April 2005.

[46] S. Sirianunpiboon, A. R. Calderbank, and S. D. Howard, "Fast essentially maximum likelihood decoding of the golden code," *submitted to IEEE Trans. Information Theory*, 2008.

[47] S. D. Howard, S. Sirianunpiboon, and A. R. Calderbank, "Low complexity essentially maximum likelihood decoding of perfect space-time block codes," in *Proc. IEEE ICASSP*, (Taipei, Taiwan), Apr. 20009.

[48] S. Sirianunpiboon, A. R. Calderbank, and S. D. Howard, "Bayesian analysis of interference cancellation for alamouti multiplexing," *IEEE Trans. Inform. Theory*, vol. 54, pp. 4755–4761, Oct. 2008.

[49] O. Tirkkonen and R. Kashaev, "Performance optimal and information maximal MIMO modulations," in *Proc. IEEE ISIT*, (Lausanne, Switzerland), July 2002.

[50] O. Tirkkonen and A. Hottinen, "Improved MIMO performance with non-orthogonal space-time block codes," in *Proc. IEEE Global Telecommunications*, (Lausanne, Switzerland), Nov. 2001.

[51] D. Rife and R. Boorstyn, "Single tone parameter estimation from discrete-time observations," *IEEE Trans. Inform. Theory*, vol. 20, no. 5, pp. 591–598, 1974.

[52] K. P. Srinath and B. S. Rajan, "Low ML-Decoding Complexity, Large Coding Gain, Full-Rate, Full-Diversity STBCs for 2×2 and 4×2 MIMO Systems," *IEEE Trans. Selected Topics in Signal Processing*, vol. 3, no. 12, pp. 916–927, 2009.

[53] H. Yao and G. W. Wornell, "Achieving the full MIMO diversity multiplexing frontier with rotation-based space-time codes," October 2003.

[54] P. Dayal and M. K. Varanasi, "Optimal two transmit antenna space-time code and its stacked extensions," *IEEE Trans. Inform. Theory*, vol. 51, pp. 4348–4355, 2005.

[55] S. Sirianunpiboon, Y. Wu, A. R. Calderbank, and S. D. Howard, "Fast optimal decoding of multiplexed orthogonal designs by conditional optimization," *to appear in IEEE Trans. Info. Theory*, 2010.

[56] E. Biglieri, Y. Hong, and E. Viterbo, "On fast-decodable space-time block codes," *IEEE Trans. Inform. Theory*, vol. 55, no. 2, pp. 524–530, 2009.

[57] M. O. Sinnokrot and J. R. Barry, "The golden code is fast decodable," in *Proc. IEEE GLOBCOM*, (New Orleans), 2008.

[58] R. U. Nabar, H. Bölsekei, V. Erceg, D. Gesbert, and A. J. Paulraj, "Performance of multiantenna signaling techniques in the presence of polarization diversity," *IEEE Trans. Signal Processing*, vol. 50, no. 10, pp. 2553–2562, 2002.

[59] J. D. Jackson, *Classical Electrodynamics*. Wiley & Sons Inc., 1975.

[60] Y. Deng, A. Burr, and G. White, "Performance of MIMO systems with combined polarization multiplexing and transmit diversity," in *Proc. IEEE Trans on Vehicular Technology*, pp. 869–873, May 2005.

[61] R. U. Nabar, V. Erceg, H. Bölcskei, and A. J. Paulraj, "Performance of multi-antenna signaling strategies using dual-polarized antennas:measurement results and analysis," in *Proc. IEEE WPMC*, (Aalborg, Denmark), pp. 175–180, Sept. 2001.

[62] D. S. Baum, D. A. Gore, R. U. Nabar, S. Panchanathan, K. V. S. Hari, V. Erceg, and A. J. Paulraj, "Measurement and characterisation of broadband MIMO fixed wireless channels at 2.5 GHz," in *Proc. IEEE Int. Conf. Pers. Wireless Commun*, (Hyderabad, India), pp. 203–206, Dec. 2000.

[63] C. Degen and W. Keusgen, "Performance evaluation of MIMO systems using dual-polarized antennas," in *Proc. IEEE 10th International Conference on Telecommunications*, pp. 1520–1525, 2003.

[64] M. Andrews, P. Mitra, and R. deCarvalho, "Tripling the capacity of wireless communications using electromagnetic polarization," *Nature*, vol. 409, pp. 316–318, 2001.

[65] R. Bansal, "Triple to the rescue," *IEEE Antennas Propagat. Mag.*, vol. 43, no. 2, pp. 106–107, 2001.

[66] R. Doostnejad, T. Lim, and E. Sousa, "Space-time multiplexing for MIMO multiuser downlink channels," *IEEE Trans. Wireless Commun.*, vol. 5, no. 7, pp. 1726–1734, 2006.

[67] S. Sirianunpiboon, S. D. Howard, R. A. Calderbank, and L. Davis, "Fully polarimetric MIMO to improve throughput and reliability across propagation conditions," in *Proc. IEEE VTC Fall*, (Anchorage), Sept. 2009.

[68] S. D. Howard, A. R. Calderbank, and W. Moran, "The finite heisenberg-weyl groups in radar and communications," *EURASIP Journal on Applied Signal Processing*, 2006.

[69] Y. Hong, E. Viterbo, and J.-C. Belfiore, "A space-time blocked multiuser MIMO downlink transmission scheme," in *Proc.IEEE ISIT*, (Seattle), July 2006.